Aus dem
CharitéCentrum für Innere Medizin mit Gastroenterologie und Nephrologie
Medizinische Klinik mit Schwerpunkt Nephrologie und Internistische Intensivmedizin
Direktor: Univ.-Prof. Dr. med. Kai-Uwe Eckardt

Habilitationsschrift

Zur Erlangung der Lehrbefähigung
für das Fach Innere Medizin

Wirts- und mikrobiomseitige Einflussfaktoren auf die Inflammation bei kardiovaskulären Erkrankungen

vorgelegt dem Fakultätsrat der Medizinischen Fakultät
Charité-Universitätsmedizin Berlin

von

Dr. med. Nicola Wilck

Eingereicht: Juli 2023

Dekan: Prof. Dr. med. Joachim Spranger

1. Gutachter:

2. Gutachter:

INHALTSVERZEICHNIS

Seite

ABKÜRZUNGEN

AhR	Arylhydrocarbonrezeptor
AngII	Angiotensin II
ATP	Adenosintriphosphat
BMDM	*Engl.: Bone-marrow-derived macrophage*
CD4	*Engl.: Cluster of differentiation 4*
CD69	*Engl.: Cluster of differentiation 69*
CKD	Chronische Niereninsuffizienz, Engl.: *Chronic kidney disease*
CrP	C-reaktives Protein
COL	besiedelt, Engl.: *colonized*
CVD	Herz-Kreislauf-Erkrankungen, Engl.: *cardiovascular disease*
EAE	Experimentelle Autoimmunenzephalitis
GF	keimfrei, Engl.: *germ-free*
GPCR	G-Protein-gekoppelter Rezeptor, Engl.: *G protein-coupled receptor*
GWAS	Genomweite Assoziationsstudie, Engl.: *Genome-wide association study*
HIF-1α	Hypoxia-inducible factor 1-alpha
HSD	Hochsalzdiät, Engl.: *high-salt diet*
HTN	Hypertension, Bluthochdruck
IFN-γ	Interferon-γ
IκB-α	I-kappa-B-alpha
IL-1β	Interleukin-1β
IL-6	Interleukin-6
IL-10	Interleukin-10
IL-17A	Interleukin-17A
ILA	Indol-3-Laktat
LDLR	LDL-Rezeptor, Engl.: *low density lipoprotein receptor*
LMP2	Low molecular mass protein 2
LMP7	Low molecular mass protein 7
MM	Multiples Myelom
MCP-1	*Monocyte Chemoattractant Protein-1,* auch: CCL2 (CC-chemokine ligand 2)
MECL-1	*Multicatalytic Endopeptidase Complex-Like 1*
MHC I	MHC-Klasse-I-Komplex, Engl.: *Major histocompatibility complex class I*
MMP	Matrixmetalloproteinasen

mRNA	*Messenger ribonucleic acid*
NF-κB	*Nuclear factor 'kappa-light-chain-enhancer' of activated B-cells*
NLRP3	*NLR family pyrin domain containing 3*
NO	Stickstoffmonoxid, Engl.: *nitric oxide*
Nox4	*NADPH-Oxidase 4*
Olfr78	*Olfactory receptor-78*
RAG1	*Recombination activating gene 1*
ROS	Reaktive Sauerstoffspezies, Engl.: *reactive oxygen species*
SCFA	Kurzkettige Fettsäuren, Engl.: *short-chain fatty acid*
T_H1	Typ-1-T-Helferzelle
T_H17	Typ-17-T-Helferzelle
T_{REG}	Regulatorische T-Zellen
TMA	Trimethylamin
TMAO	Trimethylamin-N-oxid
TNF-α	Tumornekrosefaktor-α
Trp	Tryptophan
UPS	Ubiquitin-Proteasom-System
VCAM-1	*Vascular cell adhesion molecule 1*
VSMC	Vaskuläre glatte Muskelzellen, Engl. *Vascular smooth muscle cells*

1 EINLEITUNG

1.1 Die Inflammation bei kardiovaskulären Erkrankungen

Kardiovaskuläre Erkrankungen sind die führende Todesursache in weiten Teilen der Welt bei Erwachsenen ab einem Alter von 50 Jahren, angeführt von der ischämischen Herzerkrankung und dem Schlaganfall[1]. Die Atherosklerose und die essentielle (auch: primäre) arterielle Hypertonie (hier Hypertonie genannt) sind dabei zentrale, prävalente pathophysiologische „Wegbereiter" der kardiovaskulären Morbidität und des kardiovaskulären Tods[2, 3]. Deren Progression - z.B. durch fehlende oder unzureichende Behandlung trotz diverser therapeutischer Optionen - führt zu Endorganschäden, u.a. an Gefäßsystem, Herz und Nieren und schließlich fatalen kardiovaskulären Ereignissen. Wegweisende Erkenntnisse der letzten Jahrzehnte zur Pathophysiologie von Atherosklerose und Hypertonie haben sich in vielerlei Hinsicht in den aktuell etablierten medikamentösen Therapien niedergeschlagen. Medikamente aus dem kardiovaskulären Spektrum (z.B. Antihypertensiva, Statine, Thrombozytenaggregationshemmer) machen heute einen Großteil der Pharmakotherapie erwachsener PatientInnen aus [4, 5]. Dennoch verbleiben kardiovaskuläre Erkrankungen auf den vorderen Plätzen der weltweiten Morbiditäts- und Mortalitätsstatistiken. Folglich lässt sich aus diesen Statistiken ein *Medical Need*, die Notwendigkeit der Identifikation neuartiger therapeutischer Ziele und neuer therapeutischer Strategien, ableiten. Die vorliegende Arbeit konzentriert sich im komplexen Themenfeld der kardiovaskulären Erkrankungen auf die Atherosklerose und die Hypertonie.

Ein wesentlicher Fortschritt im Verständnis der Pathophysiologie kardiovaskulärer Erkrankungen ist die Erkenntnis, dass kardiovaskuläre Erkrankungen wie die Atherosklerose und die Hypertonie durch eine chronische inflammatorische Reaktion gekennzeichnet sind[6-8], welche die Krankheitsprogression befördert und die Prognose betroffener PatientInnen beeinträchtigt. Obwohl sich in beiden Erkrankungen die Auslöser der Inflammation, die beteiligten Immunzellen und Signalwege durchaus unterscheiden, ist die chronische Inflammation in beiden Erkrankungen bei betroffenen PatientInnen messbar. Biomarker der Entzündung wie das hochsensitive C-reaktive Protein (CrP) oder Zytokine wie Interleukin-1β (IL-1β) sind sowohl bei Hypertonie als auch im Rahmen der Atherosklerose erhöht und können hilfreich bei der Risikoprädiktion sein[9-13]. Viele PatientInnen weisen trotz leitliniengerechter Therapie eine Erhöhung der Entzündungsmarker auf, was die Notwendigkeit einer gezielten anti-inflammatorischen Behandlung verdeutlicht[14]. Die derzeitig in Leitlinien festgelegten Therapiestandards adressieren die Inflammation nicht direkt oder nur unzureichend.

Beide Erkrankungen sind durch eine chronische inflammatorische Aktivierung charakterisiert, die nach derzeitigem Kenntnisstand nicht durch die Präsenz von oder die Infektion mit pathogenen Mikroorganismen ausgelöst wird, sondern durch anhaltende Auslenkungen z.B. des Lipidstoffwechsels

oder Renin-Angiotensin-Aldosteron-Systems (RAAS) oder anderer Umweltfaktoren angestoßen und unterhalten wird und somit im weitesten Sinne als eine „sterile“ Inflammationen bezeichnet werden kann. Sowohl Immunzellen des angeborenen als auch des adaptiven Immunsystems sind beteiligt und vermitteln als Mediatoren der Entzündung den resultierenden Endorganschaden, indem sie in Gefäße, Herz und Nieren einwandern. Beiden Erkrankungen ist ebenfalls gemein, dass sie trotz vieler in genomweiten Assoziationsstudien (GWAS) identifizierter, begünstigender genetischer Polymorphismen[15-17] in einem hohen Maße abhängig von Umwelteinflüssen[18, 19] wie zum Beispiel der Ernährung sind. Übergewicht, eine Ernährung reich an gesättigten Fetten tierischer Herkunft bzw. eine salzreiche Ernährung sind Einflüsse, welche vielfach mit beiden Erkrankungen assoziiert worden sind[20, 21]. Aus diesem wichtigen Einfluss diätetischer Risikofaktoren leitet sich ein Schwerpunkt der vorliegenden Arbeit ab. Diese untersucht das Darmmikrobiom als Mediator zwischen Umwelt und Wirtsorganismus als einen Einflussfaktor und therapeutisches Ziel.

Motivation der vorliegenden Arbeit ist die Erforschung neuartiger therapeutischer Angriffspunkte, um die Inflammation bei Atherosklerose und Hypertonie zu reduzieren. Dabei liegt der Fokus der Studien zum einen auf dem Ubiquitin-Proteasom-System als einem zellulären, wirtsseitigem System und zum anderen auf dem Mikrobiom des Darms als eine Schnittstelle zwischen Umwelt und Immunsystem.

1.1.1 Atherosklerose und Inflammation

Die Atherosklerose trägt wesentlich zur globalen Morbidität und Mortalität von kardiovaskulären Erkrankungen bei. Unter den drei häufigsten Todesursachen kardiovaskulärer Ursache in Deutschland führte das Statistische Bundesamt im Jahr 2022 mit der chronisch-ischämischen Herzerkrankung, dem akuten Myokardinfarkt und der Herzinsuffizienz drei ICD-10-Diagnosen auf, welche direkt oder indirekt Folge einer atherosklerotischen Erkrankung sein können[22]. Damit spiegeln die deutschen Zahlen in vergleichbarer Weise den globalen Trend wider[23].

Pathophysiologisch hat insbesondere die Erkenntnis, dass die Atherosklerose eine Lipid-getriebene Erkrankung darstellt, zwar zur äußerst erfolgreichen Translation in die medizinische Grundversorgung, jedoch nicht zur Verdrängung der kardiovaskulären Erkrankungen von den vorderen Plätzen der Statistiken geführt. Statine zählen heute zu den am meisten verschriebenen Medikamenten weltweit[24]. Zudem werten wir die Atherosklerose seit mehr als zwei Dekaden als eine chronische Erkrankung mit ausgeprägter inflammatorischer Komponente[6, 7]. Dass eine anti-inflammatorische Behandlung z.B. mit einem Antikörper gegen Interleukin-1 β nach stattgehabtem Myokardinfarkt das Überleben verbessert, konnte zwar in der großen CANTOS-Studie gezeigt werden[14], hat sich jedoch unter anderem wegen eines erhöhten Infektionsrisikos noch nicht in der klinischen Routine durchgesetzt.

Auch therapeutische Ansätze mit Methotrexat[25] und Colchizin[26] haben zum Teil einen klinischen Vorteil gezeigt, sich allerdings nicht durchgesetzt.

Neben diesen relativ breiten anti-inflammatorischen Therapien bietet jedoch die komplexe Pathophysiologie der Atherosklerose mit den verschiedenen involvierten Zelltypen vielfältige alternative Ansatzpunkte, um zukünftig die Entstehung und Progression der Atherosklerose zu verlangsamen oder gar zu verhindern: Kurz zusammengefasst führt die Exposition gegenüber Risikofaktoren (Hypercholesterinämie im Zusammenspiel mit Risikofaktoren wie Hypertension, Adipositas, Rauchen) zu einer endothelialen Schädigung und Dysfunktion, zur Retention von Lipiden im subendothelialen Raum sowie zur Expression endothelialer Adhäsionsmoleküle und Sekretion chemotaktischer Substanzen, welche die Rekrutierung, Adhäsion und Transmigration von Leukozyten aus dem Blut in die Gefäßwand fördern. Die hier relevanten Immunzellen umfassen u.a. Monozyten/Makrophagen, neutrophile Granulozyten aber auch T-Zellen. Monozyten werden über Integrine und Chemokin-Rezeptoren in die Gefäßwand aus dem Blut rekrutiert. Als subendotheliale Makrophagen internalisieren diese dann modifizierte Lipoproteine, was zur Bildung der sogenannten Schaumzellen führt. Modifizierte Lipide aktivieren das NLRP3-Inflammasom in Makrophagen, was zur Produktion von IL-1β führt. Die Interaktion von Makrophagen, T-Zellen und anderen Leukozyten unterhält die Inflammation, reaktive Sauerstoffspezies (ROS), Wachstumsfaktoren und Zytokine werden freigesetzt. Vaskuläre glatte Muskelzellen (VSMC) proliferieren und verändern ihren Phänotyp von einem kontraktilen hin zu einem Makrophagen-ähnlichen Phänotyp und wandern in die Intima, wo sie extrazelluläre Matrixproteine sezernieren und eine fibröse Kappe der Plaque bilden. Schließlich führt die Apoptose der in der Plaque ansässigen Zellen zur Entstehung eines nekrotischen Kerns. Hypoxie-induzierte Neovaskularisation und die Sekretion von Matrixmetalloproteinasen (MMP) durch Makrophagen können die fibröse Plaque weiter destabilisieren und zu einer Ruptur der Plaque mit Thrombusbildung führen.

Die vorliegende Arbeit beschreibt zum einen den experimentellen Ansatz, oxidativen Stress durch den Einsatz niedrigdosierter Proteasominhibition zu reduzieren und somit auch inflammatorische Prozesse einzudämmen. Oxidativer Stress und Inflammation sind bekanntermaßen in der Atherosklerose gleichzeitig nachweisbar und können einander fördern. So kann oxidativer Stress pro-inflammatorische Genexpression über Transkriptionsfaktoren wie NF-κB und HIF-1α sowie das NLRP3-Inflammasom aktivieren, wodurch pro-inflammatorische Zytokine, Chemokine und andere Mediatoren gebildet werden. Die von Immunzellen ausgeschütteten Zytokine und Chemokine fördern wiederum die Rekrutierung weiterer Immunzellen und eine zusätzliche ROS-Produktion, womit sich dieser Kreislauf verselbständigen kann und die Progression der Atherosklerose weiter gefördert wird. Da in der Atherosklerose vermehrt oxidativ geschädigte Proteine anfallen und über das Proteasom abgebaut werden müssen, untersucht die vorliegende Arbeit zudem das Immunoproteasom, dem eine wichtige Rolle bei der Bewältigung oxidativen Stresses zugeschrieben wurde.

1.1.2 Hypertonie, T-Zellen und Endorganschaden

Die arterielle Hypertonie ist eine Systemerkrankung, welche sich nicht ausschließlich auf das Gefäßsystem beschränkt, sondern mehrere Organsysteme inklusive Immunsystem einschließt. Oft als „stiller Killer“ bezeichnet, werden die klinischen Folgen der Hypertonie oft erst langfristig apparent, als Dysfunktionen von Gefäßsystem, Nieren, Gehirn und Herz und führen so zu einer beträchtlichen Mortalität und Morbidität weltweit. Unter den weltweit prävalentesten Risikofaktoren für nicht übertragbare Erkrankungen belegt die Hypertonie den ersten Rang[2, 20]. Pathophysiologisch sind ebenfalls eine Vielzahl von Organen und Regelkreisen an der Entstehung von Bluthochdruck beteiligt und interagieren. Hierzu zählen (Dys)regulationen der vaskulären, renalen und kardialen Struktur und Funktion, des Natriumhaushalts und der Blutvolumenregulation, des Renin-Angiotensin-Aldosteron-Systems und des vegetativen Nervensystems[27].

Die Hypothese, dass das Immunsystem im Rahmen des Bluthochdrucks eine wichtige Rolle spielt, kam vergleichsweise früh, bereits in den 1960er Jahren, auf, als man Lymphozyten aus Ratten mit unilateralem Niereninfarkt in Empfänger-Ratten transferierte, welche daraufhin Bluthochdruck entwickelten[28]. Experimentelle Studien konnten bereits damals und vermehrt in etwas jüngeren Arbeiten zeigen, dass – zum Nachweis des Konzepts - eine immunsuppressive Behandlung den Bluthochdruck sowie den hypertensiven Endorganschaden eindämmen kann[8, 29-33]. Allerdings verhindern potentiell schwere Nebenwirkungen (z.B. Infektionen) eine langfristige, breite Immunsuppression bei PatientInnen.

Experimentelle, hypertensive Stimuli wie Angiotensin II (AngII) oder ein hoher Salzgehalt in der Nahrung führen zu einer Aktivierung von angeborenen und adaptiven Immunzellen. Der Rolle der T-Zellen wurde große Aufmerksamkeit zuteil, obwohl die Mechanismen, die zur T-Zellen-Aktivierung führen, nach wie vor nur unzureichend definiert sind. Es ist bekannt, dass T-Zellen bei experimenteller Hypertonie eine wichtige Rolle spielen. RAG1-Knockout-Mäuse, denen B- und T-Zellen fehlen, haben einen abgeschwächten Blutdruckanstieg in Reaktion auf AngII, die durch den adoptiven Transfer von T-, aber nicht von B-Zellen wiederhergestellt werden kann[34]. T-Zellen exprimieren als Reaktion auf hypertensive Stimuli Aktivierungsmarker (z. B. CD69). Es wurde gezeigt, dass sowohl $CD8^+$ zytotoxische T-Zellen als auch $CD4^+$ T-Helferzellen hierbei eine entscheidende Rolle spielen. Aktivierte T-Zellen infiltrieren Zielorgane wie die Niere, wo sie pro-inflammatorische Zytokine wie Interleukin-17A (IL-17A) und Interferon-γ (IFN-γ) freisetzen, die zu Zellschäden, oxidativem Stress und endothelialer Dysfunktion, Fibrose und schließlich zum Verlust der Organfunktion führen[35, 36]. Sowohl IL-17A als auch IFN-γ sind nachweislich an der Entstehung von Hypertonie und Organschäden beteiligt. Außerdem wurde nachgewiesen, dass IL-17A den Blutdruck erhöht, indem es die Natriumrückresorption in der Niere stimuliert[37, 38]. Hypertone Stimuli fördern die Differenzierung von T-Helferzellen in pro-inflammatori-

sche T-Helfer-Subtypen wie z.B. Typ17- (T_H17) und Typ1-(T_H1) Helferzellen, die durch eine erhöhte Produktion von IL-17A bzw. IFN-γ gekennzeichnet sind[39]. T-Zellen mit einem Effektor-Gedächtnis-Phänotyp (T_{EM}; $CD44^+$ $CD62L^-$ $CCR7^-$) akkumulieren bei Bluthochdruck in der Niere und sind die vorherrschenden Quellen von IL-17A und IFN-γ. Interessanterweise können wiederholte hypertensive Stimuli die Ansammlung von T_{EM} in der Niere verstärken[39], was auf die Ausbildung eines immunologischen Gedächtnisses im Rahmen der Hypertonie hindeutet. Entzündungshemmende Interleukin-10 (IL-10) produzierende regulatorische T-Helferzellen (T_{REG}) können die pro-inflammatorische Funktion der Effektor-T-Zellen ausbalancieren und schützen vor Hypertonie und Endorganschäden[40-42]. Daher ist das Gleichgewicht zwischen pro- und anti-inflammatorischen T-Zell-Untergruppen bei Hypertonie entscheidend. Therapeutische Strategien, die zur Wiederherstellung des Gleichgewichts von pro- und anti-inflammatorischen T-Zellen führen, könnten eine Option zur Organprotektion bei Hypertonie darstellen.

1.2 Das Ubiquitin-Proteasom-System in der Atherosklerose

Das Ubiquitin-Proteasom-System (UPS) ist zentral für die Proteinhomöostase der Zelle. Das 26S Proteasom ist eine ATP-abhängige Protease, bestehend aus dem katalytischen Kern, dem 20S Proteasom, und zwei 19S Regulator-Komplexen, welche für Substraterkennung und Transport der abzubauenden Proteinketten in das katalytische Zentrum verantwortlich sind[43]. Das 20S Proteasom besteht aus vier übereinander gelagerten Ringen, welche jeweils aus sieben Untereinheiten bestehen. Dabei bestehen die beiden äußeren Ringe aus den α-Untereinheiten (α1-α7), die beiden inneren Ringe aus den β-Untereinheiten (β1-β7)[43].

Das UPS ist bedeutsam für den Abbau fehlgefalteter Proteine[44], als auch für die Degradation zentraler regulatorischer Proteine des Zellzyklus, der Transkriptionsmaschinerie und des Stoffwechsels[45]. Der selektive Abbau solcher Proteine wird über die kovalente Bindung von Ketten multipler Ubiquitin-Moleküle vermittelt, die als Erkennungssignal für das 26S Proteasom dienen.

Eine wichtige Funktion des UPS besteht in der Antigenprozessierung und Immunabwehr. Die nach proteasomaler Degradation entstandenen Peptide werden in den Major Histocompatibility Complex I (MHC I) integriert und auf der Zelloberfläche präsentiert. Vor allem in diesem Zusammenhang wurde man erstmals auf eine alternative Form des Proteasoms, das Immunoproteasom, aufmerksam. Unter Zytokin-Stimulation (z. B. durch IFN-γ) erfolgt der Austausch der β-Untereinheiten des konstitutiven Proteasoms (β1, β2, β5) gegen die immunoproteasomalen Untereinheiten *low molecular mass protein* 2 und 7 (LMP2, LMP7) und *multicatalytic endopeptidase complex subunit* 1 (MECL-1). Neben der Induktion durch Zytokin-Stimulation werden Immunoproteasomen gewebsspezifisch in immunrelevanten Geweben konstitutiv exprimiert. Immunoproteasomen verfügen über eine alternative Schnittstellenpräferenz bei der Degradation von Proteinen und führen zur effizienten Generierung von Peptiden zur Präsentation über MHC I. Die transiente, Zytokin-vermittelte Hochregulation von Immunoproteasomen scheint ein wichtiges Element in der Immunantwort bei viralen Infektionen zu sein[46]. Weitere Studien zeigten, dass die Bedeutung des Immunoproteasoms nicht auf die Antigenpräsentation beschränkt ist. Beispielsweise führt eine LMP2-Defizienz zu einer verminderten Proteasomaktivität und Akkumulation oxidierter Proteine[47]. Weitere Regulatoren der immunoproteasomalen Expression, z. B. NO und Hitzeschock, wurden identifiziert und sind auch in der Atherogenese relevant[48, 49]. Eine NO-vermittelte Expressionszunahme von immunoproteasomalen Untereinheiten schützt Endothelzellen vor oxidativem Stress[48]. Das Proteasom ist beteiligt an der Aktivierung des Transkriptionsfaktors *nuclear factor 'kappa-light-chain-enhancer' of activated B-cells* (NF-κB), der die Expression vieler inflammatorischer Proteine induziert:zum einen an der Entstehung der p50-Untereinheit aus dem p105 Vorläuferprotein und zum anderen an der Degradation der inhibitorischen Proteine *nuclear factor of kappa light polypeptide gene enhancer in B-cells inhibitor* (IκB) α und β, welche die Translokation von NF-κB aus dem Zytoplasma in den Zellkern verhindern. Pro-inflammatorische Stimuli aktivieren

Signalkaskaden, welche zur Phosphorylierung, Ubiquitinierung und anschließenden proteasomalen Degradation der IκB-Proteine führen und damit die Translokation von NF-κB in den Zellkern ermöglichen[50]. Es gibt Hinweise darauf, dass ein erhöhter Anteil von Immunoproteasomen in inflammatorischem Gewebe in direktem Zusammenhang mit einer erhöhten Aktivierung von NF-κB steht. Experimentell konnte gezeigt werden, dass Immunoproteasomen IκB-Proteine schneller abbauen als konstitutive Proteasomen[51].

Experimentelle Daten lassen darauf schließen, dass das UPS eine Rolle in der Entstehung und Progression der Atherosklerose spielt. Ob das UPS dabei einen anti- oder proatherogenen Einfluss ausübt, ist jedoch nicht eindeutig geklärt und möglicherweise abhängig vom Stadium der Atherosklerose. Einen inflammationsfördernden Einfluss des UPS mit gesteigerter Aktivität legten Marfella *et al.* in Plaques der *Arteria carotis* von symptomatischen Patienten nahe[52]. Auch der entgegengesetzte Effekt – eine Aktivitätsminderung des UPS in späten Stadien der Atherosklerose – wurde von einer anderen Arbeitsgruppe im Tiermodell beschrieben[53]. Ausgehend von diesen Beobachtungen wurde für das UPS eine duale Rolle in der Atherosklerose postuliert: Einerseits könnte eine erhöhte Aktivität des UPS für eine gesteigerte Aktivierung des pro-inflammatorischen Transkriptionsfaktors NF-κB verantwortlich sein, andererseits könnte eine erhöhte Proteasomaktivität notwendig sein, um die durch oxidativen Stress vermehrt anfallenden dysfunktionalen Proteine zu eliminieren und damit die Zelle vor toxischen Effekten aggregierter dysfunktionaler Proteine und vor dem Zelltod zu bewahren[54]. Dem Immunoproteasom könnte in beiden Prozessen eine besondere Bedeutung zukommen. Die im Rahmen der atherosklerotischen Inflammation vermehrt produzierten Zytokine könnten einen zusätzlichen Stimulus für die Assemblierung von Immunoproteasomen darstellen.

Die in dieser Habilitationsschrift dargelegten Arbeiten untersuchen in Mausmodellen den Einfluss des Immunoproteasoms auf die Entwicklung der Atherosklerose sowie den Effekt einer niedrigdosierten Proteasominhibition in der frühen Atherosklerose.

1.3 Die Rolle des Mikrobioms und bakterieller Metabolite in der Hypertonie

Das intestinale Mikrobiom (hier fortan als Mikrobiom bezeichnet), d.h. die Gesamtheit der im Darm vorhandenen Bakterien sowie deren Gene, ist ein auf Umwelteinflüsse höchst responsives Ökosystem mit profundem Einfluss auf das Immunsystem. Verschiedenen Umweltfaktoren, insbesondere Bestandteile der Nahrung (z.B. Salz, Fasern oder sog. Ballaststoffe) können Veränderungen der Zusammensetzung und der Funktion des Mikrobioms verursachen und somit inflammatorische Prozesse vorteilhaft oder aber zum Nachteil des Wirts beeinflussen. Essentiell in diesem Zusammenhang ist die Tatsache, dass Bakterien aus Nahrungsbestandteilen Metabolite (z.B. Tryptophan (Trp)-Metabolite oder Fettsäuren) generieren, die vom Wirt resorbiert werden und die Differenzierung und die Funktion von Immunzellen beeinflussen können. Auf diese Weise beeinflussen die Mikrobiota auch Darm-ferne Organe (z.B. Niere, Herz), wodurch sich verschiedene Kommunikationsachsen identifizieren lassen (z.B. Darm-Niere, Darm-Herz). Leitlinien zur Behandlung der arteriellen Hypertonie betonen die gesunde Ernährung [55-57], u.a. charakterisiert durch einen hohen Ballaststoff- und niedrigen Salzgehalt. Die vorliegende Arbeit demonstriert für diese Nahrungsbestandteile, dass das Mikrobiom in diesem Zusammenhang eine wichtige Vermittlerrolle zwischen Umwelt und Wirt einnimmt. Ein genaues Verständnis der Wechselwirkung von Ernährung und Mikrobiom, Metaboliten mikrobieller Herkunft und Immunsystem sowie der Auswirkungen auf die Hypertonie könnte zukünftig eine gezielte, personalisierte Beeinflussung des Mikrobioms zur Organprotektion in der Hypertonie ermöglichen.

Die wohl prominenteste Klasse bakterieller Metabolite sind die kurzkettigen Fettsäuren (Engl. *short-chain fatty acids*, SCFA): Fettsäuren mit einer kurzen Kettenlänge von zwei bis sechs Kohlenstoffatomen, die durch bakterielle Fermentation im Darm aus unverdaulichen Kohlenhydraten der Nahrung entstehen können. Die wichtigsten Vertreter sind Acetat (C2), Propionat (C3) und Butyrat (C4). SCFA sind im Blut in zum Teil hohen Konzentrationen messbar[58]. Mehrere Studien belegen, dass die Hypertonie mit einer verminderten SCFA-Produktion assoziiert ist[59, 60]. Umgekehrt kann eine Ballaststoff-reiche Ernährung über SCFA eine Blutdruck-senkende Wirkung erzielen. Die verschiedenen SCFA binden an G-Protein-gekoppelte Rezeptoren (Engl. *G protein-coupled receptors*, GPR), beispielsweise über GPR41 (auch: FFAR3), GPR43 (auch: FFAR2), GPR109A und Olfr78 (olfactory receptor 78)[61], mit jeweils unterschiedlicher Affinität[62, 63]. Pluznick *et al.* zeigten, dass SCFA den Blutdruck über GPR41 und Olfr78 modulieren können, da Propionat zu einem Blutdruckabfall im Mausmodell führte, außer in GPR41-defizienten Mäusen[64]. GPR41 wird u.a. im vaskulären Endothel exprimiert und vermittelt eine endothelabhängige Vasodilatation[65]. GPR41 Knockout-Mäuse weisen einen erhöhten systolischen Blutdruck und eine höhere Gefäßsteifigkeit auf[65]. Propionat führt über den Olfr78-Rezeptor am juxtaglomerulären Apparat zur Renin-Sekretion, möglicherweise als Gegenregulation zum Blutdruck-senkenden Effekt von Propionat am vaskulären Endothel[64]. Eine Ballaststoff-reiche Diät sowie die Behandlung mit Acetat führen im hypertensiven Rattenmodell zur Senkung des Blutdrucks[66].

Weitere, im kardiovaskulären Spektrum bedeutsame bakterielle Metabolite sind TMA/TMAO und Indole. Trimethylamin-N-oxid (TMAO), das durch hepatische Sulfatierung aus dem bakteriellen Metaboliten Trimethylamin (TMA) entsteht, wird durch Bakterien aus Phosphatidylcholin oder L-Carnitin der Nahrung gebildet und gilt (in erhöhten Konzentrationen) als ein proatherogener Mediator[67]. Auch bei PatientInnen mit chronischer Nierenschädigung (*chronic kidney disease*, CKD) ist TMAO im Blut erhöht und mit einem erhöhten Mortalitätsrisiko assoziiert[68]. Im Rahmen der CKD können weitere bakterielle Metabolite in erhöhten Konzentrationen im Blut detektiert werden – zum Teil wegen der reduzierten renalen Clearance, zum Teil jedoch auch wegen der erhöhten Produktion durch intestinale Bakterien. Indole – bakterielle Trp-Metabolite - können über den Arylhydrocarbon-Rezeptor (AhR) immunmodulatorische Effekte ausüben (insbesondere an der Darmbarriere)[69], als auch toxische Effekte bei CKD-PatientInnen auslösen. Indoxylsulfat ist hier sicherlich der bekannteste Metabolit bakterieller Herkunft[70], der mit einer Reihe kardiovaskulärer Pathologien in Verbindung gebracht wurde.

Die in diese Habilitationsschrift eingehenden Studien haben zum Ziel, die Rolle des Mikrobioms bei Bluthochdruck näher zu charakterisieren und den Beitrag des Mikrobioms näher zu quantifizieren. Dabei steht der Einfluss des Mikrobioms auf die Inflammation bei Bluthochdruck im besonderen Fokus. Zum einen werden Einflussfaktoren der Umwelt (z. B. die salzreiche Ernährung) in Bezug auf Zusammensetzung und Funktion des Mikrobioms näher charakterisiert und die Auswirkung auf die inflammatorische Antwort untersucht. Zum anderen wird der Einfluss von bakteriellen Metaboliten (z. B. Trp-Metabolite (Indole), SCFA) des Darmmikrobioms auf die Inflammation und den Endorganschaden bei Bluthochdruck charakterisiert. Langfristiges Ziel ist, über die Beeinflussung des Mikrobioms eine vorteilhafte, anti-inflammatorische Immunmodulation und Organprotektion bei Bluthochdruck zu erreichen.

2 EIGENE ARBEITEN

2.1 Attenuation of early atherogenesis in low-density lipoprotein receptor-deficient mice by proteasome inhibition

Die Bedeutung der chronischen Inflammation[6, 7] und des oxidativen Stresses[71, 72] für die Entwicklung von atherosklerotischen Läsionen ist anerkannt. Als chronische Erkrankung der Gefäßwand ist die Entwicklung der Atherosklerose durch eine endotheliale Dysfunktion[73] und Aktivierung[74], die Migration zirkulierender Leukozyten in den subendothelialen Raum, die Akkumulation Cholesterol-beladener Makrophagen in der Gefäßwand[6], die Freisetzung einer Reihe von Zytokinen und Chemokinen durch Leukozyten[75], die phänotypische Transformation glatter Gefäßwandmuskelzellen[76] und somit Wachstum der atherosklerotischen Plaque gekennzeichnet. Vorarbeiten haben *in vitro*[77-82] und *in vivo*[83] gezeigt, dass die Inhibition des Proteasoms in niedrigdosierter, nicht toxischer Konzentration die Expression der endothelialen NO-Synthase erhöht und endothelabhängige Vasodilatation verbessert[78, 81], die anti-oxidative Funktion stärkt[79, 80, 82] und darüber hinaus anti-inflammatorische Effekte bei Hypertonie-induzierter Inflammation[83] hat.

In Kenntnis der beschriebenen Effekte niedrigdosierter Proteasominhibition auf vaskuläre Zellen untersucht diese experimentelle Studie, ob eine niedrigdosierte Proteasominhibition *in vivo* tatsächlich die Entstehung von Atherosklerose günstig beeinflussen kann. Als Modell wurde die Low-density Lipoprotein Rezeptor–defiziente Maus (LDLR-/-) gewählt. Um ein frühes Stadium der Atherosklerose zu untersuchen, wurden 10 Wochen alte Mäuse mit einer Western Diät für 6 Wochen gefüttert. Als klinisch relevanter Proteasominhibitor kam in diesen 6 Wochen Bortezomib zum Einsatz, allerdings in weitaus niedrigerer Dosis (50µg/kg Körpergewicht zweimalig pro Woche i.p.) als bei der Behandlung des Multiplen Myeloms. Die Arbeit beschreibt zunächst die Dosisfindung einer effektiven, jedoch nicht toxischen Dosis im Mausmodell und stellt die Reduktion früher atherosklerotischer Läsionen anhand von histologischen Schnitten durch die Aortenklappenebene dar. Die anti-inflammatorische Wirkung ließ sich insbesondere durch eine signifikante Verminderung der Serumspiegel von IL-6 und MCP-1 nachweisen. Zudem reduzierte Bortezomib die Lipidperoxidation und die Expression der Nox4-Untereinheit der NADPH-Oxidase. Die Untersuchung des aortalen Expressionsprofils mittels eines mRNA Microarrays offenbarte eine Dysregulation von Adhäsionsmolekülen, inflammatorischen Mediatoren und der oxidativen Stressantwort, welche durch die niedrigdosierte Bortezomib-Behandlung in Richtung des Expressionsprofils der gesunden Kontrollen verändert werden konnte. Interessanterweise war die Reduktion der atherosklerotischen Läsionen durch Bortezomib unabhängig von den Mausmodell-typisch hohen Cholesterol- und Triglyzerid-Spiegeln, was die Bedeutung der anti-inflammatorischen und anti-oxidativen Wirkungen niedrigdosierter Proteasominhibition unterstreicht.

Originalpublikation 1

Wilck N, Fechner M, Dreger H, Hewing B, Arias A, Meiners S, Baumann G, Stangl V, Stangl K and Ludwig A. Attenuation of early atherogenesis in low-density lipoprotein receptor-deficient mice by proteasome inhibition. ***Arteriosclerosis, thrombosis, and vascular biology***. 2012;32:1418-26. https://doi.org/10.1161/ATVBAHA.112.249342

Nachfolgend die Zusammenfassung (Abstract), reproduziert aus der Originalveröffentlichung:

Objective: Low and nontoxic proteasome inhibition has anti- inflammatory, antiproliferative, and antioxidative effects on vascular cells in vitro and in vivo. We hypothesized that low- dose inhibition of the proteasome could provide antiatherogenic protection. The present study investigated the effect of low- dose proteasome inhibition on early lesion formation in low- density lipoprotein receptor–deficient mice fed a Western- type diet.

Methods and Results: Male low- density lipoprotein receptor–deficient mice, 10 weeks old, were fed a Western- type diet for 6 weeks with intraperitoneal injections of bortezomib or solvent. Bortezomib was injected at a dose of 50 mg/kg body weight. Cholesterol plasma levels were not affected by bortezomib treatment. En face Oil Red O staining of aortae and aortic root cryosections demonstrated significant reduction of atherosclerotic lesion coverage in bortezomib- treated animals. Bortezomib significantly reduced vascular cellular adhesion molecule-1 expression and macrophage infiltration as shown by histological analysis. Bortezomib treatment resulted in a significant reduction of superoxide content, lipid peroxidation and protein oxidation products, serum levels of monocyte chemoattractant protein-1, and interleukin-6. Gene expression microarray analysis showed that expressional changes induced by Western- type diet were attenuated by treatment with low- dose bortezomib.

Conclusion: Low- dose proteasome inhibition exerts antioxidative and anti- inflammatory effects and attenuates development of atherosclerotic lesions in low- density lipoprotein receptor–deficient mice.

novel deubiquitinating enzyme in the vasculature, attenuates NF-kappaB activation. *Arterioscler Thromb Vasc Biol*. 2007;27:2184–2190.
19. Stangl K, Stangl V. The ubiquitin-proteasome pathway and endothelial (dys)function. *Cardiovasc Res*. 2010;85:281–290.
20. Dantuma NP, Lindsten K, Glas R, Jellne M, Masucci MG. Short-lived green fluorescent proteins for quantifying ubiquitin/proteasome-dependent proteolysis in living cells. *Nat Biotechnol*. 2000;18:538–543.
21. Dreger H, Westphal K, Weller A, Baumann G, Stangl V, Meiners S, Stangl K. Nrf2-dependent upregulation of antioxidative enzymes: a novel pathway for proteasome inhibitor-mediated cardioprotection. *Cardiovasc Res*. 2009;83:354–361.
22. Griendling KK, Sorescu D, Ushio-Fukai M. NAD(P)H oxidase: role in cardiovascular biology and disease. *Circ Res*. 2000;86:494–501.
23. Herrmann J, Saguner AM, Versari D, Peterson TE, Chade A, Olson M, Lerman LO, Lerman A. Chronic proteasome inhibition contributes to coronary atherosclerosis. *Circ Res*. 2007;101:865–874.
24. Chade AR, Herrmann J, Zhu X, Krier JD, Lerman A, Lerman LO. Effects of proteasome inhibition on the kidney in experimental hypercholesterolemia. *J Am Soc Nephrol*. 2005;16:1005–1012.
25. Tedgui A, Mallat Z. Cytokines in atherosclerosis: pathogenic and regulatory pathways. *Physiol Rev*. 2006;86:515–581.
26. Nencioni A, Schwarzenberg K, Brauer KM, Schmidt SM, Ballestrero A, Grünebach F, Brossart P. Proteasome inhibitor bortezomib modulates TLR4-induced dendritic cell activation. *Blood*. 2006;108:551–558.
27. Ogura M, Ayaori M, Terao Y, Hisada T, Iizuka M, Takiguchi S, Uto-Kondo H, Yakushiji E, Nakaya K, Sasaki M, Komatsu T, Ozasa H, Ohsuzu F, Ikewaki K. Proteasomal inhibition promotes ATP-binding cassette transporter A1 (ABCA1) and ABCG1 expression and cholesterol efflux from macrophages in vitro and in vivo. *Arterioscler Thromb Vasc Biol*. 2011;31:1980–1987.
28. Fukai T. Targeting proteasome worsens atherosclerosis. *Circ Res*. 2007;101:859–861.
29. Ludwig A, Meiners S. Targeting of the proteasome worsens atherosclerosis? *Circ Res*. 2008;102:e37.
30. Van Herck JL, De Meyer GR, Martinet W, Bult H, Vrints CJ, Herman AG. Proteasome inhibitor bortezomib promotes a rupture-prone plaque phenotype in ApoE-deficient mice. *Basic Res Cardiol*. 2010;105:39–50.
31. Meiners S, Laule M, Rother W, Guenther C, Prauka I, Muschick P, Baumann G, Kloetzel PM, Stangl K. Ubiquitin-proteasome pathway as a new target for the prevention of restenosis. *Circulation*. 2002;105:483–489.

2.2 Immunoproteasome subunit ss5i/LMP7-deficiency in atherosclerosis

In dieser Studie wurde die Fragestellung untersucht, inwiefern die genetische Defizienz der immunoproteasomalen Untereinheit β5i/LMP7 das Ubiqutin-Proteasom-System (UPS) in Makrophagen sowie die frühe und späte Atherosklerose im LDLR-/- Mausmodell beeinflusst.

Der zugrundeliegenden Fragestellung gehen zwei wichtige Erkenntnisse zur Pathophysiologie der Atherosklerose voraus: erstens die bereits diskutierten Beobachtungen, dass die Atherosklerose durch eine chronisch-inflammatorische Reaktion der Gefäßwand[6, 7] sowie durch oxidativen Stress[71] gekennzeichnet ist. Oxidativer Stress führt zur Modifikation von zellulären Proteinen mit verstärkter Notwendigkeit der proteasomalen Degradation dieser geschädigten und dysfunktionalen Proteine[84].
Die zweite Grundlage ist das Wissen um den besonderen Aufbau des Proteasoms unter Bedingungen der Inflammation und oxidativem Stress. Unter dem Einfluss von Zytokinen (z.B. Interferon-γ, TNF-α) werden anstelle der konstitutiven katalytischen Untereinheiten sogenannte immunoproteasomale Untereinheiten (β5i/LMP7, β1i/LMP2 and β2i/MECL-1) exprimiert und in das 20S Proteasom eingebaut[85-88]. Von Bedeutung ist das Immunoproteasom insbesondere bei der Herstellung antigener Peptide für die MHC Klasse I-abhänge Antigenpräsentation[85, 89, 90]. Vorarbeiten anderer Arbeitsgruppen haben zudem die Frage diskutiert, ob das Immunoproteasom von besonderer Bedeutung für die Proteinhomöostase bei Zytokin-induziertem oxidativen Stress ist und das Immunoproteasom polyubiquitinierte Proteine womöglich schneller abbaut – mit gegensätzlichen Ergebnissen[91, 92]. Die pharmakologische Inhibition der β5i/LMP7 Untereinheit zeigte vorteilhafte Effekte in verschiedenen experimentellen Modellen inflammatorischer Erkrankungen[93-95].

Für diese Studie wurden β5i/LMP7-defiziente LDLR-/- Mäuse („Doppelknockout“) gezüchtet, mit β5i/LMP7-exprimierenden LDLR-/- („Einfachknockout“) verglichen und ausschließlich Wurfgeschwister (Engl. *Littermates*) verwendet. Die Arbeit zeigt, dass die β5i/LMP7-Defizienz die Atherosklerose in LDLR-/- Mäusen weder zu einem frühen (d.h. nach 6 Wochen Western Diät) noch zu einem späteren Zeitpunkt (d.h. nach 24 Wochen Western Diät) verstärkt. Auch die *in vitro* Polarisation von Knochenmarksmakrophagen (Engl. *bone marrow-derived macrophages*) war nicht unterschiedlich zwischen β5i/LMP7-defizienten und -exprimierenden Makrophagen. Interessanterweise konnten auch keine wesentlichen, durch den β5i/LMP7-Knockout verursachten Änderungen der proteasomalen proteolytischen Aktivitäten festgestellt werden. Insbesondere war ersichtlich, dass die β5i/LMP7-Defizienz durch den Einbau der konstitutiven β5i-Isoform kompensiert wurde, was zum einen die Bedeutung intermediärer Proteasomformen und zum anderen enorme Plastizität des Proteasoms hinsichtlich seiner Zusammensetzung unterstreicht.

Originalpublikation 2

Hewing B, Ludwig A, Dan C, Potzsch M, Hannemann C, Petry A, Lauer D, Gorlach A, Kaschina E, Muller DN, Baumann G, Stangl V, Stangl K and **Wilck N**. Immunoproteasome subunit ss5i/LMP7-deficiency in atherosclerosis. ***Scientific reports***. 2017;7:13342. https://doi.org/10.1038/s41598-017-13592-w

Nachfolgend die Zusammenfassung (Abstract), reproduziert aus der Originalveröffentlichung:

Management of protein homeostasis by the ubiquitin-proteasome system is critical for atherosclerosis development. Recent studies showed controversial results on the role of immunoproteasome (IP) subunit β5i/LMP7 in maintenance of protein homeostasis under cytokine induced oxidative stress. The present study aimed to investigate the effect of β5i/LMP7-deficiency on the initiation and progression of atherosclerosis as a chronic inflammatory, immune cell driven disease. LDLR−/−LMP7−/− and LDLR−/− mice were fed a Western-type diet for either 6 or 24 weeks to induce early and advanced stage atherosclerosis, respectively. Lesion burden was similar between genotypes in both stages. Macrophage content and abundance of polyubiquitin conjugates in aortic root plaques were unaltered by β5i/LMP7-deficiency. In vitro experiments using bone marrow-derived macrophages (BMDM) showed that β5i/LMP7-deficiency did not influence macrophage polarization or accumulation of polyubiquitinated proteins and cell survival upon hydrogen peroxide and interferon-γ treatment. Analyses of proteasome core particle composition by Western blot revealed incorporation of standard proteasome subunits in β5i/LMP7-deficient BMDM and spleen. Chymotrypsin-, trypsin- and caspase-like activities assessed by using short fluorogenic peptides in BMDM whole cell lysates were similar in both genotypes. Taken together, deficiency of IP subunit β5i/LMP7 does not disturb protein homeostasis and does not aggravate atherogenesis in LDLR−/− mice.

www.nature.com/scientificreports

OPEN

Immunoproteasome subunit ß5i/ LMP7-deficiency in atherosclerosis

Bernd Hewing[1,2,7], Antje Ludwig[1,2], Cristian Dan[1,2], Max Pötzsch[1,2], Carmen Hannemann[1,2], Andreas Petry[3,4], Dilyara Lauer[5], Agnes Görlach[3,4], Elena Kaschina[5], Dominik N. Müller[2,6,7,8], Gert Baumann[1], Verena Stangl[1,2], Karl Stangl[1,2] & Nicola Wilck[1,2,6,8]

Received: 30 November 2016
Accepted: 17 August 2017
Published online: 17 October 2017

Management of protein homeostasis by the ubiquitin-proteasome system is critical for atherosclerosis development. Recent studies showed controversial results on the role of immunoproteasome (IP) subunit β5i/LMP7 in maintenance of protein homeostasis under cytokine induced oxidative stress. The present study aimed to investigate the effect of β5i/LMP7-deficiency on the initiation and progression of atherosclerosis as a chronic inflammatory, immune cell driven disease. LDLR$^{-/-}$LMP7$^{-/-}$ and LDLR$^{-/-}$ mice were fed a Western-type diet for either 6 or 24 weeks to induce early and advanced stage atherosclerosis, respectively. Lesion burden was similar between genotypes in both stages. Macrophage content and abundance of polyubiquitin conjugates in aortic root plaques were unaltered by β5i/LMP7-deficiency. *In vitro* experiments using bone marrow-derived macrophages (BMDM) showed that β5i/LMP7-deficiency did not influence macrophage polarization or accumulation of polyubiquitinated proteins and cell survival upon hydrogen peroxide and interferon-γ treatment. Analyses of proteasome core particle composition by Western blot revealed incorporation of standard proteasome subunits in β5i/LMP7-deficient BMDM and spleen. Chymotrypsin-, trypsin- and caspase-like activities assessed by using short fluorogenic peptides in BMDM whole cell lysates were similar in both genotypes. Taken together, deficiency of IP subunit β5i/LMP7 does not disturb protein homeostasis and does not aggravate atherogenesis in LDLR$^{-/-}$ mice.

Dysregulation of the ubiquitin-proteasome system (UPS) has been associated with atherosclerosis development[1–3]. The UPS is essential for the intracellular degradation of proteins in all eukaryotic cells. Proteolytic degradation takes place in the 26 S core proteasome, a multicatalytic peptidase carrying standard chymotrypsin-like (β5 subunit), trypsin-like (β2 subunit) and caspase-like (β1 subunit) activities. Under cytokine stress these standard catalytic activities of the proteasome are replaced by distinct isoforms (β5i/LMP7, β1i/LMP2 and β2i/MECL-1), leading to the formation of the immunoproteasome (IP)[4]. Moreover, replacement of solely one or two standard β subunits results in the formation of intermediate-type proteasomes, which have been detected in various tissues[5]. Whereas non-immune cells predominantly express standard proteasomes, IPs are the predominant proteasomes in leukocytes. The IP is long known to mediate immune responses, as it efficiently generates peptides for MHC class I restricted antigen presentation[6].

An increasing number of reports indicate an important role of IP subunit β5i/LMP7 in inflammatory diseases. Hereditary inflammatory disorders have been linked to mutations in the β5i/LMP7 gene[7–10]. Selective pharmacological inhibition of β5i/LMP7 showed anti-inflammatory effects in several experimental inflammatory models[11–13]. Besides its function in immune responses, a recent study highlighted an involvement of β5i/LMP7 in the management of protein homeostasis under cytokine-induced oxidative stress[14]. It was shown that β5i/LMP7-deficiency leads to the formation of intracellular protein aggregates and aggravates experimental autoimmune encephalomyelitis. Interestingly, these finding were challenged by others using similar methods[15]. Yet,

[1]Medizinische Klinik m.S. Kardiologie und Angiologie, Charité-Universitätsmedizin Berlin, Campus Mitte, Berlin, Germany. [2]DZHK (German Centre for Cardiovascular Research), partner site Berlin, Berlin, Germany. [3]Experimental and Molecular Pediatric Cardiology, German Heart Center Munich, Technical University Munich, Munich, Germany. [4]DZHK (German Centre for Cardiovascular Research), partner site Munich, Munich, Germany. [5]Institute of Pharmacology, Center for Cardiovascular Research, Charité-Universitätsmedizin Berlin, Berlin, Germany. [6]Experimental and Clinical Research Center, a joint cooperation of Max Delbrück Center for Molecular Medicine and Charité Medical Faculty, Berlin, Germany. [7]Berlin Institute of Health (BIH), Berlin, Germany. [8]Max Delbrück Center for Molecular Medicine in the Helmholtz Association, Berlin, Germany. Correspondence and requests for materials should be addressed to N.W. (email: nicola.wilck@charite.de)

	6 weeks WD			24 weeks WD		
	LDLR$^{-/-}$	LDLR$^{-/-}$LMP7$^{-/-}$	*p*	LDLR$^{-/-}$	LDLR$^{-/-}$LMP7$^{-/-}$	*p*
Body weight, g	31.2 ± 1.5	29.4 ± 2.2	0.045	36.6 ± 4.5	34.6 ± 5.5	0.36
Body weight gain, g	6.6 ± 0.2	6.4 ± 0.8	0.732	12.1 ± 2.4	10.0 ± 3.9	0.323
TC, mg/dl	1318.7 ± 138.6	1281.2 ± 181.0	0.591	1289.5 ± 265.4	1398.4 ± 417.1	0.47
HDL-C, mg/dl	127.7 ± 23.4	135.6 ± 24.7	0.448	247.6 ± 74.6	247.1 ± 78.3	0.989
Non-HDL-C, mg/dl	1191.0 ± 135.6	1145.6 ± 168.3	0.494	1041.9 ± 232.8	1151.3 ± 376.4	0.417
Triglycerides, mg/dl	539.7 ± 165.7	708.2 ± 187.3	0.023	393.9 ± 155.6	482.4 ± 195.8	0.26

Table 1. Body weight and lipid levels. n = 11 per group, except LDLR$^{-/-}$LMP7$^{-/-}$ 24 weeks WD n = 12; data are shown as mean ± SD. Statistical analysis using unpaired *t*-test or Mann-Whitney *U* test. WD, Western-type diet; TC, total cholesterol; HDL-C, high-density lipoprotein cholesterol.

given its proposed significance for inflammation and cellular protein homeostasis, we questioned the impact of β5i/LMP7 on atherosclerosis development. Atherosclerosis represents an inflammatory, immune cell driven disease[16] and defective removal of protein aggregates was proposed to aggravate atherosclerosis development[17]. However, studies investigating the impact of β5i/LMP7-deficiency on atherosclerosis are currently not available.

Therefore, the present study aims at elucidating the effect of β5i/LMP7-deficiency on the composition and function of the UPS in macrophages and its consequences for atherosclerosis as a chronic inflammatory, immune cell driven disease.

Results

β5i/LMP7-deficient atherosclerosis mouse model. In order to study the effect of β5i/LMP7-deficiency on atherosclerosis, we generated low-density lipoprotein receptor-deficient and β5i/LMP7-deficient mice (LDLR$^{-/-}$LMP7$^{-/-}$); LDLR$^{-/-}$ littermate mice served as controls. Upon control diet for 6 or 24 weeks, respectively, serum levels of total cholesterol (TC), high-density lipoprotein cholesterol (HDL-C) and non-HDL-C were similar between both genotypes (Supplement Table S1). Serum levels of triglycerides were lower in LDLR$^{-/-}$LMP7$^{-/-}$ mice compared to LDLR$^{-/-}$ littermates solely at 6 weeks of control diet and were found to be equal at 24 weeks of control diet (Supplement Table S1). Serum glucose levels were similar between both genotypes (Fig. S1). Body weight was similar after 6 weeks of diet, but lower in the group of LDLR$^{-/-}$LMP7$^{-/-}$ mice after 24 weeks compared to LDLR$^{-/-}$ littermates (Supplement Table S1). β5i/LMP7-deficiency did not influence cardiac dimensions and function as assessed by echocardiography (Supplement Table S2).

Feeding of a high-fat Western-type diet (WD) for 6 or 24 weeks, respectively, resulted in hyperlipidemia with similar serum levels of TC, HDL-C, non-HDL-C, and glucose between both genotypes (Table 1, Fig. S1). LDLR$^{-/-}$LMP7$^{-/-}$ mice exhibited a trend to higher levels of triglycerides compared to LDLR$^{-/-}$ littermates, which was statistically significant solely after 6 weeks of WD (Table 1). Body weight was lower in LDLR$^{-/-}$ mice (statistically significant after 6 weeks of WD), while the actual body weight gain over the course of the WD did not differ between both genotypes (Table 1). Serum levels of lipid peroxidation products measured as thiobarbituric acid reactive substances (TBARS) were similar in both genotypes (Fig. S2).

β5i/LMP7-deficiency does not aggravate atherosclerotic lesion progression in LDLR$^{-/-}$ mice. LDLR$^{-/-}$LMP7$^{-/-}$ and LDLR$^{-/-}$ littermate mice developed early lesions in atherosclerosis-prone sites such as the aortic root and arch after being fed a WD for 6 weeks. Mice fed a WD over 24 weeks exhibited advanced lesions in the entire aorta, as shown by *en face* and histologic analyses of the aortic root and the *truncus brachiocephalicus* (Figs 1A and S3). Lesion quantification did not reveal significant differences in atherosclerotic plaque burden between both genotypes at either stage of atherosclerosis (Fig. 1A). Plaque macrophage (Mac-2) and T cell (CD4) content in advanced aortic root plaques did not differ between both genotypes (Figs 1B and S4). Cells associated with strong FK2 staining, a marker for accumulation of ubiquitinated proteins, were detectable in macrophage-rich areas and were not significantly affected by β5i/LMP7-deficiency (Fig. 1B). Necrotic core size was similar between both genotypes (Fig. 1B).

β5i/LMP7-deficiency does not influence macrophage polarization and stress response in BMDM of LDLR$^{-/-}$ mice. Macrophage activation states have been shown to differentially influence atherosclerosis[18]. Therefore, we assessed the influence of β5i/LMP7-deficiency on BMDM polarization towards M1 and M2 phenotypes induced by IFN-γ and IL-4, respectively. Figure 2A shows that IFN-γ induced mRNA levels of the M1 marker genes tumor necrosis factor-α (TNF-α) and monocyte chemoattractant protein-1 (MCP-1) to a similar extent in BMDM from LDLR$^{-/-}$LMP7$^{-/-}$ and LDLR$^{-/-}$ littermate mice. Likewise, superoxide anion production of IFN-γ stimulated BMDM was not affected by β5i/LMP7-deficiency (Fig. 2B). IL-4 stimulation induced mRNA expression of M2 marker arginase-1 similarly in BMDM of both genotypes (Fig. 2A).

Next, we determined the influence of cytokine-stimulation and oxidative stress on the content of polyubiquitin conjugates in BMDM by Western blot. The amount of polyubiquitinated proteins was not changed after IFN-γ stimulation up to 24 hours in BMDM of both genotypes (Figs 2C and S5A). After hydrogen peroxide (H_2O_2) challenge, we detected a similar increase in polyubiquitinated proteins in BMDM of both genotypes (Figs 2D and S5B). BMDM survival following H_2O_2 challenge was similar for both genotypes (Fig. 2E).

Impact of β5i/LMP7-deficiency on proteasome composition and proteolytic activity in cells and tissues of LDLR$^{-/-}$ mice. To determine the impact of β5i/LMP7-deficiency on proteasome

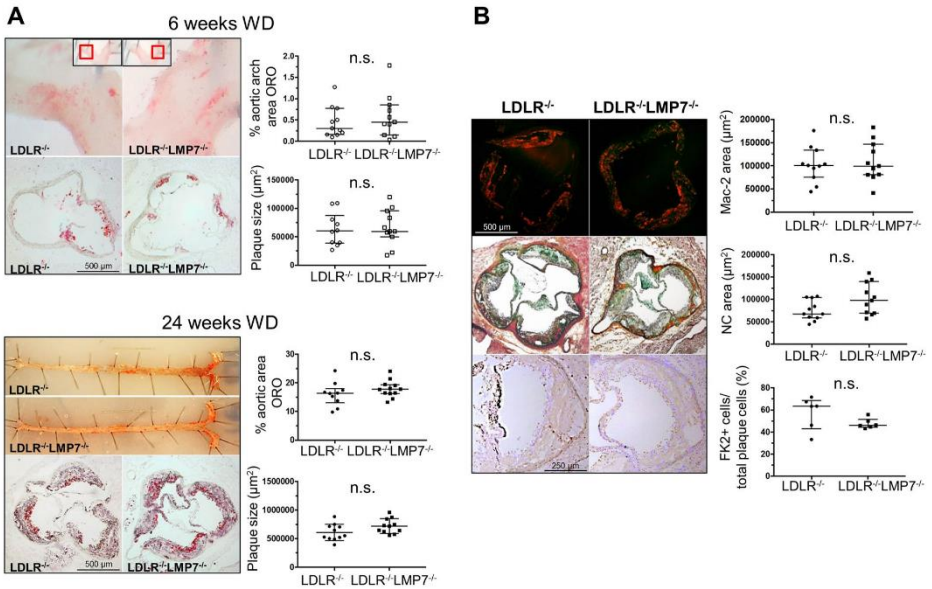

Figure 1. β5i/LMP7-deficiency does not aggravate atherosclerotic lesion progression in LDLR$^{-/-}$ mice. LDLR$^{-/-}$LMP7$^{-/-}$ and LDLR$^{-/-}$ littermate mice were fed a high-fat Western-type diet (WD) for either 6 or 24 weeks to induce early and advanced stage atherosclerosis, respectively. (**A**) Representative *en face* stainings of aortic arch/whole aorta (upper rows) and Oil Red O stainings with hematoxylin counterstain of aortic root cross-sections (bottom rows) for early (upper panels) and advanced (lower panels) stage atherosclerosis with quantification of lesion sizes. (**B**) Representative stainings and quantifications of (upper row) macrophages (MAC-2), (middle row) necrotic core (NC; Movat pentachrome staining), and (bottom row) ubiquitinated proteins (FK2; magnification: 10x) of aortic root cross-sections of advanced stage atherosclerosis. Data in graphs are presented as individual values with median and interquartile ranges indicated. n.s. = statistically non-significant. Unpaired *t*-test (Welch test for unequal variances) or Mann-Whitney *U* test.

subunit composition, we performed Western blots in BMDM, spleen and liver lysates of LDLR$^{-/-}$LMP7$^{-/-}$ and LDLR$^{-/-}$ littermate mice. In BMDM lysates from LDLR$^{-/-}$ mice we detected expression of all standard and IP β subunits (Fig. 3A). Standard proteasome subunits β5, β2, β1 and mature forms of IP subunit β1i were detectable in β5i/LMP7-deficient BMDM (under native and IFN-γ stimulated conditions) and in splenic lysates of β5i/LMP7-deficient mice (Fig. 3A). Mature forms of IP subunit β2i were detectable in splenic lysates of β5i/LMP7-deficient mice. In β5i/LMP7-deficient fibroblasts standard proteasome subunits β5, β2, β1 and induction of IP subunit β1i after IFN-γ stimulation were detectable (Fig. S6). Enhanced bands for β5i/LMP7 were observable in spleens and livers of LDLR$^{-/-}$ mice fed a WD compared to tissues from CD fed mice (baseline) indicative of a systemic inflammatory response under WD (Figs 3A and S6).

To examine the composition of β subunits incorporated into proteasomal core particles, we isolated 26 S proteasomes from BMDM and splenic lysates using native gel electrophoresis and determined their subunit composition by Western blot (Fig. 3B). BMDM and spleens of LDLR$^{-/-}$ mice assembled IP subunits β5i/LMP7, β2i, β1i and standard proteasome subunits β1 and β2, indicating the presence of immuno- and intermediate proteasomes. In proteasomes of β5i/LMP7-deficient BMDM and spleen standard subunits β5, β2, β1 and IP subunit β1i (and β2i in spleen) were detectable indicating the presence of standard and intermediate proteasomes. Incorporated β2i was hardly detectable in β5i/LMP7-deficient BMDM. Except for β5i/LMP7, mRNA expression levels of proteasome subunits in BMDM did not differ between both genotypes (Fig. S7).

Next, we determined whether alterations in proteasomal composition ultimately lead to alterations in proteasomal proteolytic activities. However, chymotrypsin-, trypsin- and caspase-like activities were similar in BMDM of both genotypes, as measured by using short fluorogenic peptides in BMDM whole cell lysates (Fig. 3C).

Discussion

The major finding of the current study is that the deficiency of the IP subunit β5i/LMP7 does not aggravate initiation and progression of atherosclerosis in LDLR$^{-/-}$ mice. This is of particular interest, since β5i/LMP7 expression was suggested to be required for the efficient elimination of damaged proteins after cytokine induced oxidative stress[14]. However, this relationship was questioned by others[15], leading to a debate on the role of β5i/LMP7 in the pathogenesis of inflammatory disorders[19]. The present study contributes to this debate, as our observations do

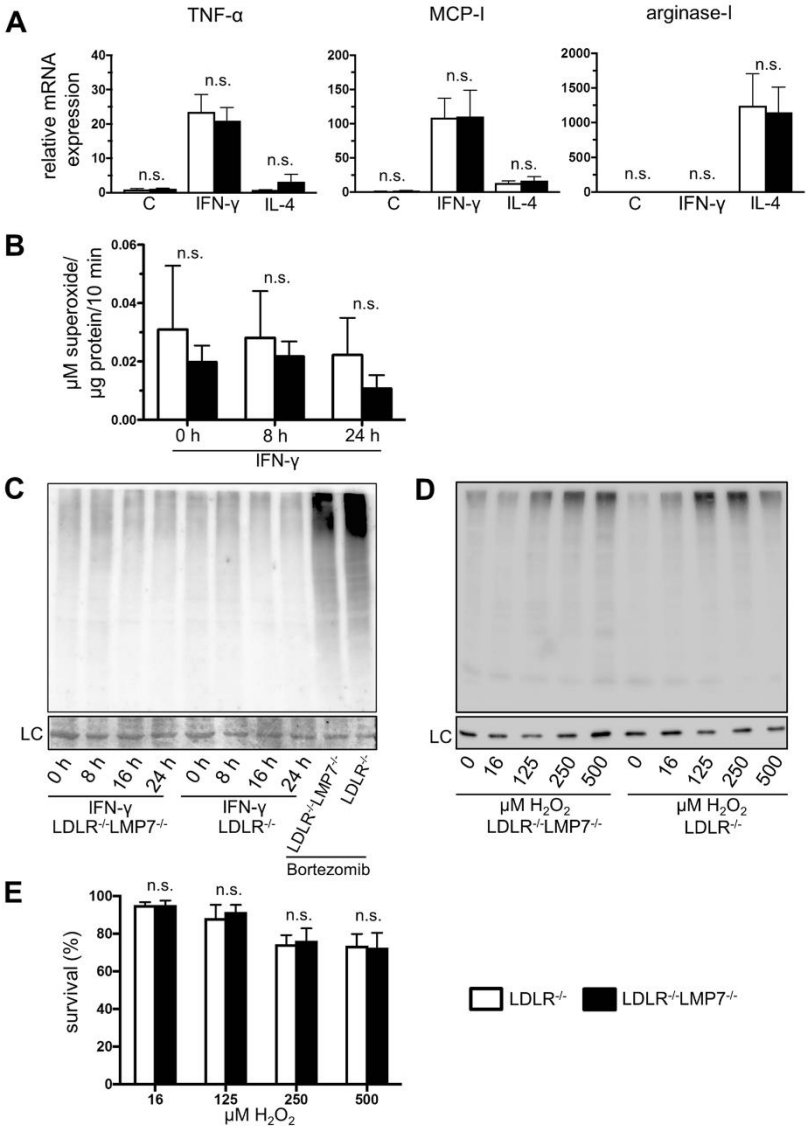

Figure 2. β5i/LMP7-deficiency does not influence macrophage polarization and stress response in BMDM of LDLR$^{-/-}$ mice. BMDM isolated from LDLR$^{-/-}$LMP7$^{-/-}$ and LDLR$^{-/-}$ littermate mice: (**A**) M1/M2 polarization – mRNA expression of tumor necrosis factor-α (TNF-α), monocyte chemoattractant protein-1 (MCP-1) and arginase-1 determined by quantitative real-time RT-PCR after treatment of BMDM with IFN-γ (100 U/ml) and IL-4 (4 U/ml) over 6 hours for M1 and M2 macrophage phenotype polarization, respectively; C = untreated cells; graphs show fold-change in mRNA expression levels relative to untreated BMDM of LDLR$^{-/-}$ mice; n = 5 experiments. Unpaired *t*-test (Welch test for unequal variances) or Mann-Whitney *U* test. (**B**) Superoxide production of IFN-γ-treated (100 U/ml) BMDM determined by electron paramagnetic resonance (EPR) technique; n = 5–7 per group. Two-way ANOVA followed by Sidak's multiple comparisons test. (**C**) Representative Western blot with anti-ubiquitin antibody of lysates of IFN-γ (100 U/ml) treated BMDM; Bortezomib (5 ng/ml) treated BMDM served as positive controls; n = 4 experiments; LC indicates amidoblack staining as loading control. (**D**) Representative Western blot with anti-ubiquitin antibody of lysates of BMDM

after treatment with hydrogen peroxide (H_2O_2) over 1 hour; n = 3 experiments. LC indicates GAPDH staining as loading control. (**E**) Survival of BMDM treated with H_2O_2 over 1 hour; n = 4 experiments. Kruskal-Wallis test with post hoc comparison by Dunn's multiple comparison test. Data in graphs are presented as mean ± SEM. n.s. = statistically non-significant.

not point to an impact of β5i/LMP7-deficiency on atherosclerosis, which is considered a chronic inflammatory vascular disease[20].

It has been hypothesized that the UPS is dysregulated in atherosclerosis[20,21] and that the accumulation of dysfunctional proteins is associated with cell death within atherosclerotic lesions[3]. Given the proposed importance of β5i/LMP7 for the removal of damaged proteins[14], aggravation of atherosclerosis in β5i/LMP7-deficient mice would have been conceivable. However, we did not detect augmented ubiquitin accumulation in plaques of β5i/LMP7-deficient mice. In line with previous reports[3,20], ubiquitin enrichment was associated with macrophages, but was equally present in the plaques of both genotypes (considering the limited sample size). Furthermore, the similar extent of necrotic cores in atherosclerotic lesions of both genotypes does not indicate increased cell death in β5i/LMP7-deficient mice. Finally, atherosclerotic plaque size was not affected by β5i/LMP7-deficiency for early or advanced stage atherosclerosis. Thus, these findings do not favor the perception that β5i/LMP7-containing proteasomes have a higher capacity to degrade polyubiquitinated proteins compared to standard proteasomes.

Recently, beneficial effects of β5i/LMP7-deficiency on obesity and glucose homeostasis have been described in the presence of mild hypercholesteremia[22]. β5i/LMP7-deficient mice fed a high fat diet showed an improved glucose intolerance, lower triglyceride levels and a decreased weight gain when compared to C57BL/6 wild-type mice[22]. Such metabolic alterations are potentially important to atherogenesis. However, in our study β5i/LMP7-deficiency on a $LDLR^{-/-}$ background did not lead to significant alterations of glucose levels. Also, weight gain during short and long term high-fat WD was not affected by β5i/LMP7-deficiency. We observed higher triglyceride levels in β5i/LMP7-deficient mice fed a WD over 6 weeks; triglycerides are associated with risk of cardiovascular disease in humans. However, atherosclerosis outcome was not affected by β5i/LMP7-deficiency in our model. We cannot exclude the possibility that a potential impact of elevated triglycerides on atherogenesis has been outweighed by other (yet unidentified) effects of β5i/LMP7-deficiency. Thus, further in depth characterization of lipoprotein forms in β5i/LMP7-deficient models should be performed in future studies.

Macrophages play a key role in atherosclerotic lesion formation, progression and plaque destabilization. Depending on the cytokine milieu within atherosclerotic lesions macrophages are polarized towards distinct subsets, which critically affect plaque development[18]. It was recently reported that β5i/LMP7-deficiency and selective inhibition of β5i/LMP7 promotes M2 polarization of alveolar macrophages[23]. Our data derived from BMDM do not suggest an impact of β5i/LMP7 on M1 and M2 polarization as well as on macrophage survival under oxidative stress.

In line with previous reports, we observed that β5i/LMP7-deficiency leads to the formation of proteasome subtypes with β5i/LMP7 being replaced by its corresponding standard subunit β5[24,25]. Structure and function of various proteasome subpopulations and -types have been investigated in different species and organs[24,26–29]. Studies comparing the enzymatic activities of different isolated proteasome subtypes *in vitro* using fluorogenic peptide substrates revealed varying activities and differential cleavage characteristics depending on the proteasomal subunit composition[5,25,27]. However, despite differences in subunit composition we found similar proteolytic activities when measured in BMDM whole cell lysates of both genotypes using short fluorogenic peptides. In addition, the detection of similar amounts of accumulated polyubiquitinated proteins in hydrogen peroxide stimulated BMDM of both genotypes further confirmed an equal capacity for the removal of damaged proteins under oxidative stress; taken together, these observations are in accordance with the findings of Nathan *et al.*[15].

In conclusion, deficiency of IP subunit β5i/LMP7 does not alter initiation and progression of atherosclerosis in $LDLR^{-/-}$ mice. Our data indicate that protein homeostasis in atherosclerosis is not disturbed by deficiency of β5i/LMP7.

Methods

Materials. Unless otherwise specified, all reagents and media were purchased from Sigma Chemicals, Germany. Bortezomib was kindly provided by Millenium Pharmaceuticals.

Animal experiments. Animal experiments were approved by the local authority (Landesamt für Gesundheit und Soziales, Berlin, Germany) and were performed according to institutional guidelines.

Low-density lipoprotein receptor-deficient ($LDLR^{-/-}$) mice (B6.129S7-*Ldlr*^{tm1Her}/J; JAX Mice, Boston) and β5i/$LMP7^{-/-}$ mice (kindly provided by Antje Voigt, Department of Biochemistry, Charité-Universitätsmedizin Berlin, Germany) were crossed to generate double heterozygous mice. Both, $LDLR^{-/-}$ and β5i/$LMP7^{-/-}$ mice were originally backcrossed at least 10 times to C57BL/6 mice. The resulting F1 generation was crossed and the offsprings genotyped for LDLR and β5i/LMP7. Male mice homozygous for LDLR-deficiency ($LDLR^{-/-}$) or homozygous for LDLR-deficiency and β5i/LMP7-deficiency ($LDLR^{-/-}LMP7^{-/-}$) were fed a high fat diet containing 21% butterfat, 17% casein, and 0.21% cholesterol (Western-type diet, Ssniff, Soest, Germany) for 6 or 24 weeks *ad libitum* beginning from 10 weeks of age. Mice of both genotypes fed a low-fat control diet (CD) served as additional controls. General condition and body weight were monitored regularly.

For harvesting, mice were fasted for two hours, anesthetized with isoflurane- and euthanized by blood withdrawal. After perfusion with PBS, heart and aorta were dissected under a stereomicroscope (Leica), shock-frozen in liquid nitrogen and stored at −80 °C or fixed in formalin. Livers and spleens were collected, shock-frozen and stored at −80 °C.

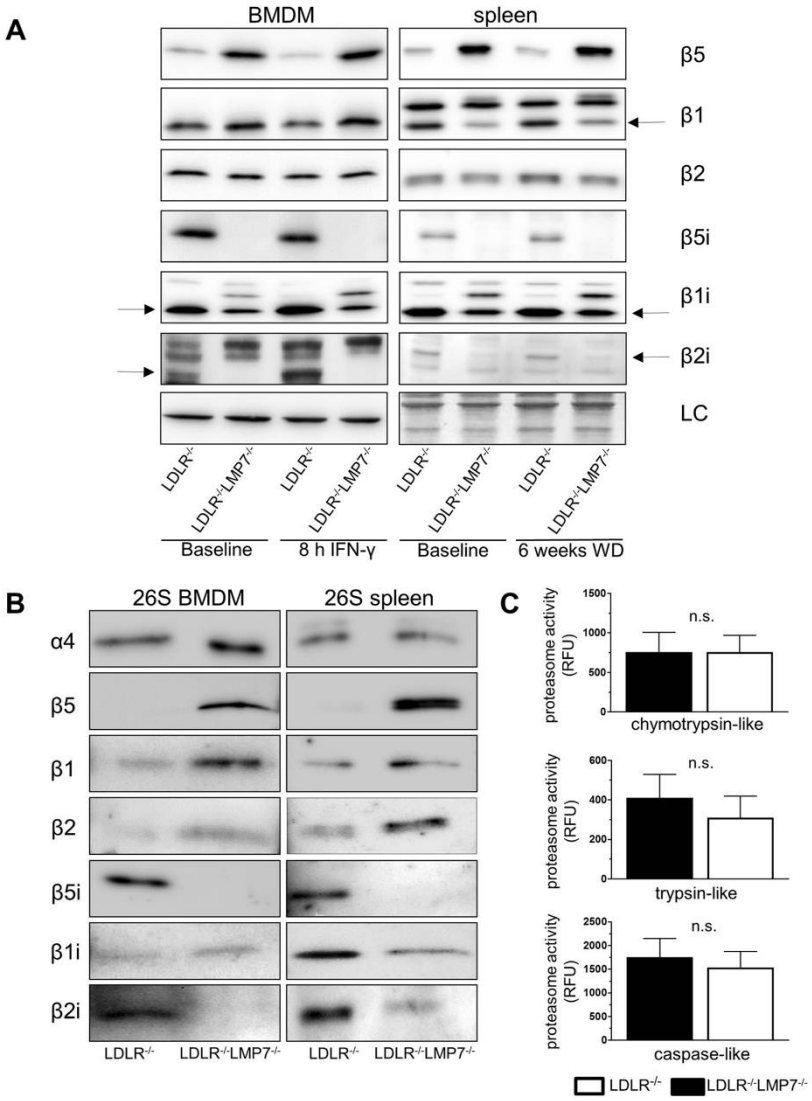

Figure 3. Impact of β5i/LMP7-deficiency on proteasome composition and proteolytic activity in cells and tissues of LDLR$^{-/-}$ mice. **(A)** Western blot analysis of standard proteasome (β1, β2, and β5) and immunoproteasome (β1i, β2i, and β5i) subunit expression in BMDM of LDLR$^{-/-}$LMP7$^{-/-}$ and LDLR$^{-/-}$ at baseline and after treatment with IFN-γ (100 U/ml) over 8 hours (left panel). Right panel shows Western blot analyses of pooled spleen protein samples from LDLR$^{-/-}$LMP7$^{-/-}$ and LDLR$^{-/-}$ mice at baseline and after feeding a high-fat Western-type diet (WD) over 6 weeks (n = 11 mice per group). LC indicates actin staining (for BMDM) or amidoblack staining (for spleen) as loading controls. **(B)** Representative Western blots of standard proteasome and immunoproteasome subunits of isolated 26 S proteasome derived from murine LDLR$^{-/-}$LMP7$^{-/-}$ and LDLR$^{-/-}$ BMDM (left panel) and spleen (right panel) lysates. **(C)** Chymotrypsin-, trypsin- and caspase-like proteasome activities (expressed as relative fluorescence units, RFU) of murine LDLR$^{-/-}$LMP7$^{-/-}$ and LDLR$^{-/-}$ BMDM; n = 4 experiments. Unpaired *t*-test or Mann-Whitney *U* test. Data in graphs are presented as mean ± SEM.

Echocardiography. Transthoracic Doppler echocardiography was performed in mice anesthetized with isoflurane (2%) with the use of the high-resolution imaging system Vevo 770 (VisualSonics). M-mode tracings were recorded from the short-axis view of the left ventricle (LV) at the level of the papillary muscles with two-dimensional image guidance through the anterior and posterior walls. Left ventricular internal dimensions were measured at the end of diastole (LVIDd) and systole (LVIDs). Ejection fraction (EF) and fractional shortening (FS) were calculated from linear measurements of LVIDd and LVIDs.

Measurement of serum glucose and lipids. Serum glucose levels were measured using a Fuji DRI-CHEM NX500 system (Fujifilm). Serum total cholesterol and triglyceride concentrations were measured by colorimetric enzymatic assay (CHOL-PAP, and TG GPO-PAP, Roche-Diagnostics). High-density lipoprotein cholesterol concentration was separated by the phosphotungstate-magnesium precipitation technique. Briefly, 100 µl of serum were supplemented with 10 µl sodium phosphotungstate solution (40 g of phosphotungstic acid per liter in 160 mM NaOH) and 5 µl 1 M MgCl2. After mixing and incubation for 2 hours; samples were centrifuged (1500 g, 30 minutes, 4 °C) and cholesterol was determined in the supernatant.

Measurement of thiobarbituric-acid reactive substances (TBARS). Lipid hydroperoxides were determined in mouse serum by spectrophotometric measurement of formation of thiobarbituric-acid reactive substances (TBARS), as described previously[30].

Staining and analysis of atherosclerotic lesions. The dissected aorta was fixed in formalin overnight, opened longitudinally under a stereomicroscope, and pinned flat on a silicon gel. For *en face* aortic lesion analysis, pinned aortae were stained with Oil Red O (Sigma-Aldrich) and digitally photographed at standardized magnification and illumination. Total aortic area and atherosclerotic lesion area were determined using ImageJ software. Atherosclerotic lesion area was calculated as percentage of total *en face* aortic area.

Cross sections of formalin-fixed, paraffin-embedded brachiocephalic arteries (BCA, *truncus brachiocephalicus*) were stained with the original Movat pentachrome according to the manufacturers' protocol (Morphisto). Frozen acetone-fixed cross sections (5 µm) of aortic roots were stained with Oil Red O (counterstained with hematoxylin) or with Movat pentachrome. Sections were digitally photographed under standardized conditions using Zeiss AxioCam MrC and analyzed using Zeiss AxioVision software. Absolute plaque size (in μm^2) was determined as well as absolute cell free necrotic core area. Plaque macrophages and ubiquitinated proteins were detected in cross sections by immunohistochemistry using anti-Mac-2 antibody (Cedarlane Laboratories), or anti-FK2 ubiquitin monoclonal antibody (Enzo Life Sciences), respectively. Biotin-conjugated goat anti-mouse IgG (Jackson Immunoresearch) was used as secondary antibody, followed by 10 minutes incubation with streptavidin-peroxidase (Zymed) and visualization with diaminobenzidine (DAB, Zymed). For macrophage content Mac-2 positive plaque area was determined (in μm^2). After ubiquitin staining, sections were stained with 4', 6-diamidino-2-phenylindole (DAPI) to visualize cell nuclei. Images of 3–4 regions of interest per plaque were analyzed and the mean percentage of cells with strong ubiquitin signal was calculated. CD4 immunofluorescence for analysis of plaque T cells was performed using rat anti-mouse anti-CD4 (BD Biosciences) and Cy3-conjugated donkey anti-rat IgG (Jackson Immunoresearch) as secondary antibody. Nuclei were stained with DAPI. Sections were photographed with a Zeiss Axioplan-2 microscope and HrC AxioCam, plaque area was measured using AxioVison software, CD4 cell numbers per plaque area were counted.

Cell Culture and treatments. Primary bone marrow derived macrophages (BMDM) were recovered from bone marrow suspensions of tibia and femur of $LDLR^{-/-}LMP7^{-/-}$ and $LDLR^{-/-}$ littermate mice as described previously[31]. For differentiation in macrophages, cells were incubated in RPMI-1640 (Gibco Life Technologies) containing 10% fetal calf serum, 1% penicillin/streptomycin, and 10% of L929-conditioned RPMI (as a source of Macrophage Colony Stimulating Factor, M-CSF) for 7 days. Macrophage differentiation was verified by flow cytometry via staining for CD45 (APC, BioLegend), F4/80 (PE, Abcam) and C11b (V450, BD Horizon) on day 7. Mouse ear fibroblasts have been isolated and cultivated as described previously[32].

For individual experiments, BMDM or fibroblasts were treated with 100 U/ml IFN-γ (recombinant, Biomol) for varying times or with medium containing varying concentrations of hydrogen peroxide (H_2O_2; Sigma) at 37 °C for 60 minutes. For survival analyses, H_2O_2-treated BMDM were harvested by scraping, and counted in a hemocytometer. Numbers of survived cells were expressed as percentage of cell count of the corresponding untreated control. For polarization of macrophages into the M1 and M2 state, BMDMs were incubated with 100 U/ml IFN-γ or 5 U/ml IL-4 (Promokine) at 37 °C for 6 hours, respectively.

Quantitative real-time RT-PCR. RNA was isolated using RNeasy kit (Qiagen) according to the manufacturer's instructions. 500 ng of total RNA was reversed-transcribed with random hexamers (TIB Molbiol) using Reverse Transcriptase Kit (Invitrogen). TaqMan assays (Applied Biosystems) were used to quantify the expression of tumor necrosis factor-α (TNF-α; Mm00443260_g1), monocyte chemoattractant protein-1 (MCP-1; Mm00441242_m1), arginase-1 (Mm00475988_m1), and proteasome subunits β1 (Mm01245590_g1), β2 (Mm00650844_g1), β5 (Mm01615821_g1), β1i/LMP2 (Mm00479004_m1), β5i/LMP7 (Mm01278979_m1), β2i/MECL1 (Mm00479052_g1) using the 7300 Real Time PCR System (Applied Biosystems). RPL19 (Mm02601633_g1) was used as housekeeping gene. Expression of the target gene relative to housekeeping gene expression was calculated as the difference between the threshold values for the two genes.

Measurement of superoxide production. Superoxide production was measured using electron paramagnetic resonance (EPR) technique as described previously[33,34]. Briefly, BMDM were washed twice in Krebs HEPES buffer, pH 7.35 (99 mM NaCl, 4.69 mM KCl, 25 mM $NaHCO_3$, 1.03 mM KH_2PO_4, 5.6 mM d-glucose,

20 mM Na-HEPES, 2.5 mM $CaCl_2$, 1.2 mM $MgSO_4$) and incubated in Krebs-HEPES buffer supplemented with 25 µM desferoxamine, 5 µM diethyldithiocarbamate and 100 µM of the spintrap 1-hydroxy-3-methoxycarbonyl-2 ,2,5,5-tetramethylpyrrolidine (CMH; Noxygen) for 20 minutes on ice followed by snap freezing in liquid nitrogen. Superoxide generation was analyzed at 37 °C for 10 minutes with 20 scannes in an Escan EPR spectrometer with temperature control (Noxygen) with the following starting parameters: microwave power 23.89 mW; center field 3459–3466 G; steep width 10 G, frequency 9.7690 GHz and modulation amplitude 2.93 G. Superoxide generation rate was calculated using linear regression and normalized to the protein content of cells.

Western blot analysis. BMDM and spleen specimen were lysed in extraction buffer containing (in mmol/L): Tris/HCl 50 (pH 7.4), KCl 154, glucose 5, EDTA 0.5, Complete protease inhibitor, and 1% Triton X-100. We isolated protein from livers and spleens separately for each animal, and used equal amounts of protein per animal to prepare one pooled sample per group. Total protein (10 µg per lane) was subjected to SDS-PAGE and membranes were probed with the respective antibodies: anti-Ubiquitin (DAKO), anti-β5 (Abcam), anti-β1 (Abcam), anti-β2 (Abcam), anti-β1i/LMP2 (Abcam), anti-β5i/LMP7 (Epitomics), anti-β2i/MECL-1, anti-α4 (kindly provided by the Department of Biochemistry, Charité-Universitätsmedizin Berlin, Germany). After probing with the respective secondary antibodies, bands were visualized using ECL detection system (Amersham) and chemiluminescence system Fusion Solo (Vilber Lourmat). Amidoblack staining or probing with antibodies against GAPDH (Santa Cruz) or β-actin (MAB150, Millipore) served as controls for equal protein loading. Densitometry was performed using ImageJ software.

Proteasomal activity assay and assessment of proteasome subunit composition. Proteasome chymotrypsin-like (ChTL), trypsin-like (TL) and caspase-like (CaspL) activities of BMDM lysates were determined fluorometrically in a spectramax GEMINI-EM (Molecular Devices) by using synthetic peptides linked to the fluorophor 7-amino-4-methylcoumarin (AMC). ChTL activity was measured by SLLVY-AMC, TL by BzVGR-AMC and CaspL activity by ZLLE-AMC hydrolysis with 360-nm excitation and 460-nm emission wavelengths. BMDM were lysed under hypotonic conditions with three cycles of thawing and freezing in liquid nitrogen. Lysates were centrifuged and the protein content of the supernatant was estimated using the BCA Protein Assay kit (Pierce).

For activity assays, 10 µg of protein were incubated at 37 °C for 30 minutes in incubation buffer containing an ATP-regenerating system (225 mM Tris–HCl, pH 8.2, 45 mM KCl, 7.5 mM $Mg(CH_3COO)_2$, 7.5 mM $MgCl_2$, 1.1 mM dithiothreitol, 6 mM ATP, 5 mM phosphocreatine, 0.2 unit of phosphocreatinekinase) and 0.2 mM of the appropriate fluorogenic substrate. Proteasomal activity was determined by calculating the difference of AMC formation in the absence and presence of 10 µM MG262 and 20 µM epoxomicin and the results were expressed as AMC formation (relative fluorescence units).

For assessment of proteasome subunit composition, lysates were separated on non-denaturing 3–8% Tris-acetate polyacrylamide gels (Life Technologies) and 26 S proteasomes were localized after overlay with 100 µM SLLVY-AMC and 5 mM ATP at 37 °C for 30 minutes using an UV transilluminator. 26 S proteasome containing gel slices were extracted by centrifugation through Amicon Ultra-2 Centrifugal Filter Devices (Millipore) in 120 mM Tris HCl pH 6.8, 0.2 M DTT, 4% SDS, 0.002% bromophenol blue and 20% glycine at 4 °C. Protein extracts were separated under denaturing conditions on 10% polyacrylamide gels and proteasome subunits were detected by Western blot with the respective specific antibodies. At first, a Western blot with anti-α4 antibody was performed and signal intensities were used for the adjustment of equal proteasomal protein loading in subsequent Western blots.

Statistical analysis. Data were analyzed using GraphPad Prism software version 7. Data variability about the mean is generally expressed as standard error of the mean (SEM), except where otherwise indicated. Continuous variables were tested for normal distribution by Shapiro-Wilk test and skewness and for equality of variances by F test. Unpaired Student's *t*-test (Welch test for unequal variances) was used for normally distributed variables. A two-way analysis of variance (ANOVA) followed by Sidak's multiple comparisons test was used to analyze experiments with multiple independent factors across genotypes. Mann-Whitney *U* test or Kruskal-Wallis test with post hoc comparison by Dunn's multiple comparison test was used for non-normally distributed variables. $p < 0.05$ was considered statistically significant.

References

1. Marfella, R. *et al.* Role of the ubiquitin-proteasome system in carotid plaque instability in diabetic patients. *Acta cardiologica* **61**, 630–636 (2006).
2. Marfella, R. *et al.* Increased activity of the ubiquitin-proteasome system in patients with symptomatic carotid disease is associated with enhanced inflammation and may destabilize the atherosclerotic plaque: effects of rosiglitazone treatment. *Journal of the American College of Cardiology* **47**, 2444–2455, https://doi.org/10.1016/j.jacc.2006.01.073 (2006).
3. Versari, D. *et al.* Dysregulation of the ubiquitin-proteasome system in human carotid atherosclerosis. *Arteriosclerosis, thrombosis, and vascular biology* **26**, 2132–2139, https://doi.org/10.1161/01.ATV.0000232501.08576.73 (2006).
4. Kloetzel, P. M. Generation of major histocompatibility complex class I antigens: functional interplay between proteasomes and TPPII. *Nature immunology* **5**, 661–669, https://doi.org/10.1038/ni1090 (2004).
5. Dahlmann, B. Mammalian proteasome subtypes: Their diversity in structure and function. *Archives of biochemistry and biophysics* **591**, 132–140, https://doi.org/10.1016/j.abb.2015.12.012 (2016).
6. Kincaid, E. Z. *et al.* Mice completely lacking immunoproteasomes show major changes in antigen presentation. *Nature immunology* **13**, 129–135, https://doi.org/10.1038/ni.2203 (2012).
7. Agarwal, A. K. *et al.* PSMB8 encoding the beta5i proteasome subunit is mutated in joint contractures, muscle atrophy, microcytic anemia, and panniculitis-induced lipodystrophy syndrome. *American journal of human genetics* **87**, 866–872, https://doi.org/10.1016/j.ajhg.2010.10.031 (2010).

8. Arima, K. *et al.* Proteasome assembly defect due to a proteasome subunit beta type 8 (PSMB8) mutation causes the autoinflammatory disorder, Nakajo-Nishimura syndrome. *Proceedings of the National Academy of Sciences of the United States of America* **108**, 14914–14919, https://doi.org/10.1073/pnas.1106015108 (2011).
9. Egerer, T. *et al.* Tissue-specific up-regulation of the proteasome subunit beta5i (LMP7) in Sjogren's syndrome. *Arthritis and rheumatism* **54**, 1501–1508, https://doi.org/10.1002/art.21782 (2006).
10. Liu, Y. *et al.* Mutations in proteasome subunit beta type 8 cause chronic atypical neutrophilic dermatosis with lipodystrophy and elevated temperature with evidence of genetic and phenotypic heterogeneity. *Arthritis and rheumatism* **64**, 895–907, https://doi.org/10.1002/art.33368 (2012).
11. Basler, M., Dajee, M., Moll, C., Groettrup, M. & Kirk, C. J. Prevention of experimental colitis by a selective inhibitor of the immunoproteasome. *Journal of immunology* **185**, 634–641, https://doi.org/10.4049/jimmunol.0903182 (2010).
12. Kalim, K. W., Basler, M., Kirk, C. J. & Groettrup, M. Immunoproteasome subunit LMP7 deficiency and inhibition suppresses Th1 and Th17 but enhances regulatory T cell differentiation. *Journal of immunology* **189**, 4182–4193, https://doi.org/10.4049/jimmunol.1201183 (2012).
13. Muchamuel, T. *et al.* A selective inhibitor of the immunoproteasome subunit LMP7 blocks cytokine production and attenuates progression of experimental arthritis. *Nature medicine* **15**, 781–787, https://doi.org/10.1038/nm.1978 (2009).
14. Seifert, U. *et al.* Immunoproteasomes preserve protein homeostasis upon interferon-induced oxidative stress. *Cell* **142**, 613–624, https://doi.org/10.1016/j.cell.2010.07.036 (2010).
15. Nathan, J. A. *et al.* Immuno- and constitutive proteasomes do not differ in their abilities to degrade ubiquitinated proteins. *Cell* **152**, 1184–1194, https://doi.org/10.1016/j.cell.2013.01.037 (2013).
16. Libby, P., Lichtman, A. H. & Hansson, G. K. Immune effector mechanisms implicated in atherosclerosis: from mice to humans. *Immunity* **38**, 1092–1104, https://doi.org/10.1016/j.immuni.2013.06.009 (2013).
17. Herrmann, J., Soares, S. M., Lerman, L. O. & Lerman, A. Potential role of the ubiquitin-proteasome system in atherosclerosis: aspects of a protein quality disease. *Journal of the American College of Cardiology* **51**, 2003–2010, https://doi.org/10.1016/j.jacc.2008.02.047 (2008).
18. Moore, K. J., Sheedy, F. J. & Fisher, E. A. Macrophages in atherosclerosis: a dynamic balance. *Nature reviews. Immunology* **13**, 709–721, https://doi.org/10.1038/nri3520 (2013).
19. Ebstein, F. *et al.* Immunoproteasomes are important for proteostasis in immune responses. *Cell* **152**, 935–937, https://doi.org/10.1016/j.cell.2013.02.018 (2013).
20. Wilck, N. & Ludwig, A. Targeting the ubiquitin-proteasome system in atherosclerosis: status quo, challenges, and perspectives. *Antioxidants & redox signaling* **21**, 2344–2363, https://doi.org/10.1089/ars.2013.5805 (2014).
21. Herrmann, J., Lerman, L. O. & Lerman, A. On to the road to degradation: atherosclerosis and the proteasome. *Cardiovascular research* **85**, 291–302, https://doi.org/10.1093/cvr/cvp333 (2010).
22. Kimura, H. *et al.* Immunoproteasome subunit LMP7 Deficiency Improves Obesity and Metabolic Disorders. *Scientific reports* **5**, 15883, https://doi.org/10.1038/srep15883 (2015).
23. Chen, S. *et al.* Immunoproteasome dysfunction augments alternative polarization of alveolar macrophages. *Cell death and differentiation* **23**, 1026–1037, https://doi.org/10.1038/cdd.2016.3 (2016).
24. Joeris, T. *et al.* The proteasome system in infection: impact of beta5 and LMP7 on composition, maturation and quantity of active proteasome complexes. *PloS one* **7**, e39827, https://doi.org/10.1371/journal.pone.0039827 (2012).
25. Kirschner, F. *et al.* Proteasome beta5i Subunit Deficiency Affects Opsonin Synthesis and Aggravates Pneumococcal Pneumonia. *PloS one* **11**, e0153847, https://doi.org/10.1371/journal.pone.0153847 (2016).
26. Kloss, A., Meiners, S., Ludwig, A. & Dahlmann, B. Multiple cardiac proteasome subtypes differ in their susceptibility to proteasome inhibitors. *Cardiovascular research* **85**, 367–375, https://doi.org/10.1093/cvr/cvp217 (2010).
27. Dahlmann, B., Ruppert, T., Kuehn, L., Merforth, S. & Kloetzel, P. M. Different proteasome subtypes in a single tissue exhibit different enzymatic properties. *Journal of molecular biology* **303**, 643–653, https://doi.org/10.1006/jmbi.2000.4185 (2000).
28. Guillaume, B. *et al.* Two abundant proteasome subtypes that uniquely process some antigens presented by HLA class I molecules. *Proceedings of the National Academy of Sciences of the United States of America* **107**, 18599–18604, https://doi.org/10.1073/pnas.1009778107 (2010).
29. Drews, O. *et al. Mammalian proteasome subpopulations wit*h distinct molecular compositions and proteolytic activities. *Molecular & cellular proteomics: MCP* **6**, 2021–2031, https://doi.org/10.1074/mcp.M700187-MCP200 (2007).
30. Wilck, N. *et al.* Attenuation of early atherogenesis in low-density lipoprotein receptor-deficient mice by proteasome inhibition. *Arteriosclerosis, thrombosis, and vascular biology* **32**, 1418–1426, https://doi.org/10.1161/atvbaha.112.249342 (2012).
31. Zhang, X., Goncalves, R. & Mosser, D. M. The isolation and characterization of murine macrophages. *Current protocols in immunology/edited by John* E. *Coligan… et al.* Chapter 14, Unit14 11, https://doi.org/10.1002/0471142735.im1401s83 (2008).
32. Korotkov, V. S. *et al.* Synthesis and biological activity of optimized belactosin C congeners. *Organic & biomolecular chemistry* **9**, 7791–7798, https://doi.org/10.1039/c1ob05661a (2011).
33. Rzymski, T. *et al.* The unfolded protein response controls induction and activation of ADAM17/TACE by severe hypoxia and ER stress. *Oncogene* **31**, 3621–3634, https://doi.org/10.1038/onc.2011.522 (2012).
34. Diebold, I., Petry, A., Hess, J. & Gorlach, A. The NADPH oxidase subunit NOX4 is a new target gene of the hypoxia-inducible factor-1. *Molecular biology of the cell* **21**, 2087–2096, https://doi.org/10.1091/mbc.E09-12-1003 (2010).

Acknowledgements

We are grateful for the excellent assistance of Susanne Metzkow, Anke Stach, and Nicole Rösener. This work was supported by a grant from German Center for Cardiovascular Research (DZHK) to A.L. and V.S. and a grant from the Charité-Universitätsmedizin Berlin to A.L. B.H. is a participant in the Charité Clinical Scientist Program funded by the Charité-Universitätsmedizin Berlin and the Berlin Institute of Health (BIH).

Author Contributions

B.H., A.L. and N.W. designing research studies, conducting experiments, acquiring data, analyzing data and writing the manuscript; C.D., M.P., C.H., A.P. and D.L.: conducting experiments, acquiring data, analyzing data and revising the manuscript; A.G., E.K., D.N.M., V.S., G.B. and K.S.: analyzing data and revising the manuscript.

Additional Information

Supplementary information accompanies this paper at https://doi.org/10.1038/s41598-017-13592-w.

Competing Interests: The authors declare that they have no competing interests.

Publisher's note: Springer Nature remains neutral with regard to jurisdictional claims in published maps and institutional affiliations.

2.3 Quantifying the impact of gut microbiota on inflammation and hypertensive organ damage

Hypertonie ist einer der wichtigsten kardiovaskulären Risikofaktoren weltweit[96, 97] und in besonderem Maß eine von Umweltbedingungen abhängige chronische Erkrankung[18]. In diesem Zusammenhang ist die Ernährung[98, 99] sehr relevant, da beispielsweise eine salzreiche[100, 101] und ballaststoffarme[102, 103] Ernährung Hypertonie begünstigt. Die dem Umwelteinfluss zugrundeliegenden Mechanismen sind komplex. Das Darmmikrobiom rückt - als Mediator zwischen Umwelt und Organismus - zunehmend in den Fokus der Hypertonieforschung. Mehrere experimentelle Studien belegen den Einfluss des Darmmikrobioms auf die Hypertonie[59, 60, 66].

Die vorliegende Studie nutzt ein experimentelles Mausmodell der Hypertonie (Infusion von Angiotensin II s.c. über eine osmotische Minipumpe über 14 Tage, zusätzlich Gabe von 1 %igem NaCl über das Trinkwasser) und vergleicht den resultierenden Organschaden an Herz und Niere zwischen konventionell kolonisierten Mäusen und keimfreien Mäusen. Dazu wurden keimfreie C57BL/6J Wurfgeschwister nach dem Absetzen entweder mit Darmbakterien einer gesunden C57BL/6J-Mauszucht kolonisiert oder keimfrei belassen. Keimfreie Mäuse blieben auch nach Hypertonie-Induktion keimfrei. Ziel dieser Studie war die erstmalige Quantifizierung des Ausmaßes, mit dem das Darmmikrobiom den hypertensiven Endorganschaden beeinflusst.

Die Studie zeigt, dass die renale als auch die kardiale hypertensiven Schädigung von der Anwesenheit einer Darmmikrobiota abhängig und in keimfreien Mäusen ausgeprägter ist. Ursächlich dafür könnte die Abwesenheit protektiver bakterieller Metabolite in keimfreien Mäusen sein, wie z.B. *short-chain fatty acids* (SCFA). Die Tatsache, dass sich der Unterschied im Nierenschaden beim Vergleich von keimfreien und kolonisierten Mäusen ausgeprägter als beim kardialen Schaden darstellte, lässt eine besondere Suszeptibilität der Niere für darmmikrobielle Einflüsse vermuten. Im Umkehrschluss könnte dies auf ein therapeutisches Potential des Darmmikrobioms für neuartige nephroprotektive Behandlungsstrategien bei Hypertonie hinweisen.

Originalpublikation 3

Avery EG, Bartolomaeus H, Rauch A, Chen CY, N'Diaye G, Lober U, Bartolomaeus TUP, Fritsche-Guenther R, Rodrigues AF, Yarritu A, Zhong C, Fei L, Tsvetkov D, Todiras M, Park JK, Marko L, Maifeld A, Patzak A, Bader M, Kempa S, Kirwan JA, Forslund SK, Muller DN and **Wilck N**. Quantifying the impact of gut microbiota on inflammation and hypertensive organ damage. ***Cardiovascular research***. 2023; 119:1441-1452 DOI: 10.1093/cvr/cvac121. https://doi.org/10.1093/cvr/cvac121

Nachfolgend die Zusammenfassung (Abstract), reproduziert aus der Originalveröffentlichung:

Aims: Hypertension (HTN) can lead to heart and kidney damage. The gut microbiota has been linked to HTN, although it is difficult to estimate its significance due to the variety of other features known to influence HTN. In the present study, we used germ-free (GF) and colonized (COL) littermate mice to quantify the impact of microbial colonization on organ damage in HTN.

Methods and results: Four-week-old male GF C57BL/6J littermates were randomized to remain GF or receive microbial colonization. HTN was induced by subcutaneous infusion with angiotensin (Ang) II (1.44 mg/kg/d) and 1% NaCl in the drinking water; sham-treated mice served as control. Renal damage was exacerbated in GF mice, whereas cardiac damage was more comparable between COL and GF, suggesting that the kidney is more sensitive to microbial influence. Multivariate analysis revealed a larger effect of HTN in GF mice. Serum metabolomics demonstrated that the colonization status influences circulating metabolites relevant to HTN. Importantly, GF mice were deficient in anti-inflammatory fecal short-chain fatty acids (SCFA). Flow cytometry showed that the microbiome has an impact on the induction of anti-hypertensive myeloid-derived suppressor cells and pro-inflammatory T_H17 cells in HTN. In vitro inducibility of T_H17 cells was significantly higher for cells isolated from GF than conventionally raised mice.

Conclusions: Microbial colonization status of mice had potent effects on their phenotypic response to a hypertensive stimulus, and the kidney is a highly microbiota-susceptible target organ in HTN. The magnitude of the pathogenic response in GF mice underscores the role of the microbiome in mediating inflammation in HTN.

Translation perspective: To assess the potential of microbiota-targeted interventions to prevent organ damage in hypertension, an accurate quantification of microbial influence is necessary. We provide evidence that the development of hypertensive organ damage is dependent on colonization status and suggest that a healthy microbiota provides anti-hypertensive immune and metabolic signals to the host. In the absence of normal symbiotic host-microbiome interactions, hypertensive damage to the kidney in particular is exacerbated. We suggest that hypertensive patients experiencing perturbations to the microbiota, which are common in CVD, may be at a greater risk for target-organ damage than those with a healthy microbiome.

ESC European Society of Cardiology
Cardiovascular Research (2022) **00**, 1–12
https://doi.org/10.1093/cvr/cvac121

Quantifying the impact of gut microbiota on inflammation and hypertensive organ damage

Ellen G. Avery [1,2,3,4†], Hendrik Bartolomaeus [1,2,3,5†], Ariana Rauch [1,2,3,5], Chia-Yu Chen [1,2,3,6], Gabriele N'Diaye[1,2,6], Ulrike Löber [1,2,3], Theda U. P. Bartolomaeus [1,2,3,6], Raphaela Fritsche-Guenther [2,7], André F. Rodrigues [2,3,4], Alex Yarritu[1,2,3,5], Cheng Zhong[8], Lingyan Fei[8], Dmitry Tsvetkov [1,3,6,9], Mihail Todiras [2,10], Joon-Keun Park[11], Lajos Markó [1,2,3,6], András Maifeld[1,2,3,6], Andreas Patzak[8], Michael Bader [2,3,6], Stefan Kempa [2,12], Jennifer A. Kirwan [2,7], Sofia K. Forslund [1,2,3,6], Dominik N. Müller [1,2,3,6]*, and Nicola Wilck [1,2,3,5]*

[1]Experimental and Clinical Research Center, A Cooperation of Charité-Universitätsmedizin Berlin and Max-Delbrück-Center for Molecular Medicine, Berlin, Germany; [2]Max-Delbrück-Center for Molecular Medicine in the Helmholtz Association, Berlin, Germany; [3]DZHK (German Centre for Cardiovascular Research), partner site Berlin, Germany; [4]Department of Biology, Chemistry, and Pharmacy, Freie Universität Berlin, Berlin, Germany; [5]Department of Nephrology and Internal Intensive Care Medicine, Charité-Universitätsmedizin Berlin, Corporate member of Freie Universität Berlin and Humboldt-Universität zu Berlin, Berlin, Germany; [6]Charité-Universitätsmedizin Berlin, Corporate member of Freie Universität Berlin and Humboldt-Universität zu Berlin, Berlin, Germany; [7]Metabolomics Platform, Berlin Institute of Health at Charité-Universitätsmedizin Berlin, Berlin, Germany; [8]Institute of Translational Physiology, Charité-Universitätsmedizin Berlin, Corporate Member of Freie Universität Berlin and Humboldt-Universität zu Berlin, Charitéplatz 1, 10117 Berlin, Germany; [9]Department of Geriatrics, University of Greifswald, University District Hospital Wolgast, Greifswald, Germany; [10]Nicolae Testemianu State University of Medicine and Pharmacy, Chisinau, Moldova; [11]Hannover Medical School, Hannover, Germany; and [12]Integrative Proteomics and Metabolomics Platform, Berlin Institute for Medical Systems Biology BIMSB, Berlin, Germany

Received 23 September 2021; revised 4 July 2022; editorial decision 8 July 2022; online publish-ahead-of-print 29 July 2022

Time of primary review: 44 days
This article was guest edited by Thomas F. Lüscher.

Aims Hypertension (HTN) can lead to heart and kidney damage. The gut microbiota has been linked to HTN, although it is difficult to estimate its significance due to the variety of other features known to influence HTN. In the present study, we used germ-free (GF) and colonized (COL) littermate mice to quantify the impact of microbial colonization on organ damage in HTN.

Methods and results 4-week-old male GF C57BL/6J littermates were randomized to remain GF or receive microbial colonization. HTN was induced by subcutaneous infusion with angiotensin (Ang) II (1.44 mg/kg/day) and 1% NaCl in the drinking water; sham-treated mice served as control. Renal damage was exacerbated in GF mice, whereas cardiac damage was more comparable between COL and GF, suggesting that the kidney is more sensitive to microbial influence. Multivariate analysis revealed a larger effect of HTN in GF mice. Serum metabolomics demonstrated that the colonization status influences circulating metabolites relevant to HTN. Importantly, GF mice were deficient in anti-inflammatory faecal short-chain fatty acids (SCFA). Flow cytometry showed that the microbiome has an impact on the induction of anti-hypertensive myeloid-derived suppressor cells and pro-inflammatory Th17 cells in HTN. *In vitro* inducibility of Th17 cells was significantly higher for cells isolated from GF than conventionally raised mice.

Conclusion The microbial colonization status of mice had potent effects on their phenotypic response to a hypertensive stimulus, and the kidney is a highly microbiota-susceptible target organ in HTN. The magnitude of the pathogenic response in GF mice underscores the role of the microbiome in mediating inflammation in HTN.

Keywords Hypertension • Microbiome • Inflammation • Kidney • Heart

* Corresponding authors. Tel: +49 30 450540459, E-mail: nicola.wilck@charite.de (N.W.); Tel: +49 30 450540286, E-mail: dominik.mueller@mdc-berlin.de (D.N.M.)
† These authors contributed equally.

1. Introduction

Hypertension (HTN) is the leading risk factor for non-communicable diseases worldwide,[1] and is known as a multifactorial disease, where complex mechanisms often co-occur to lead to a persistent increase in blood pressure (BP). Several studies have indicated that alterations in the composition and function of the intestinal microbiota may contribute to the burden of hypertensive disease.[2–6] However, it is difficult to estimate the contribution of the microbiota, especially in human studies, where the added complexities of other contributing factors easily obstruct our understanding. The aim of our study is to understand the relative contribution that the microbiota has to the burden of hypertensive disease.

Mounting evidence suggests that inflammation is not only characteristic of hypertensive cardiovascular disease (CVD) but is causally linked to disease progression and severity.[3] Components of both the innate and adaptive immune system have been implicated.[3] T-helper 17 (Th17) cells and Type 1 helper T-cells (Th1) have been shown to be integrally interlinked with hypertensive disease, and have been demonstrated to exacerbate cardiac and renal damage.[5,7,8] Moreover, myeloid-derived suppressor cells (MDSCs) derived from hypertensive mice were shown to have immunosuppressive properties, and upon adoptive transfer were able to mitigate BP increase in response to angiotensin II (Ang II) infusion.[9] MDSC, Th17, and Th1 cells have each been shown in different settings to be influenced by the microbiota.[5,9–11]

We and others could recently demonstrate the role of several anti-inflammatory microbial metabolites in HTN. Short-chain fatty acids (SCFA) such as acetate, propionate, and butyrate, are produced by gut microbiota through the fermentation of indigestible dietary fibre.[12] Acetate has been shown to ameliorate hypertensive damage to the kidney and heart in mice.[13] Our recent work elucidated the protective role of propionate in Ang II-induced inflammation and cardiovascular damage.[14] Furthermore, low butyrate levels have been associated with worsened CVD in several models.[15] In addition to SCFA, we have recently shown that a bacterially produced indole metabolite derived from tryptophan suppresses Th17-driven inflammation in salt-sensitive HTN.[5] In contrast, metabolites of microbial origin can also exacerbate disease in some contexts. For example, pro-inflammatory metabolites like trimethylamine N-oxide (TMAO) and indoxyl sulfate (IS) have been shown to aggravate CVD.[16,17]

To address our central aim, we utilized germ-free (GF) mice. C57BL/6J GF littermates were randomized at 4 weeks of age to either receive a microbiota transfer from our in-house C57BL/6J colony, or to remain GF for the duration of the experiment. Here, we have uncovered several differences between GF and colonized (COL) mice in response to Ang II and 1% NaCl in the drinking water, which underscores the importance of the microbiota in the pathogenesis of HTN-induced organ damage. Of note, we show an exacerbation of damage in GF mice compared with COL mice, which is more distinct in the kidney than in the heart.

2. Materials and Methods

Detailed description of all analytical methods and data analysis used are available in the Supplementary material online.

2.1 Animal ethics

All experiments performed complied with the German/European law for animal protection and were approved by the local ethics committee (G0280/13, G0028/21).

2.2 Animal protocol

Wild-type C57BL/6J mice were bred under axenic conditions in an isolator (Metall + Plastic, Radolfzell-Stahringen, Germany). Mice were maintained on a 12:12 h day: night cycle with constant access to food and water. Until Week 4, mice in both experimental groups grew under GF conditions. At 4 weeks of age, male mice were randomized to either remain GF in the isolator or receive passive bacterial colonization (COL). For colonization, mice were introduced in the regular SPF animal facility and placed in cages from healthy wild-type male C57BL/6J mice. Until 12 weeks of age mice received sterilized tap water as drinking water. At 12 weeks of age, COL and GF mice received Angiotensin II (Ang II, 1.44 mg/kg/day) by subcutaneous infusion via an osmotic minipump (Alzet) and 1% NaCl (Carl Roth) in the drinking water or sham treatment. Sham-treated animals received the same operation procedure without minipump implantation. Minipumps were implanted under sterile conditions, GF mice were kept sterile throughout the experiment. Sterile drinking water was delivered via the Hydropac system (Plexx B.V., Elst, the Netherlands). Throughout the experiment mice were fed autoclaved standard breeding chow (V1124, Ssniff, Soest, Germany). After 2 weeks of Ang II + 1% NaCl or sham treatment mice were euthanized by isoflurane anaesthesia and blood, spot urine (where possible), faeces, and organs were collected. The Ang II infusion model was performed in 40 mice (GF $n = 5$, COL $n = 5$, GF + HTN $n = 16$, COL + HTN $n = 14$). Over the course of the experiments, five animals were taken out of the experiment (GF + HTN $n = 3$, COL + HTN $n = 2$), due to pre-specified ethical termination criteria in order to counteract severe distress in this experiment. These five mice were not included in the analysis. Additionally, invasive BP measurements were performed in 10 animals (GF $n = 5$, COL $n = 5$), these animals were not included in any other analysis. As a control group for *in vitro* experiments, cells, and tissues from age-matched conventionally raised SPF C57BL/6J mice (referred to as CONV) were used.

Mice were euthanized by isoflurane anaesthesia (5% isoflurane–air mixture). Furthermore, echocardiography, BP, and Ang II pressor response measurements were performed in isoflurane inhalation anaesthesia (2–2.5% isoflurane–air mixture). Details are given in Supplementary material online.

3. Results

3.1 Absence of microbiota exacerbates cardiorenal damage

To exclude confounding effects relating to the genetic background of mice used in our study, GF littermates were randomized at 4 weeks of age for colonization with SPF microbiota (COL) or further kept under GF conditions. At 12 weeks of age, we induced HTN by subcutaneous Ang II infusion and 1% NaCl-supplemented drinking water. After 14 days, we analysed hypertensive target organ damage (*Figure 1A*). Of note, we did not include surgical uninephrectomy to avoid bacterial contamination. The standard model in our lab includes uninephrectomy to induce a more severe form of renal damage,[8,18] thus we expected a lower degree of renal damage when compared with the published literature.[19] To validate the integrity of our experiment, we first checked the colonization status of the mice. Gross morphological changes were assessed, and the characteristics typical of the gastrointestinal (GI) tract in GF mice (e.g. megacecum) did not persist in the mice which had been colonized (COL) (see Supplementary material online, *Figure S1A*). To confirm the microbial status of the respective group, we examined faecal pellets

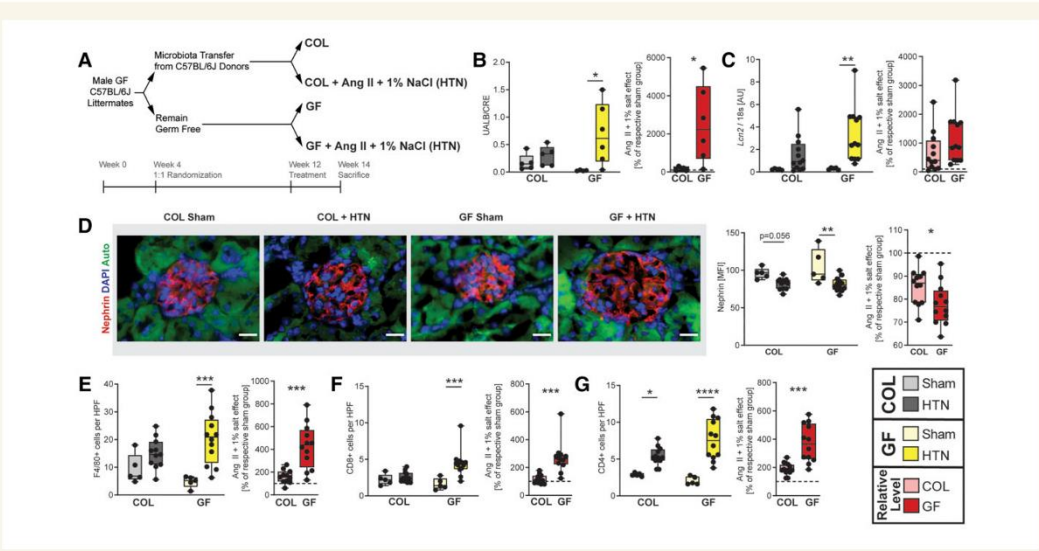

Figure 1 Renal damage is exacerbated under GF conditions. (*A*) Description of experimental protocol (unless otherwise stated, GF Sham $n = 5$, GF + HTN $n = 12$, COL Sham $n = 5$, COL + HTN $n = 12$ for further analyses). (*B*) Urinary albumin-to-creatinine ratio from spot urine collected upon sacrifice from a subset of mice (COL $n = 5$, COL + HTN $n = 5$, GF $n = 4$, GF + HTN $n = 6$). (*C*) *Lcn2* gene expression was measured from kidney tissue by qPCR. (*D*) Histological kidney sections were stained for nephrin. Representative glomeruli are shown (left). Nephrin immunofluorescence was quantified as mean fluorescence intensity (MFI) in the glomerular space averaged per mouse. The scale bar represents 20 µm. (*E*) Macrophages (F4/80+), (*F*) CD8+, and (*G*) CD4+ T-cells from kidney sections were counted from five representative high-power fields within the cortex. For (*B*–*G*), the left graph was tested using a two-way ANOVA and *post hoc* Sidak multiple comparison's test and depicts the raw values for each variable. For (*B*–*F*), HTN was identified as the source of variation using two-way ANOVA, and *post hoc* multiple comparison between sham and HTN within each group revealed that the GF comparison was the source of variation. In (*G*), HTN was identified as the source of variation using two-way ANOVA, and *post hoc* multiple comparison between sham and HTN within each group revealed that both the GF and COL comparison were significant. For *B* through *G*, the right plot depicts the relative change induced by Ang II + 1% NaCl in comparison with the respective sham group, tested using an unpaired two-tailed *t*-test. No change (100%) depicted as dotted line. For all plots, *P*-values are as follows; $*P \leq 0.05$, $**P \leq 0.01$, $***P \leq 0.001$, $****P \leq 0.0001$.

produced on the final day of experimentation. First, pellets were incubated in a thioglycolate medium for 96 h, and GF mice were found to show no bacterial growth (see Supplementary material online, *Figure S1B*). Second, 16S rDNA copies per gram stool measured by qPCR were found to be similar in COL (Sham and HTN) and conventional SPF mice (CONV), whereas GF mice did not have more 16S rDNA copies than blank samples (see Supplementary material online, *Figure S1C*). Finally, unimputed serum metabolomics confirmed the presence of bacterially-derived metabolites in COL mice only (see Supplementary material online, *Figure S1D*). Shotgun metagenomics revealed that the grafted bacteria in COL mice showed the largest overlap with mouse gut metagenomes published in the global microbial gene catalogue (GMGC) (see Supplementary material online, *Figure S2*). We therefore concluded that the GF and COL groups were maintained as intended to confidently proceed with further analyses. Of note, it has been previously reported for the Ang II infusion model that HTN induction leads to changes in the microbiome composition.[20] Likewise, we found Ang II infusion influenced the abundance of various taxa in COL mice (see Supplementary material online, *Figure S1E*) as shown by shotgun sequencing. Indeed, both the caecal and faecal compartments displayed differences between the COL sham and HTN groups on phylum and genus levels (see Supplementary material online, *Figure S1F* and *G*, and *File S1–4*).

One of the hallmarks of hypertensive target organ damage is renal damage, which is characterized by abnormally high excretion of albumin with the urine (albuminuria), fibrosis, and inflammation. In line with the literature,[19] our HTN induction without uninephrectomy lead to a moderate increase in albuminuria in COL mice (*Figure 1B*). GF mice developed a greater degree of albuminuria upon HTN induction, which is abundantly clear when comparing the relative increase of GF and COL mice compared with their respective sham groups (*Figure 1B*). HTN also lead to a significant increase in renal damage marker lipocalin-2 in GF mice (Lcn2), which was not evident in COL mice (*Figure 1C*). Next, we analysed nephrin, a protein in the podocytes' slit membrane, by immunofluorescence. We observed a significant decrease of nephrin immunofluorescence in GF mice, where COL mice exhibited a similar but insignificant trend (*Figure 1D*). HTN led to a significant increase of macrophages (F4/80+ cells, *Figure 1E*) and cytotoxic T-cells (CD8+ cells, *Figure 1F*) in the kidney of GF mice, not reaching significance in COL mice. Likewise, we found that mRNA expression of CC-chemokine ligand 2 (Ccl2, see Supplementary material online, *Figure S3A*) and infiltrating T-cells (CD3+, see Supplementary material online, *Figure S3B*) were selectively increased in the GF group upon HTN. While T-helper cells (CD4+ cells) were shown to increase in both GF and COL mice, GF mice displayed a stronger increase

(*Figure 1G*). The number of leukocytes (CD45+ cells) within the kidney confirms the stronger effect of HTN on renal inflammation in GF (see Supplementary material online, *Figure S3C*). For all immune populations in the kidney, the change in HTN relative to sham was consistently exacerbated in GF compared with COL (*Figure 1E–G*, and see Supplementary material online, *Figure S3B and C*). Finally, we investigated kidney fibrosis. Expression of *Col3a1* was significantly increased only in GF + HTN mice (see Supplementary material online, *Figure S3D*). Perivascular fibrosis analysed by Masson's trichrome staining was accentuated in GF mice but not statistically different between the groups using two-way analysis of variance (ANOVA); although when comparing the relative increase from sham to HTN, there was a significant difference between GF and COL (see Supplementary material online, *Figure S3E*). Similar to what was previously shown,[21] GF mice tended to have lower baseline values for several damage markers when comparing sham-treated GF and COL mice. Overall, renal pathology upon HTN induction was greater in GF mice when compared with their COL littermates.

Next, we examined the cardiac phenotype. HTN induction led to greater hypertrophy in GF compared with COL mice, as measured by heart weight-to-tibia length ratio (*Figure 2A*). Left ventricular weight taken from echocardiography relative to the tibia length (*Figure 2B*) as well as cardiac *Nppb* expression (*Figure 2C*) confirmed this finding. Neither the GF + HTN nor COL + HTN mice had a reduced ejection fraction (*Figure 2D*), indicating none of these mice were experiencing systolic heart failure. Using two-way ANOVA, both perivascular (*Figure 2E*) and interstitial (*Figure 2F*) fibrosis were significantly increased in GF + HTN and not in COL + HTN mice compared with their respective sham group. Interestingly, when assessing the relative increase in HTN compared with sham for markers of cardiac fibrosis, there was no difference in GF compared with COL mice (*Figure 2E and F*). Next, we examined cardiac inflammation. Despite an increase in *Ccl2* expression in GF and not COL (see Supplementary material online, *Figure S4A*), macrophages (F4/80+) were increased in both GF and COL hearts upon HTN; and GF + HTN showed significantly less macrophages than COL + HTN mice (*Figure 2G*). The change in overall leukocytes (CD45+) within the heart mimics the changes seen for macrophages (see Supplementary material online, *Figure S4B*). Furthermore, no significance was reached when comparing CD4+ T-helper cell infiltration (*Figure 2H*), whereas CD8+ cytotoxic T-cells in the hearts increased in both GF + HTN and COL + HTN mice compared with sham (*Figure 2I*). We also observed an increase in the cardiac expression of pro-inflammatory cytokine *Tnfa* selectively in the GF + HTN group compared with sham (see Supplementary material online, *Figure S4C*). Altogether, cardiac hypertrophy and inflammation following HTN were affected to a greater extent in GF, but when assessing the relative change for GF and COL mice in HTN compared with sham we saw many similarities in the development of the cardiac fibrosis. Whereas in the kidney, there was a clear difference in the development of HTN damage between GF and COL mice, these distinctions were less evident in the heart.

3.2 Hypertensive kidney damage is more sensitive to microbial status than cardiac damage

The aforementioned findings indicate that GF mice respond more sensitively to HTN. Within the context of our initial statistical approach (two-way ANOVA) we often saw a loss of significance for the HTN effect in COL mice under equal statistical power; and the differences between GF and COL response where much clearer when assessing the relative increase for a given marker in HTN (unpaired *t*-test). To expand on this idea to increase our understanding of the differences between GF and COL, we assessed the size of the HTN-induced effect by calculating an effect size (Cliff's delta) and fold change for each marker. Using a comprehensive univariate testing strategy, we assessed the significance in the different tissue spaces using a robust false discovery rate (FDR) correction within GF and COL groups to root out any spurious findings. From the majority of kidney parameters assessed, across the subcategorizations of damage, fibrosis, and inflammatory markers, a very consistent pattern emerged in that the GF mice experienced worsened kidney outcomes compared with COL mice (*Figure 3A*, see Supplementary material online, *Table S1*). In contrast to the renal damage, both GF and COL mice experienced a more similar cardiac damage pattern, particularly regarding markers of cardiac fibrosis (*Figure 3B*, and see Supplementary material online, *Table S2*). Albeit several cardiac parameters reached significance in GF and COL mice, the fold changes observed in GF mice were often larger (e.g. *Nppb*, perivascular fibrosis, *Ccn2*, *Lcn2*, F4/80, CD8; see Supplementary material online, *Table S2*). GF + HTN mice develop a significant increase in lung weight-to-tibia length ratio (*Figure 3B*), indicating the development of lung congestion[22] due to aggravated cardiac dysfunction. Taken together, there was more overlap in the cardiac response to HTN in GF and COL groups than was seen for the kidney parameters.

To further quantify the HTN effect across the renal (*Figure 3C*) and cardiac (*Figure 3D*) tissue space, we performed a multivariate principal coordinate analysis (PCoA) summarizing the overall (dis)similarities amongst the groups. To assess pairwise comparisons of interest, the overall dataset was divided and tested using PERMANOVA (*Figure 3C*). The pairwise comparisons of the kidney phenotypic data show a significant distance in the COL group from sham to HTN (P-value = 0.012, F-value = 4.8). However, the effect of HTN, as measured by the F-value, was greater in the GF mice (P-value = 0.001, F-value = 8.2). In line with our initial univariate targeted analysis (*Figure 1*), this indicates that the overall phenotypic change in the kidney in response to HTN was larger in GF mice than in COL mice. Furthermore, the pairwise PERMANOVA between GF + HTN and COL + HTN groups (P-value = 0.044, F-value = 3.2) indicates that HTN induction resulted in a different outcome on a multivariate level. Despite some slight differences within some univariate kidney data in the sham groups (e.g. albuminuria, F4/80 + cells), pairwise comparison of GF and COL sham samples was insignificant (P-value = 0.262, F-value = 1.4).

For the multivariate analysis of our cardiac data, pairwise comparisons were also used to assess the trajectory of each group (*Figure 3D*). Consistent with our conclusions from the univariate assessment of the overall cardiac phenotype (*Figure 3B*), we saw that the comparison between GF + HTN and COL + HTN group showed significant overlap in the PCoA plot, and the pairwise comparison between these samples was not significant (P-value = 0.391, F-value = 1.1). Conversely, the difference between sham GF and COL samples was significant, suggesting that perhaps the basal cardiac phenotype is sensitive to the host's microbiome status (P-value = 0.01, F-value = 5.6). As expected, the comparison of HTN with sham samples within the GF (P-value = 0.01, F-value = 4.8) and COL (P-value = 0.046, F-value = 3.2) samples were both significant. The cardiac data again indicate larger phenotypic shifts in GF mice most likely driven by significantly different sham groups.

Taken together, our univariate and multivariate approaches indicate a larger effect of HTN in GF mice. In the case of the kidney, this increased effect is indeed driven by a stronger adverse response of GF mice to

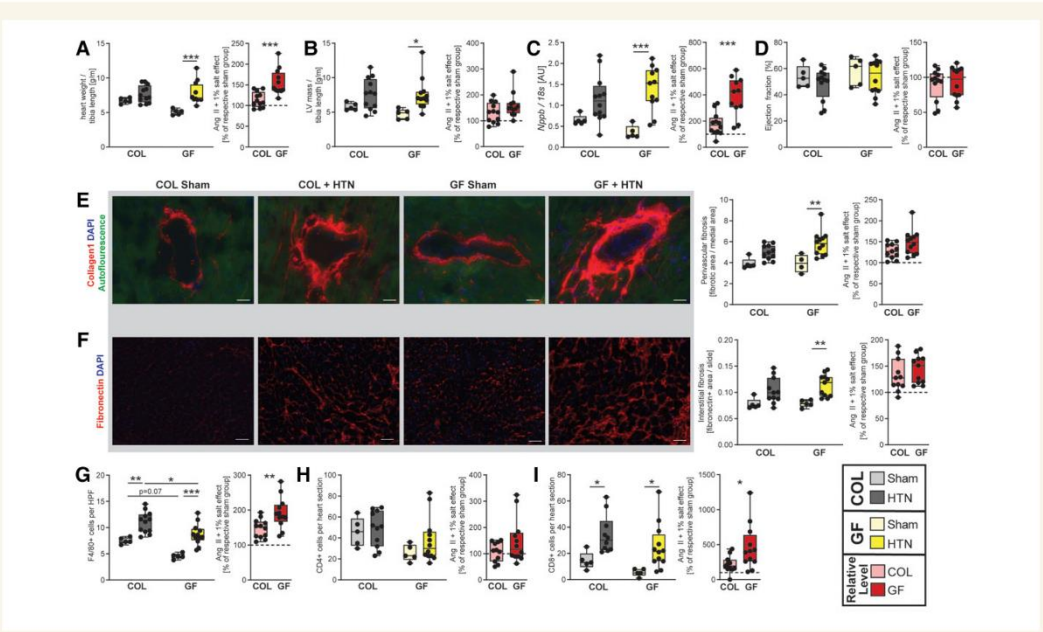

Figure 2 Cardiac inflammation and hypertrophy are aggravated in GF mice. Unless otherwise stated, GF Sham $n = 5$, GF + HTN $n = 12$, COL Sham $n = 5$, COL + HTN $n = 12$. (*A*) Heart weight-to-tibia length (g/m) from mice taken at sacrifice. (*B*) Left ventricular (LV) mass was estimated using echocardiography and normalized to tibia length (g/m). (*C*) Cardiac ventricular natriuretic peptide gene expression (*Nppb*) measured by qPCR. COL + HTN $n = 11$, otherwise as stated above. (*D*) Echocardiography prior to sacrifice revealed no change in the ejection fraction upon HTN induction in GF or COL mice. (*E*) Perivascular fibrosis from cardiac vessels, evaluated by measuring the fibrotic area relative to the medial area of vessels from Collagen 1-stained histology slides. GF Sham $n = 4$, otherwise as stated above. (*F*) Cardiac interstitial fibrosis was evaluated as fibronectin positive area proportionate to total area from five representative 40× magnification pictures from histological slides. In scale bar represents 40 µm. (*G*) Macrophages (F4/80+) were counted from five representative high-power fields, and (H) CD4+, and (*I*) CD8+ T-cells were counted from whole heart sections. Two-way ANOVA and *post hoc* Sidak multiple comparison's test for (*A–I*) was used to test significance in the left plot. In (*A–C*) and (*E and F*), HTN was identified as the source of variation using two-way ANOVA, and *post hoc* multiple comparison between sham and HTN within each group revealed that the GF comparison was the source of variation. In (*G*) HTN and the microbiome were both identified as sources of variation using two-way ANOVA, and significant *post hoc* comparisons are shown. In (*I*), HTN was identified as the source of variation using two-way ANOVA, and *post hoc* multiple comparison between sham and HTN within each group revealed that both the GF and COL comparison were significant. To the right in (*A–I*), the relative change induced by Ang II + 1% NaCl in comparison with the respective sham group was tested using an unpaired two-tailed *t*-test. No change (100%) depicted as dotted line. For all plots, *P*-values are as follows; $*P \leq 0.05$, $**P \leq 0.01$, $***P \leq 0.001$.

HTN, whereas in the case of the heart, this effect is driven by phenotypic differences in the healthy groups (sham-treated mice).

3.3 Vascular response to Angiotensin II is similar in GF and COL mice

There is some evidence from the literature that vascular reactivity may be dependent on microbial colonization.[23,24] We opted not to implant telemetry devices for the measurement of BP in our primary experimental animals, as microscopic vascular surgery was not possible under sterile conditions. Although we decided to forgo this gold-standard for BP measurement, we still questioned whether the axenic status of our GF mice would impact the basal mean arterial pressure (MAP), or BP reactivity to Ang II. We therefore colonized additional mice using the same colonization procedure as previously outlined, and we performed *in vivo* BP measurements using an implanted arterial catheter in freely moving mice. Interestingly, we found that GF mice had a significantly higher MAP (*Figure 4A*) than their colonized counterparts, although the mean of each group (GF mean value = 118.4 mmHg, COL mean value = 107.8 mmHg) was still in a range considered normal for untreated C57BL/6J mice.[25] Acute intravenous infusion of Ang II induced an increase in BP (*Figure 4B*) which was nearly identical for GF and COL mice, suggesting that Ang II-dependent reactivity of the vasculature is similar in these mice. Similarly, we investigated *ex vivo* vascular contractility of mesenteric arteries isolated from conventionally colonized mice (CONV) or GF mice (GF). CONV mice were used for this *in vitro* experiment due to ease of availability because colonization of GF mice is a lengthy procedure. GF mice showed similar contractile response compared with CONV mice in response to Ang II (see Supplementary material online, *Figure S5A*). Additionally, mesenteric arterial rings from GF mice showed similar contraction force in response to KCl to CONV mice (see Supplementary material online, *Figure S5B*). Similarly,

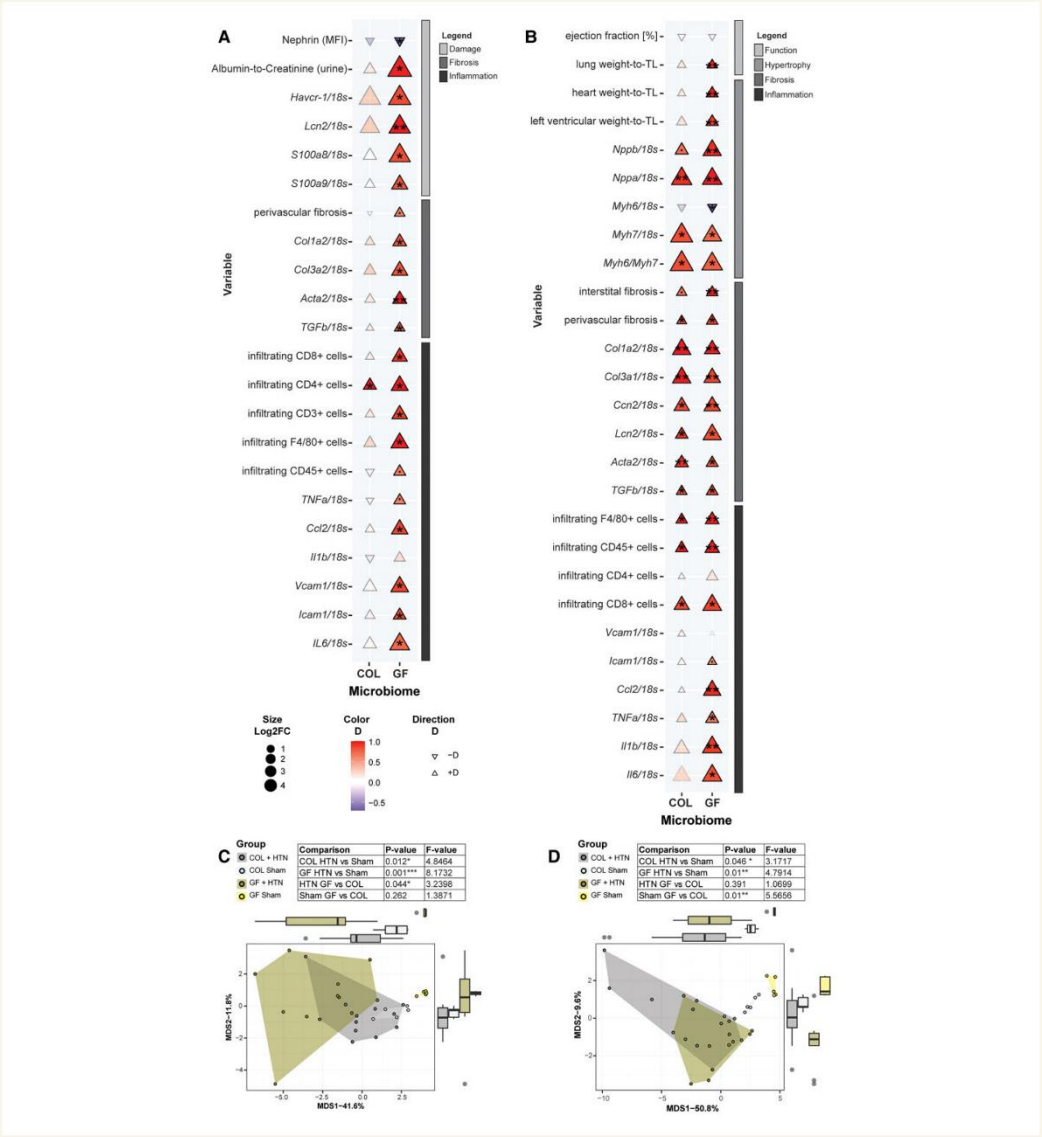

Figure 3 Unbiased assessment of kidney and heart damage in HTN-treated GF vs. COL mice. Unless otherwise stated, GF Sham $n = 5$, GF + HTN $n = 12$, COL Sham $n = 5$, COL + HTN $n = 12$. For cardiac RNA expression COL + HTN $n = 11$, otherwise as stated before. (*A*) Effect sizes [Cliff's delta (*D*)] and fold changes are shown to assess the effect of HTN treatment relative to the respective sham group in GF and COL on the kidney phenotype. Colour and triangle direction indicates effect size. Size indicates log2-transformed fold change (Log2FC) of HTN compared with the respective sham group. Significance was calculated using the Mann–Whitney *U*-test and was FDR-corrected with the Benjamini–Hochberg procedure to account for multiple testing. Markers for significant *Q*-values are superimposed, and transparency indicates non-significant effects. °$q < 0.1$, *$q < 0.05$, **$q < 0.01$. Variables are organized by subcategory (damage, fibrosis, inflammation). (*B*) Same univariate analysis as in (*A*) was performed on cardiac phenotypic data. Variables are organized by subcategory (function, hypertrophy, fibrosis, inflammation). (*C*) PCoA was performed based on Euclidean distance scaling of kidney phenotypic data to demonstrate the dissimilarities between study groups in a quantitative phenotypic state space (GF + HTN = 11, otherwise as stated). Pairwise comparisons between groups were preformed using PERMANOVA and reported in the inset table. (*D*) PCoA as in (*C*) was performed on the cardiac phenotypic data.

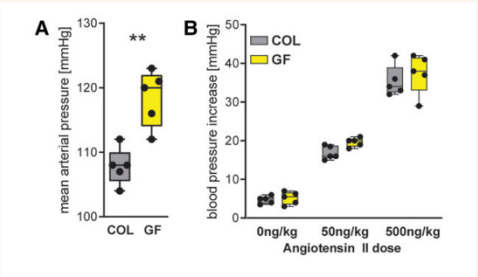

Figure 4 BP and Angiotensin II reactivity in GF and COL mice. $N = 5$ animals per group. (*A*) GF and COL mice were implanted an arterial catheter for BP measurement. MAP was measured in resting and awake animals, and the difference was tested using an unpaired two-tailed *t*-test (**$P \leq 0.01$). (*B*) The increase in BP after acute intravenous infusion of Angiotensin II as a bolus was measured. No statistical difference between GF and COL mice was found using a two-way repeated measurement ANOVA ($P = 0.14$), whereas Ang II dose had a significant influence ($P \leq 0.0001$, not shown).

endothelial-dependent (see Supplementary material online, *Figure S5C*) and –independent (see Supplementary material online, *Figure S5D*) relaxation was not influenced by colonization status.

3.4 Microbiota and microbial metabolites shape serum metabolome changes in HTN

Although the vascular reactivity of GF mice was similar to those housing microbes, we were interested to understand the different phenotypic and inflammatory response to HTN. We therefore decided to investigate the microbiome itself and associated metabolite production, as our group and others have previously shown that some metabolites of microbial origin can be anti-inflammatory in HTN.[5,13,14]

Consistent with the literature,[20] the metabolome of GF and COL animals was affected by HTN induction. We found a multitude of differences when analyzing the serum metabolome (MxP Quant 500, Biocrates) from GF and COL mice in HTN compared with the respective sham, which we grouped together by class to show the composite shift of over 300 individually measured metabolites (*Figure 5A*, and see Supplementary material online, *Table S3*). Of the 15 classes of metabolites where HTN induction had an effect, four of those classes (phosphatidylcholines, hexosylceramides, alkaloids, fatty acids) showed similar trajectories, suggesting these classes changed in a microbiome-independent manner upon HTN (*Figure 5A*, individual metabolites shown in see Supplementary material online, *Figure S6A–D*). For individual metabolites, we compared the impact of HTN induction on metabolite trajectories. When comparing sham with HTN, there was little overlap between the metabolites that decreased (*Figure 5B*) or increased (*Figure 5C*) within GF or COL. Overall, in GF mice more metabolites were regulated by HTN than in COL mice (see Supplementary material online, *Table S11*) (*Figure 5D*). Of note, a subset of metabolites which were upregulated in GF mice were downregulated in COL mice in response to HTN and vice versa (*Figure 5D*, shown in black). Taken together, the alterations of the metabolome in response to HTN show little overlap in GF and COL mice (*Figure 5D*, referred to as 'both'). Unsurprisingly, the serum metabolome was significantly impacted by the microbiome, and we saw a wide range of correlations between individual metabolites and microbial species, as well as functional modules derived from shotgun sequencing data (see Supplementary material online, *Figure S7*). Although the serum metabolite measurements used here were very comprehensive, they did not cover SCFA metabolites, which we and others have shown to have high importance in the progression of HTN. It has been demonstrated elsewhere that GF mice are devoid of some important SCFA.[26] We confirmed this for our mouse colonies (GF and CONV, which were the source populations for our experiments) by performing mass spectrometry measurements of faecal acetate, propionate, and butyrate (*Figure 5E*). We expect that the lack of the potent anti-hypertensive metabolites propionate and butyrate influences the phenotype seen in GF mice.

3.5 Inflammation contributes to the differing phenotypic response to HTN in GF and COL mice

It has been shown that the immune system and the gut microbiome are strongly interconnected, and several studies have shown the importance of immune cells in HTN.[2,3] We and others have also shown that metabolites of microbial origin can influence inflammation in HTN.[5,13,14] We examined the splenic immune cell composition a surrogate for systemic inflammation in GF and COL mice by flow cytometry (gating strategies are shown in see Supplementary material online, *Figure S8*). Of the 23 immune cell subsets we investigated, 12 were differentially influenced by HTN when compared with the respective sham group (*Figure 6A*, and see Supplementary material online, *Table S4*). We then examined all immune parameters multivariately to assess how changes in immune cells would be reflected in the distance between each group using PCoA (*Figure 6B*). It is known that the immune system of GF mice differs from their colonized counterparts.[27] Our data confirms this observation as the pairwise comparison of sham-treated GF and COL mice (*P*-value = 0.011, *F*-value = 6.6) was significant. Interestingly, this difference between COL and GF was still evident after HTN induction (*P*-value = 0.026, *F*-value = 2.8). Pairwise comparisons of individual groups using PERMANOVA indicated that the HTN to sham comparison was significant in the GF group (*P*-value = 0.006, *F*-value = 4.8), but not within the COL group (*P*-value = 0.177, *F*-value = 1.6) (*Figure 6B*). It can be concluded that overall, the inflammatory status of GF mice was disturbed to a greater degree by HTN induction.

Previous studies have shown that splenic MDSC increase in HTN and have anti-hypertensive properties.[9] In line with the literature, there was an increase in monocytic MDSC (mMDSC) upon HTN induction, and this increase was only significant in COL + HTN mice (*Figure 6C*). Furthermore, for both mMDSC and granulocytic MDSC (gMDSC) (*Figure 6D*) subtypes, COL + HTN mice showed a significantly higher frequency of these anti-hypertensive immune cells than GF + HTN mice. The relative increase in HTN compared with sham for mMDSC was lesser in GF mice but greater for gMDSC than in COL (*Figure 6C and D*). The dynamics of whether the relative increase, or absolute number of MDSCs is relevant in HTN is currently unknown. Additionally, we saw an increase in Th17 cells in both GF and COL mice, though this effect only reached significance in GF mice (*Figure 6E*). This increase was driven by pathological Th1-like Th17 cells, defined by their co-expression of RORgt and Tbet (*Figure 6F*).[28] Recent evidence suggest that pre-existing conditions can influence naive T-cell responses towards effector differentiation.[29–31] We hypothesized that the absence of microbes and their metabolites in GF mice would render naive T-cells more vulnerable to

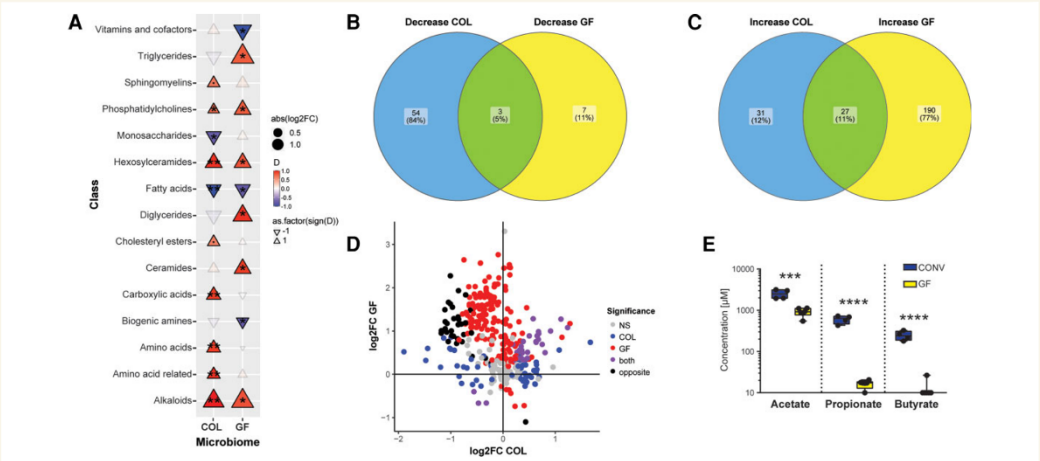

Figure 5 Microbiome heavily influences the metabolome in response to HTN. (*A*) Using the Biocrates MxP500 Quant kit, serum metabolites were analysed from GF and COL mice. Metabolites were grouped by class to demonstrate the overall effect on the serum metabolome (Sham GF $n = 5$, Sham COL $n = 5$, GF + HTN $n = 10$, COL + HTN $n = 11$). Effect size [Cliff's delta (*D*)] is shown to demonstrate the effect of HTN relative to the respective sham group in GF and COL. Colour and triangle direction indicates effect size. Size indicates log2-transformed fold change (Log2FC) of HTN mice compared with the respective sham group. Significance was calculated using the Mann–Whitney *U*-test and was FDR-corrected using the Benjamini–Hochberg procedure to account for multiple testing. Markers for significant Q-values are superimposed, and transparency indicates non-significant effects. °$q < 0.1$, *$q < 0.05$, **$q < 0.01$. For (*B*) and (*C*), individual metabolites rather than metabolite classes within the GF and COL group were compared using the effect size calculation listed in (*A*, see Supplementary material online, *Table S11*). Those metabolites which were significantly altered in the sham to HTN comparison, as tested using the Mann–Whitney *U*-test with Benjamini–Hochberg FDR correction were selected and separated based on the directionality of their shift. Metabolites which decreased (*B*) or increased (*C*) in HTN relative to sham are compared between the COL and GF conditions using a Venn diagram. The number of metabolites and the percentage within each subcategory are overlayed. In (*D*) significant changes to individual metabolites (points) are shown in GF (*y*-axis) and COL (*x*-axis) as log2-fold changes in response to HTN. Metabolites exclusively significantly regulated in GF or in COL are shown in red and blue, respectively. Purple points indicate metabolites significantly regulated similarly in GF and COL (significant in both and same trajectory), while black points indicate metabolites regulated significant in both groups but with opposite trajectories. Grey points are metabolites which were reliably measured but not significantly altered in either group. (*E*) Faecal SCFA from GF or CONV mice demonstrates the absence of potent anti-hypertensive metabolites butyrate and propionate in the GF setting (GF $n = 6$, CONV $n = 4$). Significance was tested using unpaired two-tailed Student's *t*-test (***$P \leq 0.001$, ****$P \leq 0.0001$). LC-MS, liquid chromatography-mass spectrometry; FIA-MS, flow injection analysis-mass spectrometry.

cytokines. Therefore, we performed an *in vitro* Th17 polarization of naive T-cells from GF and CONV mice (which were used in place of COL due to ease of accessibility) in the presence or absence of Ang II. Naive T-cells from GF mice more readily polarized towards Th17 cells than cells from CONV mice, particularly in the presence of Ang II (*Figure 6G*). To demonstrate that the conditions for the polarization of Th17 cells indeed exist *in vivo*, we quantified the expression of each of the Th17-polarizing cytokines (Il-6, Il-1b, and TGFb) by qPCR from kidney (see Supplementary material online, *Figure S9A*, and *Figure 3A*) and heart (see Supplementary material online, *Figure S9B*, and *Figure 3C*) tissue. These key cytokines were increased upon HTN. The comparison of effect sizes (*Figure 3A and C*) often indicated larger effects of HTN in GF mice. We suspected that the reason naive CD4+ T-cells isolated from CONV mice were less inducible toward Th17 in the presence of Ang II may be due to the priming of immune cells by SCFA in the *in vivo* microenvironment. To test this hypothesis, prior to Th17 induction in the presence of Ang II, naive CD4+ cells were pre-treated for 24 h with the SCFA butyrate and propionate. While the pre-treatment did not affect the induction of Th17 in CONV, SCFA pre-treatment prevented the enhanced Th17 induction of naive T-cells from GF mice (*Figure 6H*).

In summary, our *in vitro* findings suggest that the different preconditioning of naive T-cells within GF and COL mice may impact polarization into pro-inflammatory effector T-cells and thus severity of target organ damage. We anticipate that this effect contributes to our *in vivo* findings, where the absence of microbes and microbiota-derived metabolites like SCFA had a potent impact on immune cells relevant in HTN and cardiorenal damage.

4. Discussion

Gut microbial dysbiosis associates with HTN in humans[5,32] and in rodent models.[5,32–34] Faecal microbiota transplantation from hypertensive patients into mice has also been shown to induce an increase in BP.[32] However, few studies have focused on the overall contribution of the microbiome to the pathogenesis of HTN, such that it may be contextualized relative to other known contributors to hypertensive disease

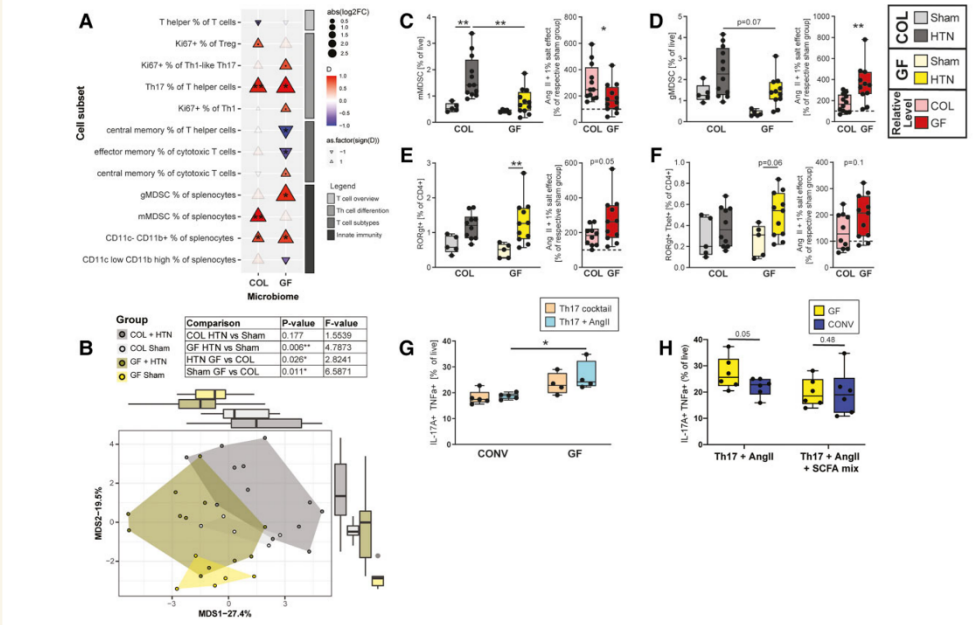

Figure 6 Colonization status influences the inflammatory reaction to HTN. Unless otherwise stated, GF Sham $n = 5$, GF + HTN $n = 12$, COL Sham $n = 5$, COL + HTN $n = 12$. (*A*) Several unique immune cell subsets were measured from the spleen, as a proxy measure of systemic inflammation. Effect size (Cliff's delta [D]) is shown to demonstrate the effect of HTN relative to the respective sham group in GF and COL. Colour and triangle direction indicates effect size. Size indicates log2-transformed fold change (Log2FC) of HTN induction compared with the respective sham group. Significance was calculated using the Mann–Whitney *U*-test and was FDR-corrected using the Benjamini–Hochberg procedure to account for multiple testing. Markers for significant Q-values are superimposed, and transparency indicates non-significant effects. $^{\circ}q < 0.1$, $^{*}q < 0.05$, $^{**}q < 0.01$. Immune cell subsets are organized by sub-category (Innate immunity and T-cell overview, differentiation, and subtypes) and subsets, and cell types where no significant effect in either GF or COL was found are not shown. (*B*) PCoA was performed based on Euclidean distance scaling of immune cell abundances to demonstrate the dissimilarities between study groups. Pairwise comparisons between groups were performed using PERMANOVA and reported in the inset table. Monocytic MDSCs (mMDSC, *C*) and granulocytic MDSCs (gMDSC, *D*), as well as Th17 (*E*) and Th1-like Th17 cells (*F*) from the spleen are shown as boxplots on the left. (*G*) naive CD4+ T-cells from mesenteric lymph nodes of either GF of CONV mice, polarized *in vitro* towards a Th17 using a cocktail of IL-1β, TGFβ, and IL-6 with or without Ang II (GF $n = 4$, CONV $n = 5$). In (H) naive CD4+ T-cells were pre-treated with 1 mM SCFA mix (0.5 mM of each butyrate and propionate) or 1 mM NaCl. Subsequently, the pre-treatment was removed, and cells were polarized toward Th17 in the presence of Ang II as described in G (GF $n = 6$, CONV $n = 6$). To the left in (*C*–*G*), two-way ANOVA and *post hoc* Sidak multiple comparison's test was used to test significance. To the right in (*C*–*F*), the relative change induced by Ang II + 1% NaCl in comparison with the respective sham group was tested using an unpaired two-tailed *t*-test. No change (100%) depicted as dotted line. In (*H*) for the Th17 + Ang II and Th17 + Ang II + SCFA mix a one-tailed *t*-test was performed per group, as a pre-specified hypothesis from *Figure 6G* was tested. For all plots in (*C*–*G*), *P*-values are as follows; $^{*}P \leq 0.05$, $^{**}P \leq 0.01$.

burden. Here we show in a presence/absence scenario, that the microbiota has a potent effect on HTN-induced cardiac and renal damage in mice. GF mice showed a stronger adverse response to HTN than their COL littermates. Interestingly, the kidney seems to be more sensitive to changes in microbial status than the heart. Finally, we propose that the altered inflammatory response in GF mice contributes to their aggravated phenotype in HTN.

We have shown robustly that the kidney damage within GF mice upon HTN is comparatively more severe than the damage experienced by their COL littermates. Some of the larger effects in our univariate analysis may be related to the slightly lower baseline level of putative markers for kidney damage within sham GF mice compared with sham COL, though these groups do not significantly differ. We surmise that the baseline differences between GF and COL mice are likely due to the immunological uniqueness of GF mice, which has been documented in the literature.[27] Indeed, across renal damage, fibrosis and inflammation markers, we consistently saw a significant effect of HTN selectively in the GF group (*Figure 3A*). Furthermore, we show on a multivariate level that the difference between sham GF and GF + HTN mice for the composite of kidney parameters is significant, while the equivalent comparison within the COL mice is insignificant (*Figure 3C*). Consistent with other inflammatory markers, we show an increase of infiltrating macrophages (F4/80+ cells, *Figure 1E*) in GF + HTN kidneys, as well as the increased expression of *Ccl2* (see Supplementary material online,

Figure S3A), which has been implicated as a major player in worsening kidney damage in mice[35] and humans.[36] Infiltrating macrophages during renal injury are known to contribute to the secretion of cytokines like IL-1β, which enhances the activation and differentiation of Th17 cells.[37] A previous study additionally showed that SCFA-treatment in ischaemia-reperfusion injury (IRI) radically reduced kidney *Ccl2*, *Il-1b*, and associated kidney damage.[38] SCFA have been shown to have anti-inflammatory properties in several cell types,[39–42] which could contribute to the lessened damage in COL mice, since only mice harbouring microbiota have significant SCFA production within the GI tract (*Figure 5C*). Our results are highly compatible with previous studies showing that GF status exacerbates kidney damage in the context of IRI[43] and adenine-induced chronic kidney disease.[21,44]

Intriguingly, we found that the cardiac phenotype was less influenced by the microbial status of the host. Here we have shown that particularly for markers of fibrosis (*Figure 3B*), regardless of the microbiome status, the mice developed significant injury. For CD8+ T-cells, F4/80+ macrophages and overall CD45+ leukocytes, we observed significant changes in GF and COL mice, although GF mice tended to show a higher fold change in response to HTN (see Supplementary material online, *Table S2*). Despite these similarities, both cardiac hypertrophy (*Figure 2A*) and left ventricular mass-to-tibia length (*Figure 2B*) were significantly altered upon HTN induction in the GF but not COL mice. Nonetheless, our data suggest that the kidney, more so than the heart, represents a subspace of hypertensive target organ damage, which is more susceptible to microbial colonization. It is conceivable that cardiac damage could be further exacerbated as renal function declines. Thus, the gut microbiota could be added as an important modulator of the well-known cardiorenal axis. Further research to follow up this idea is required, perhaps using several iterations of variations to a defined community of microbes, to test the universality of this hypothesis.

Metabolites of microbial origin, some of which are known to be associated with CVD and accumulate in chronic kidney disease,[16,17] were measurable within the serum metabolome of our COL but not our GF mice, such as IS and TMAO (see Supplementary material online, *Figure S1D*). Our results very clearly indicate that GF mice experience robust kidney damage to a greater extent than COL mice, despite GF mice being devoid of these harmful metabolites. However, we suggest that the reason COL mice experience less overall damage is likely due to the presence of SCFA. We and others have shown the potent effect of SCFA in mouse models.[13,14] Here we have shown again, for a representative set of animals, that SCFA are depleted in GF mice (*Figure 5C*). We hypothesize that the potency of SCFA in COL mice counterbalances the presence of IS and TMAO. Further research on this topic is required to definitively conclude the effects of the co-occurrence of these various metabolites of microbial origin.

Furthermore, we show that systemic inflammatory response to HTN is altered by colonization status. MSDC, which represent an important subset of innate anti-inflammatory cells in HTN,[9] reacted differently GF mice compared with COL (*Figure 6C and D*). Additionally, we found that Th17 cells were increased during HTN in GF mice (*Figure 6E*). Th1-like Th17 cells, which are known to be pathogenic, trended towards enrichment in GF + HTN mice (*Figure 6F*). We wanted to explore *in vitro* that naive T-cells from GF mice were more sensitive to polarizing cytokines and Ang II. We found that upon polarization, naive T-cells from GF mice skewed more towards Th17, particularly when Ang II was added (*Figure 6G*). As it has been recently demonstrated that the SCFA propionate can decrease the rate of Th17 cell differentiation,[41,42] we suspected that this could be part of the reason naive cells from COL mice were less inducible toward Th17. Indeed, when we pre-treated naive CD4+ T-cells with butyrate and propionate, we observed a decline in Th17 inducibility in the presence of Ang II in GF; an effect that was not seen in cells isolated from CONV mice (*Figure 6H*). Recently, Krebs and colleagues showed that the development of Th17 cells in the kidney is dependent on the cytokine micromilieu and can be blocked with specific antibodies against IL-1b and IL-6.[45] We also could show that the polarization conditions used in our Th17 *in vitro* assay were practically available *in vivo*, and the expression of each polarizing cytokine was increased within heart and kidney tissue of hypertensive mice.

To our knowledge, one study similar to ours exists within the literature, published by Karbach *et al.*[46] It is clear from the extensive phenotyping performed in our study that our findings were not congruent with their data, where they showed that GF mice were protected from developing HTN and related vascular damage. Though this was initially a surprise, upon further examination, there are two likely scenarios that may explain this. First, the protocol of our experiments did differ from one another. The study from Karbach and colleagues compared GF mice with conventionally raised mice, whereas we compared GF mice with littermates that had been colonized early in life. Therefore, our study was able to account for known genetic drifts in gnotobiotic colonies. Additionally, Ang II infusion was only performed for seven days, while we studied a more chronic phenotype. Furthermore, our mice ate different diets, and as Kaye and colleagues recently demonstrated, the composition of the diet can have a profound impact on the resultant hypertensive phenotype.[47] Second, it is highly likely that the microbiome used in our study and in the study by Karbach and colleagues may be distinct from one another. Incongruencies like ours have also been found in other contexts. The comparison of microbiome-rich and GF mice in one study showed the amelioration of an IRI of the kidney by the microbiome,[43] where another study demonstrated the opposite effect.[48]

To investigate the second scenario further, we hypothesized that the microbiome background used in any given study might have drastic implications for the study outcome. Our group and others have shown that microbially-produced metabolites have a potent effect on the pathogenesis of HTN.[5,13,14,49] In reference to that, if the microbiota itself were to change, we expect the circulating metabolites to be likewise altered within the host. Unfortunately, the study from Karbach *et al.*[46] did not include any information regarding the microbiome and metabolome of their microbiota-rich mice. Although, we did find a recent study from Cheema and Pluznick[20] where these data were made available, but their phenotypic data is not reported.[20] Nevertheless, to test our hypothesis regarding the putative comparability of the colonizing microbiome between studies, and the impact this may have on resultant study outcome, we decided to compare our microbiome and metabolome with the published data from Cheema and Pluznick. To compare the microbiomes from these two studies, we re-annotated our shotgun microbiome sequencing data such that it would be comparable to the 16s rDNA sequencing data from Cheema and Pluznick. The microbiome of CONV between the two studies were starkly contrasting in sham and HTN mice (shown as a multivariate PCoA plot derived from genus level information from each of the studies, see Supplementary material online, *Figure S10A*). We surmised that because of the lack of overlapping microbiome signatures within our study and the Pluznick dataset, that the metabolome signal would likewise be dichotomous. We compared the serum metabolome dataset from the two studies by using metabolites which could be measured in both studies from all COL and GF mice. We found that interestingly, there was significantly less distance

between the effect of HTN on individual metabolites within the serum metabolome of GF mice from these two studies than in the equivalent COL mice comparison (see Supplementary material online, *Figure S10B and C*). This result suggests that the congruence of the serum metabolome in GF groups within these two datasets is higher than the COL groups. These exploratory data support the idea that the structure of the implanted microbiome has a measurable impact on serum metabolome alterations in response to HTN. Because of our and others' findings regarding the importance of microbial metabolites in HTN, we believe that this could be a driving factor behind the contradictory phenotypic results of our study compared with the data from Karbach *et al.*[46] It is nonetheless critical in future studies for the microbiome to be well documented and openly accessible to avoid questions regarding the reproducibility of existing studies.

5. Conclusion

We have shown that the microbiota has a profound effect on hypertensive disease pathogenesis. Furthermore, we have shown that GF mice, when compared with their colonized littermates, experienced an aggravation of target organ damage, which was more distinct in the kidney than in the heart. Additionally, we demonstrated that the metabolome is influenced significantly by the microbiome used for experimentation, which underscores the need for standardization of experimentation and reporting within the field. The immunophenotype of HTN mice, and in particular, the alteration of MDSC and Th17 cells, which have been previously implicated in HTN, give us some indication of how GF mice may have developed an exacerbated hypertensive phenotype in our study. *In vitro*, SCFA rescued the pro-inflammatory phenotype of T-cells isolated from GF mice. We propose that the COL mice were protected from damage in comparison with their GF counterparts due to the absence of the potent anti-inflammatory SCFA metabolites under GF conditions.

Supplementary material

Supplementary material is available at *Cardiovascular Research* online.

Authors' Contributions

N.W., D.N.M., and H.B. designed the study. E.G.A., H.B., A.R., G.N., D.T., A.Y., C.Z., L. Y., L.M., A.M., A.P., and N.W. performed animal experiments and analysed the data. A.F.R, M.T., and M.B. performed *in vivo* BP measurement. C.-Y.C., U.L., and T.U.P.B. performed the microbiome analysis. E.G.A., R.F.G., S.K., and J.A.K. performed and analysed the metabolomics experiments. S.K.F. helped with data analysis and interpretation. E.G.A., N.W., H.B., and D.N.M. wrote the manuscript with input from all authors.

Acknowledgments

We thank Petra Voss, Ilona Kramer, May-Britt Köhler, Jana Czychi, Ute Gerhardt, Alina Eisenberger, Martin Taube, and Stefanie Schelenz for their technical assistance.

Conflict of interest: none declared.

Funding

N.W. is supported by the European Research Council (ERC) under the European Union's Horizon 2020 research and innovation programme (852796) and by a grant from the Corona-Stiftung, Deutsches Stiftungszentrum, Essen, Germany. A.P., N.W., D.N.M., and S.K.F. are supported by the Deutsche Forschungsgemeinschaft (DFG, German Research Foundation) Projektnummer 394046635—SFB 1365. The DZHK (German Centre for Cardiovascular Research, 81Z1100101) supported D.N.M. N.W. was participant in the Clinician Scientist Programme funded by the Berlin Institute of Health (BIH).

Data availability

The data underlying this article are available in the article and in its online supplementary material. The microbiome data underlying this article are available in NCBI database and can be accessed as BioProject PRJNA812410. The metabolomics data underlying this article are available via FigShare, please see Supplementary material online, *Table S10* for access links.

References

1. Ezzati M, Riboli E. Behavioral and dietary risk factors for noncommunicable diseases. *N Engl J Med* 2013;**369**:954–964.
2. Avery EG, Bartolomaeus H, Maifeld A, Marko L, Wiig H, Wilck N, Rosshart SP, Forslund SK, Muller DN. The gut microbiome in hypertension: recent advances and future perspectives. *Circ Res* 2021;**128**:934–950.
3. Madhur MS, Elijovich F, Alexander MR, Pitzer A, Ishimwe J, Van Beusecum JP, Patrick DM, Smart CD, Kleyman TR, Kingery J, Peck RN, Laffer CL, Kirabo A. Hypertension: do inflammation and immunity hold the key to solving this epidemic? *Circ Res* 2021;**128**:908–933.
4. Verhaar BJH, Collard D, Prodan A, Levels JHM, Zwinderman AH, Backhed F, Vogt L, Peters MJL, Muller M, Nieuwdorp M, van den Born BH. Associations between gut microbiota, faecal short-chain fatty acids, and blood pressure across ethnic groups: the HELIUS study. *Eur Heart J* 2020;**41**:4259–4267.
5. Wilck N, Matus MG, Kearney SM, Olesen SW, Forslund K, Bartolomaeus H, Haase S, Mahler A, Balogh A, Marko L, Vvedenskaya O, Kleiner FH, Tsvetkov D, Klug L, Costea PI, Sunagawa S, Maier L, Rakova N, Schatz V, Neubert P, Fratzer C, Krannich A, Gollasch M, Grohme DA, Corte-Real BF, Gerlach RG, Basic M, Typas A, Wu C, Titze JM, Jantsch J, Boschmann M, Dechend R, Kleinewietfeld M, Kempa S, Bork P, Linker RA, Alm EJ, Muller DN. Salt-responsive gut commensal modulates TH17 axis and disease. *Nature* 2017;**551**:585–589.
6. Yang T, Santisteban MM, Rodriguez V, Li E, Ahmari N, Carvajal JM, Zadeh M, Gong M, Qi Y, Zubcevic J, Sahay B, Pepine CJ, Raizada MK, Mohamadzadeh M. Gut dysbiosis is linked to hypertension. *Hypertension* 2015;**65**:1331–1340.
7. Madhur MS, Lob HE, McCann LA, Iwakura Y, Blinder Y, Guzik TJ, Harrison DG. Interleukin 17 promotes angiotensin II-induced hypertension and vascular dysfunction. *Hypertension* 2010;**55**:500–507.
8. Marko L, Kvakan H, Park JK, Qadri F, Spallek B, Binger KJ, Bowman EP, Kleinewietfeld M, Fokuhl V, Dechend R, Muller DN. Interferon-γ signaling inhibition ameliorates angiotensin II-induced cardiac damage. *Hypertension* 2012;**60**:1430–1436.
9. Shah KH, Shi P, Giani JF, Janjulia T, Bernstein EA, Li Y, Zhao T, Harrison DG, Bernstein KE, Shen XZ. Myeloid suppressor cells accumulate and regulate blood pressure in hypertension. *Circ Res* 2015;**117**:858–869.
10. Ivanov II, Atarashi K, Manel N, Brodie EL, Shima T, Karaoz U, Wei D, Goldfarb KC, Santee CA, Lynch SV, Tanoue T, Imaoka A, Itoh K, Takeda K, Umesaki Y, Honda K, Littman DR. Induction of intestinal Th17 cells by segmented filamentous bacteria. *Cell* 2009;**139**:485–498.
11. Zaccone P, Raine T, Sidobre S, Kronenberg M, Mastroeni P, Cooke A. Salmonella typhimurium infection halts development of type 1 diabetes in NOD mice. *Eur J Immunol* 2004;**34**:3246–3256.
12. Tan J, McKenzie C, Potamitis M, Thorburn AN, Mackay CR, Macia L. The role of short-chain fatty acids in health and disease. *Adv Immunol* 2014;**121**:91–119.
13. Marques FZ, Nelson E, Chu PY, Horlock D, Fiedler A, Ziemann M, Tan JK, Kuruppu S, Rajapakse NW, El-Osta A, Mackay CR, Kaye DM. High-fiber diet and acetate supplementation change the gut microbiota and prevent the development of hypertension and heart failure in hypertensive mice. *Circulation* 2017;**135**:964–977.
14. Bartolomaeus H, Balogh A, Yakoub M, Homann S, Marko L, Hoges S, Tsvetkov D, Krannich A, Wundersitz S, Avery EG, Haase N, Kraker K, Hering L, Maase M, Kusche-Vihrog K, Grandoch M, Fielitz J, Kempa S, Gollasch M, Zhumadilov Z, Kozhakhmetov S, Kushugulova A, Eckardt KU, Dechend R, Rump LC, Forslund SK, Muller DN, Stegbauer J, Wilck N. Short-chain fatty acid propionate protects from hypertensive cardiovascular damage. *Circulation* 2019;**139**:1407–1421.
15. Poll BG, Cheema MU, Pluznick JL. Gut microbial metabolites and blood pressure regulation: focus on SCFAs and TMAO. *Physiology (Bethesda)* 2020; **35**:275–284.
16. Zhu W, Gregory JC, Org E, Buffa JA, Gupta N, Wang Z, Li L, Fu X, Wu Y, Mehrabian M, Sartor RB, McIntyre TM, Silverstein RL, Tang WHW, DiDonato JA, Brown JM, Lusis AJ,

Hazen SL. Gut microbial metabolite TMAO enhances platelet hyperreactivity and thrombosis risk. *Cell* 2016;**165**:111–124.
17. Nakano T, Katsuki S, Chen M, Decano JL, Halu A, Lee LH, Pestana DVS, Kum AST, Kuromoto RK, Golden WS, Boff MS, Guimaraes GC, Higashi H, Kauffman KJ, Maejima T, Suzuki T, Iwata H, Barabasi AL, Aster JC, Anderson DG, Sharma A, Singh SA, Aikawa E, Aikawa M. Uremic toxin indoxyl sulfate promotes proinflammatory macrophage activation via the interplay of OATP2B1 and Dll4-notch signaling. *Circulation* 2019;**139**:78–96.
18. Marko L, Park JK, Henke N, Rong S, Balogh A, Klamer S, Bartolomaeus H, Wilck N, Ruland J, Forslund SK, Luft FC, Dechend R, Muller DN. B-cell lymphoma/leukaemia 10 and angiotensin II-induced kidney injury. *Cardiovasc Res* 2020;**116**:1059–1070.
19. Leelahavanichkul A, Yan Q, Hu X, Eisner C, Huang Y, Chen R, Mizel D, Zhou H, Wright EC, Kopp JB, Schnermann J, Yuen PS, Star RA. Angiotensin II overcomes strain-dependent resistance of rapid CKD progression in a new remnant kidney mouse model. *Kidney Int* 2010;**78**:1136–1153.
20. Cheema MU, Pluznick JL. Gut microbiota plays a central role to modulate the plasma and fecal metabolomes in response to angiotensin II. *Hypertension* 2019;**74**:184–193.
21. Mishima E, Ichijo M, Kawabe T, Kikuchi K, Akiyama Y, Toyohara T, Suzuki T, Suzuki C, Asao A, Ishii N, Fukuda S, Abe T. Germ-free conditions modulate host purine metabolism, exacerbating adenine-induced kidney damage. *Toxins (Basel)* 2020;**12**:547.
22. Richards DA, Aronovitz MJ, Calamaras TD, Tam K, Martin GL, Liu P, Bowditch HK, Zhang P, Huggins GS, Blanton RM. Distinct phenotypes induced by three degrees of transverse aortic constriction in mice. *Sci Rep* 2019;**9**:5844.
23. Joe B, McCarthy CG, Edwards JM, Cheng X, Chakraborty S, Yang T, Golonka RM, Mell B, Yeo JY, Bearss NR, Furtado J, Saha P, Yeoh BS, Vijay-Kumar M, Wenceslau CF. Microbiota introduced to germ-free rats restores vascular contractility and blood pressure. *Hypertension* 2020;**76**:1847–1855.
24. Edwards JM, Roy S, Tomcho JC, Schreckenberger ZJ, Chakraborty S, Bearss NR, Saha P, McCarthy CG, Vijay-Kumar M, Joe B, Wenceslau CF. Microbiota are critical for vascular physiology: germ-free status weakens contractility and induces sex-specific vascular remodeling in mice. *Vascul Pharmacol* 2020;**125-126**:106633.
25. Mattson DL. Comparison of arterial blood pressure in different strains of mice. *Am J Hypertens* 2001;**14**:405–408.
26. Hoverstad T, Midtvedt T. Short-chain fatty acids in germfree mice and rats. *J Nutr* 1986;**116**:1772–1776.
27. Smith K, McCoy KD, Macpherson AJ. Use of axenic animals in studying the adaptation of mammals to their commensal intestinal microbiota. *Semin Immunol* 2007;**19**:59–69.
28. Kamali AN, Noorbakhsh SM, Hamedifar H, Jadidi-Niaragh F, Yazdani R, Bautista JM, Azizi G. A role for Th1-like Th17 cells in the pathogenesis of inflammatory and autoimmune disorders. *Mol Immunol* 2019;**105**:107–115.
29. Coit P, Dozmorov MG, Merrill JT, McCune WJ, Maksimowicz-McKinnon K, Wren JD, Sawalha AH. Epigenetic reprogramming in naive CD4+ T cells favoring T Cell activation and non-Th1 effector T cell immune response as an early event in lupus flares. *Arthritis Rheumatol* 2016;**68**:2200–2209.
30. Altorok N, Coit P, Hughes T, Koelsch KA, Stone DU, Rasmussen A, Radfar L, Scofield RH, Sivils KL, Farris AD, Sawalha AH. Genome-wide DNA methylation patterns in naive CD4+ T cells from patients with primary Sjogren's syndrome. *Arthritis Rheumatol* 2014;**66**:731–739.
31. Heninger AK, Eugster A, Kuehn D, Buettner F, Kuhn M, Lindner A, Dietz S, Jergens S, Wilhelm C, Beyerlein A, Ziegler AG, Bonifacio E. A divergent population of autoantigen-responsive CD4(+) T cells in infants prior to beta cell autoimmunity. *Sci Transl Med* 2017;**9**:eaaf8848.
32. Li J, Zhao F, Wang Y, Chen J, Tao J, Tian G, Wu S, Liu W, Cui Q, Geng B, Zhang W, Weldon R, Auguste K, Yang L, Liu X, Chen L, Yang X, Zhu B, Cai J. Gut microbiota dysbiosis contributes to the development of hypertension. *Microbiome* 2017;**5**:14.
33. Adnan S, Nelson JW, Ajami NJ, Venna VR, Petrosino JF, Bryan RM Jr, Durgan DJ. Alterations in the gut microbiota can elicit hypertension in rats. *Physiol Genomics* 2017;**49**:96–104.
34. Santisteban MM, Qi Y, Zubcevic J, Kim S, Yang T, Shenoy V, Cole-Jeffrey CT, Lobaton GO, Stewart DC, Rubiano A, Simmons CS, Garcia-Pereira F, Johnson RD, Pepine CJ, Raizada MK. Hypertension-linked pathophysiological alterations in the gut. *Circ Res* 2017;**120**:312–323.
35. Kashyap S, Osman M, Ferguson CM, Nath MC, Roy B, Lien KR, Nath KA, Garovic VD, Lerman LO, Grande JP. Ccl2 deficiency protects against chronic renal injury in murine renovascular hypertension. *Sci Rep* 2018;**8**:8598.
36. Eardley KS, Zehnder D, Quinkler M, Lepenies J, Bates RL, Savage CO, Howie AJ, Adu D, Cockwell P. The relationship between albuminuria, MCP-1/CCL2, and interstitial macrophages in chronic kidney disease. *Kidney Int* 2006;**69**:1189–1197.
37. Pindjakova J, Hanley SA, Duffy MM, Sutton CE, Weidhofer GA, Miller MN, Nath KA, Mills KH, Ceredig R, Griffin MD. Interleukin-1 accounts for intrarenal Th17 cell activation during ureteral obstruction. *Kidney Int* 2012;**81**:379–390.
38. Andrade-Oliveira V, Amano MT, Correa-Costa M, Castoldi A, Felizardo RJ, de Almeida DC, Bassi EJ, Moraes-Vieira PM, Hiyane MI, Rodas AC, Peron JP, Aguiar CF, Reis MA, Ribeiro WR, Valduga CJ, Curi R, Vinolo MA, Ferreira CM, Camara NO. Gut bacteria products prevent AKI induced by ischemia-reperfusion. *J Am Soc Nephrol* 2015;**26**:1877–1888.
39. Singh N, Thangaraju M, Prasad PD, Martin PM, Lambert NA, Boettger T, Offermanns S, Ganapathy V. Blockade of dendritic cell development by bacterial fermentation products butyrate and propionate through a transporter (Slc5a8)-dependent inhibition of histone deacetylases. *J Biol Chem* 2010;**285**:27601–27608.
40. Wang F, Liu J, Weng T, Shen K, Chen Z, Yu Y, Huang Q, Wang G, Liu Z, Jin S. The inflammation induced by lipopolysaccharide can be mitigated by short-chain fatty acid. Butyrate, through upregulation of IL;10, in septic shock. *Scand J Immunol* 2017;**85**:258–263.
41. Duscha A, Gisevius B, Hirschberg S, Yissachar N, Stangl GI, Eilers E, Bader V, Haase S, Kaisler J, David C, Schneider R, Troisi R, Zent D, Hegelmaier T, Dokalis N, Gerstein S, Del Mare-Roumani S, Amidror S, Staszewski O, Poschmann G, Stuhler K, Hirche F, Balogh A, Kempa S, Trager P, Zaiss MM, Holm JB, Massa MG, Nielsen HB, Faissner A, Lukas C, Gatermann SG, Scholz M, Przuntek H, Prinz M, Forslund SK, Winklhofer KF, Muller DN, Linker RA, Gold R, Haghikia A. Propionic acid shapes the multiple sclerosis disease course by an immunomodulatory mechanism. *Cell* 2020;**180**:1067–1080.e16.
42. Haghikia A, Jorg S, Duscha A, Berg J, Manzel A, Waschbisch A, Hammer A, Lee DH, May C, Wilck N, Balogh A, Ostermann AI, Schebb NH, Akkad DA, Grohme DA, Kleinewietfeld M, Kempa S, Thone J, Demir S, Muller DN, Gold R, Linker RA. Dietary fatty acids directly impact central nervous system autoimmunity via the small intestine. *Immunity* 2015;**43**:817–829.
43. Jang HR, Gandolfo MT, Ko GJ, Satpute S, Racusen L, Rabb H. Early exposure to germs modifies kidney damage and inflammation after experimental ischemia-reperfusion injury. *Am J Physiol Renal Physiol* 2009;**297**:F1457–F1465.
44. Mishima E, Fukuda S, Mukawa C, Yuri A, Kanemitsu Y, Matsumoto Y, Akiyama Y, Fukuda NN, Tsukamoto H, Asaji K, Shima H, Kikuchi K, Suzuki C, Suzuki T, Tomioka Y, Soga T, Ito S, Abe T. Evaluation of the impact of gut microbiota on uremic solute accumulation by a CE-TOFMS-based metabolomics approach. *Kidney Int* 2017;**92**:634–645.
45. Krebs CF, Reimers D, Zhao Y, Paust HJ, Bartsch P, Nunez S, Rosemblatt MV, Hellmig M, Kilian C, Borchers A, Enk LUB, Zinke M, Becker M, Schmid J, Klinge S, Wong MN, Puelles VG, Schmidt C, Bertram T, Stumpf N, Hoxha E, Meyer-Schwesinger C, Lindenmeyer MT, Cohen CD, Rink M, Kurts C, Franzenburg S, Koch-Nolte F, Turner JE, Riedel JH, Huber S, Gagliani N, Huber TB, Wiech T, Rohde H, Bono MR, Bonn S, Panzer U, Mittrucker HW. Pathogen-induced tissue-resident memory TH17 (TRM17) cells amplify autoimmune kidney disease. *Sci Immunol* 2020;**5**:eaba4163.
46. Karbach SH, Schonfelder T, Brandao I, Wilms E, Hormann N, Jackel S, Schuler R, Finger S, Knorr M, Lagrange J, Brandt M, Waisman A, Kossmann S, Schafer K, Munzel T, Reinhardt C, Wenzel P. Gut microbiota promote angiotensin II-induced arterial hypertension and vascular dysfunction. *J Am Heart Assoc* 2016;**5**:e003698.
47. Kaye DM, Shihata WA, Jama HA, Tsyganov K, Ziemann M, Kiriazis H, Horlock D, Vijay A, Giam B, Vinh A, Johnson C, Fiedler A, Donner D, Snelson M, Coughlan MT, Phillips S, Du XJ, El-Osta A, Drummond G, Lambert GW, Spector TD, Valdes AM, Mackay CR, Marques FZ. Deficiency of prebiotic fiber and insufficient signaling through gut metabolite-sensing receptors leads to cardiovascular disease. *Circulation* 2020;**141**:1393–1403.
48. Emal D, Rampanelli E, Stroo I, Butter LM, Teske GJ, Claessen N, Stokman G, Florquin S, Leemans JC, Dessing MC. Depletion of gut microbiota protects against renal ischemia-reperfusion injury. *J Am Soc Nephrol* 2017;**28**:1450–1461.
49. Heianza Y, Ma W, Manson JE, Rexrode KM, Qi L. Gut microbiota metabolites and risk of major adverse cardiovascular disease events and death: a systematic review and meta-analysis of prospective studies. *J Am Heart Assoc* 2017;**6**:e004947.

2.4 Salt-responsive gut commensal modulates T_H17 axis and disease

Der Salzkonsum übersteigt in vielen Teilen der Welt die von Fachgesellschaften empfohlenen Grenzwerte[104, 105]. Eine salzreiche Diät gilt als Risikofaktor für die Mortalität von nichtübertragbaren Erkrankungen und wird für das Auftreten von Hypertonie maßgeblich verantwortlich gemacht[20, 97, 101, 106, 107]. Die zugrundeliegenden Mechanismen sind unvollständig verstanden; die Bedeutung des Immunsystems und insbesondere der T-Helferzellen wird vermutet. Dabei ist bekannt, dass $CD4^+$ Interleukin-17A-produzierende Typ17-T-Helferzellen (T_H17) Hypertonie und Endorganschäden fördern[35, 38] und möglicherweise eine Rolle bei der Entstehung von Autoimmunerkrankungen spielen[108]. So fördert ein salzreiches Milieu die Bildung pathogener T_H17-Zellen *in vitro.* Eine Hochsalzdiät (HSD) aggraviert den Krankheitsverlauf einer experimentellen autoimmunen Encephalomyelitis (EAE)[109].

Die Studie untersucht den Einfluss einer HSD auf das Darmmikrobiom und T_H17-Zellen in Maus und Mensch. Mittels 16S Sequenzierung von aus murinen Stuhlproben isolierter DNA wird gezeigt, dass eine HSD die Zusammensetzung des Mikrobioms ändert. *Lactobacillus murinus* wird als die am stärksten durch HSD regulierte Spezies identifiziert. Das Vorkommen nimmt unter der HSD signifikant ab. Gleichsam nimmt die Konzentration des von *L. murinus* produzierten Tryptophan-Metaboliten Indol-3-Laktat (ILA) unter HSD ab. Im EAE-Mausmodell verhindert die probiotische Gabe von *L. murinus* den HSD-induzierten Anstieg von T_H17-Zellen und mildert den Krankheitsverlauf ab. Im Mausmodell der Salz-sensitiven Hypertonie verhindert die Behandlung mit *L. murinus* sowohl die HSD-induzierte Zunahme der T_H17-Zellen und mildert den Anstieg des systolischen und diastolischen Blutdrucks ab. Mechanistisch könnten diese Effekte ILA-abhängig sein, da ILA die T_H17-Polarisation von murinen naiven T-Zellen inhibiert. Um den Einfluss einer HSD auf das Mikrobiom, T_H17-Zellen und Blutdruck im Menschen zu untersuchen, werden Ergebnisse einer Pilotstudie mit gesunden männlichen Probanden dargestellt, in der Probanden 6 g NaCl pro Tag zusätzlich zur normalen Ernährung über einen Zeitraum von 14 Tagen erhielten. Die HSD führt dabei zu signifikant höheren nächtlichen Blutdrücken sowie erhöhten T_H17-Zellen im Blut. Die Untersuchung der Stuhlproben mittels Shotgun-Sequenzierung zeigt, dass das Überleben von verschiedenen *Lactobacillus*-Stämmen im Vergleich zu Kontrollkohorten signifikant vermindert war.

Die Ergebnisse zeigen erstmals einen Zusammenhang zwischen erhöhter Salzaufnahme, Mikrobiom und Immunsystem auf. Zudem unterstreicht die Studie die mögliche Bedeutung des Darmmikrobioms bei der Behandlung Salz-sensitiver Erkrankungen.

Originalpublikation 4

Wilck N, Matus MG, Kearney SM, Olesen SW, Forslund K, Bartolomaeus H, Haase S, Mahler A, Balogh A, Marko L, Vvedenskaya O, Kleiner FH, Tsvetkov D, Klug L, Costea PI, Sunagawa S, Maier L, Rakova N, Schatz V, Neubert P, Fratzer C, Krannich A, Gollasch M, Grohme DA, Corte-Real BF, Gerlach RG, Basic M, Typas A, Wu C, Titze JM, Jantsch J, Boschmann M, Dechend R, Kleinewietfeld M, Kempa S, Bork P, Linker RA, Alm EJ and Muller DN. Salt-responsive gut commensal modulates T(H)17 axis and disease. ***Nature***. 2017; 551:585-589. https://doi.org/10.1038/nature24628

Nachfolgend die Zusammenfassung (Abstract), reproduziert aus der Originalveröffentlichung:

A Western lifestyle with high salt consumption can lead to hypertension and cardiovascular disease. High salt may additionally drive autoimmunity by inducing T helper 17 (T_H17) cells, which can also contribute to hypertension. Induction of T_H17 cells depends on gut microbiota; however, the effect of salt on the gut microbiome is unknown. Here we show that high salt intake affects the gut microbiome in mice, particularly by depleting *Lactobacillus murinus*. Consequently, treatment of mice with *L. murinus* prevented salt-induced aggravation of actively induced experimental autoimmune encephalomyelitis and salt-sensitive hypertension by modulating T_H17 cells. In line with these findings, a moderate high-salt challenge in a pilot study in humans reduced intestinal survival of *Lactobacillus spp*., increased T_H17 cells and increased blood pressure. Our results connect high salt intake to the gut-immune axis and highlight the gut microbiome as a potential therapeutic target to counteract salt-sensitive conditions.

2.5 Short-Chain Fatty Acid Propionate Protects From Hypertensive Cardiovascular Damage

Die Studie untersucht die Wirkung kurzkettiger Fettsäuren auf die inflammatorische Antwort bei Hypertonie und den resultierenden hypertensiven Endorganschaden. Kurzkettige Fettsäuren (*short-chain fatty acids*, SCFA) haben eine Kettenlänge von zwei bis sechs Kohlenstoffatomen und sind wichtige Vertreter immunmodulatorisch wirksamer bakterieller Metabolite[110]. Sie entstehen aus für Säuger unverdaubaren, langkettigen Kohlenhydraten der Nahrung (sogenannten Ballaststoffen) durch bakterielle Fermentation. Für verschiedene Modelle inflammatorischer Erkrankungen konnten bereits vorteilhafte Effekte einer Behandlung mit SCFA dargestellt werden. Unsere früheren Untersuchungen und Daten anderer Arbeitsgruppen belegen die protektive Wirkung kurzkettiger Fettsäuren (z.B. von Propionat) in Mausmodellen der Multiplen Sklerose sowie der experimentellen Colitis[111, 112] über die Verbesserung der Funktion von regulatorischen T-Zellen (T_{REG}).

Für das Mausmodell der Angiotensin II (AngII)-induzierten Hypertonie zeigt diese Studie, dass die perorale Behandlung mit der SCFA Propionat den kardialen und vaskulären hypertensiven Endorganschäden signifikant abschwächt. Die Propionat-Behandlung führt neben einer verzögert eintretenden, moderaten Blutdrucksenkung zu einer signifikant abgeschwächten inflammatorischen T-Zell-Antwort auf AngII, die sowohl in der Milz als auch im Herz nachweisbar ist. Das kardiale Remodeling als auch die Suszeptibilität für ventrikuläre Arrhythmien ist durch die Propionat-Behandlung deutlich vermindert. Zudem wird in einem weiteren Mausmodell der AngII-indizierten Hypertonie und akzelerierten Atherosklerose in der Apolipoprotein E Knockout-Maus gezeigt, dass die Behandlung mit Propionat die Inflammation und die Atherosklerose last vermindert. Dabei ist ein Großteil der organoprotektiven Wirkung von Propionat durch T_{REG} vermittelt, da die experimentelle Depletion von T_{REG} im Mausmodell die Protektion durch Propionat deutlich vermindert. Diese experimentelle Studie skizziert einen translatierbaren therapeutischen Ansatz der anti-inflammatorischen Behandlung von kardiovaskulären Erkrankungen durch SCFA.

Originalpublikation 5

Bartolomaeus H, Balogh A, Yakoub M, Homann S, Marko L, Hoges S, Tsvetkov D, Krannich A, Wundersitz S, Avery EG, Haase N, Kraker K, Hering L, Maase M, Kusche-Vihrog K, Grandoch M, Fielitz J, Kempa S, Gollasch M, Zhumadilov Z, Kozhakhmetov S, Kushugulova A, Eckardt KU, Dechend R, Rump LC, Forslund SK, Muller DN*, Stegbauer J* and **Wilck N***. Short-Chain Fatty Acid Propionate Protects From Hypertensive Cardiovascular Damage. ***Circulation***. 2019;139:1407-1421. https://doi.org/10.1161/CIRCULATIONAHA.118.036652

*Drs Müller, Stegbauer, and Wilck jointly supervised this work.

Nachfolgend die Zusammenfassung (Abstract), reproduziert aus der Originalveröffentlichung:

Background: Arterial hypertension and its organ sequelae show characteristics of T cell-mediated inflammatory diseases. Experimental anti-inflammatory therapies have been shown to ameliorate hypertensive end-organ damage. Recently, the CANTOS study (Canakinumab Anti-inflammatory Thrombosis Outcome Study) targeting interleukin-1β demonstrated that anti-inflammatory therapy reduces cardiovascular risk. The gut microbiome plays a pivotal role in immune homeostasis and cardiovascular health. Short-chain fatty acids (SCFAs) are produced from dietary fiber by gut bacteria and affect host immune homeostasis. Here, we investigated effects of the SCFA propionate in 2 different mouse models of hypertensive cardiovascular damage.

Methods: To investigate the effect of SCFAs on hypertensive cardiac damage and atherosclerosis, wild-type NMRI or apolipoprotein E knockout-deficient mice received propionate (200 mmol/L) or control in the drinking water. To induce hypertension, wild-type NMRI mice were infused with angiotensin II (1.44 mg·kg-1·d-1 subcutaneous) for 14 days. To accelerate the development of atherosclerosis, apolipoprotein E knockout mice were infused with angiotensin II (0.72 mg·kg-1·d-1 subcutaneous) for 28 days. Cardiac damage and atherosclerosis were assessed using histology, echocardiography, in vivo electrophysiology, immunofluorescence, and flow cytometry. Blood pressure was measured by radiotelemetry. Regulatory T cell depletion using PC61 antibody was used to examine the mode of action of propionate.

Results: Propionate significantly attenuated cardiac hypertrophy, fibrosis, vascular dysfunction, and hypertension in both models. Susceptibility to cardiac ventricular arrhythmias was significantly reduced in propionate-treated angiotensin II-infused wild-type NMRI mice. Aortic atherosclerotic lesion area was significantly decreased in propionate-treated apolipoprotein

E knockout-deficient mice. Systemic inflammation was mitigated by propionate treatment, quantified as a reduction in splenic effector memory T cell frequencies and splenic T helper 17 cells in both models, and a decrease in local cardiac immune cell infiltration in wild-type NMRI mice. Cardioprotective effects of propionate were abrogated in regulatory T cell-depleted angiotensin II-infused mice, suggesting the effect is regulatory T cell-dependent.

Conclusions: Our data emphasize an immune-modulatory role of SCFAs and their importance for cardiovascular health. The data suggest that lifestyle modifications leading to augmented SCFA production could be a beneficial nonpharmacological preventive strategy for patients with hypertensive cardiovascular disease.

Circulation

ORIGINAL RESEARCH ARTICLE

Short-Chain Fatty Acid Propionate Protects From Hypertensive Cardiovascular Damage

BACKGROUND: Arterial hypertension and its organ sequelae show characteristics of T cell–mediated inflammatory diseases. Experimental anti-inflammatory therapies have been shown to ameliorate hypertensive end-organ damage. Recently, the CANTOS study (Canakinumab Antiinflammatory Thrombosis Outcome Study) targeting interleukin-1β demonstrated that anti-inflammatory therapy reduces cardiovascular risk. The gut microbiome plays a pivotal role in immune homeostasis and cardiovascular health. Short-chain fatty acids (SCFAs) are produced from dietary fiber by gut bacteria and affect host immune homeostasis. Here, we investigated effects of the SCFA propionate in 2 different mouse models of hypertensive cardiovascular damage.

METHODS: To investigate the effect of SCFAs on hypertensive cardiac damage and atherosclerosis, wild-type NMRI or apolipoprotein E knockout–deficient mice received propionate (200 mmol/L) or control in the drinking water. To induce hypertension, wild-type NMRI mice were infused with angiotensin II (1.44 $mg \cdot kg^{-1} \cdot d^{-1}$ subcutaneous) for 14 days. To accelerate the development of atherosclerosis, apolipoprotein E knockout mice were infused with angiotensin II (0.72 $mg \cdot kg^{-1} \cdot d^{-1}$ subcutaneous) for 28 days. Cardiac damage and atherosclerosis were assessed using histology, echocardiography, in vivo electrophysiology, immunofluorescence, and flow cytometry. Blood pressure was measured by radiotelemetry. Regulatory T cell depletion using PC61 antibody was used to examine the mode of action of propionate.

RESULTS: Propionate significantly attenuated cardiac hypertrophy, fibrosis, vascular dysfunction, and hypertension in both models. Susceptibility to cardiac ventricular arrhythmias was significantly reduced in propionate-treated angiotensin II–infused wild-type NMRI mice. Aortic atherosclerotic lesion area was significantly decreased in propionate-treated apolipoprotein E knockout–deficient mice. Systemic inflammation was mitigated by propionate treatment, quantified as a reduction in splenic effector memory T cell frequencies and splenic T helper 17 cells in both models, and a decrease in local cardiac immune cell infiltration in wild-type NMRI mice. Cardioprotective effects of propionate were abrogated in regulatory T cell–depleted angiotensin II–infused mice, suggesting the effect is regulatory T cell–dependent.

CONCLUSIONS: Our data emphasize an immune-modulatory role of SCFAs and their importance for cardiovascular health. The data suggest that lifestyle modifications leading to augmented SCFA production could be a beneficial nonpharmacological preventive strategy for patients with hypertensive cardiovascular disease.

Hendrik Bartolomaeus et al

*Drs Müller, Stegbauer, and Wilck jointly supervised this work.

The full author list is available on page 1419

Key Words: angiotensin II ■ apolipoproteins E ■ fatty acids, volatile ■ immunology ■ inflammation ■ microbiota ■ Th17 cells ■ T-lymphocytes, regulatory

Sources of Funding, see page 1419

ORIGINAL RESEARCH ARTICLE

Clinical Perspective

What Is New?

- The present study shows that propionate, a short-chain fatty acid produced by intestinal bacteria, has profound beneficial anti-inflammatory properties limiting cardiovascular disease progression in 2 independent mouse models.
- Oral propionate administration beneficially influenced T helper cell homeostasis, thereby reducing cardiac hypertrophy and fibrosis, susceptibility to cardiac arrhythmias, and atherosclerotic lesion burden.
- Propionate exhibited antihypertensive effects in both models.
- Cardioprotective effects of propionate effects are mainly dependent on regulatory T cells.

What Are the Clinical Implications?

- The data suggest increased attention to propionate in hypertensive patients with a high cardiovascular risk and evidence of ongoing chronic inflammation.
- Oral propionate supplementation is simple, inexpensive, and regarded safe in humans.
- Further studies are needed to characterize the effect of propionate supplementation or interventions increasing propionate production by the gut microbiota in humans.

Hypertension drives cardiovascular disease by causing an array of pathological organ sequelae. Hypertensive tissue damage is largely mediated by different immune cells, which are activated in hypertension.[1] Hypertensive stimuli like angiotensin II (AngII) promote the activation of T cells and macrophages,[2] which subsequently may infiltrate target organs like the heart and the vasculature to cause tissue damage. Increased generation of effector memory T cells (T_{EM}) is indicative of a chronic inflammatory response in hypertension.[3] In particular, T helper cell subtypes Th17 and Th1 may promote hypertension and target organ injury by releasing proinflammatory cytokines like interleukin (IL)–17A and interferon-γ, respectively.[4,5] In contrast, regulatory T cells (Treg) counterbalance tissue inflammation by secreting anti-inflammatory IL-10.[6] Thus, the extent of hypertensive target organ damage is not solely dependent on the hemodynamic load, but, in addition, depends on the balance of pro- and anti-inflammatory immune cells. In clinical practice, hypertension usually coexists with atherosclerosis and accelerates atherosclerosis progression.[7] Atherosclerosis is similarly a chronic inflammatory disease of the vasculature, although the precise nature of the inflammatory response differs from hypertension.[8] Inflammation and vascular damage are intensified when both hypertension and atherosclerosis are present.[9] Furthermore, experimental and clinical anti-inflammatory approaches, as recently shown in the CANTOS trial (Canakinumab Antiinflammatory Thrombosis Outcome Study),[10] ameliorate hypertensive inflammatory tissue damage[11] and atherosclerosis.[12] In particular, enhancement of Treg by adoptive transfer has been shown to reduce effector T cells and ameliorate cardiac damage,[13] hypertension, vascular injury,[14] and atherosclerosis.[15]

The gut microbiota is considered important for cardiovascular health,[16] and abnormal bacterial communities have been associated with hypertension[17,18] and atherosclerosis.[19] Bacterial metabolites mediate interactions with the host. Through resorption and distribution, they can affect intestinal health, and distant functions of the immune system, the vasculature, and the heart, as well. Short-chain fatty acids (SCFAs) are a major class of bacterial metabolites and are mainly produced in the colon by bacterial fermentation of otherwise indigestible polysaccharides (fibers).[20] Beyond their importance for intestinal integrity, SCFAs have potent anti-inflammatory effects on immune cell functions. The SCFA propionate (C3) has been shown to induce the differentiation and suppressive capacity of $CD25^+$ $Foxp3^+$ Treg.[21,22] Propionate treatment of murine Treg donors significantly enhanced the protective effect of a Treg adoptive transfer in experimental autoimmune encephalomyelitis.[23] In vitro, propionate was shown to enhance the differentiation of different murine T cells dependent on the cytokine milieu.[24] It is interesting to note that propionate promoted a regulatory phenotype among T cells under Th17 polarization conditions.[24] Beneficial effects of SCFAs have been demonstrated in several other disease models, such as colitis, airway disease, metabolic syndrome, or ischemia-reperfusion injury of the kidney.[25] Although their mode of action has yet to be elucidated, SCFAs may exert their effects via inhibition of histone deacetylases (HDACs) or via G-protein–coupled receptors (Gpr) 41 and 43 and olfactory receptor 78.[25,26] In addition, a direct effect of SCFAs on renin release and vasomotor function leading to blood pressure reduction was recently suggested.[26–28]

Considering the prominent role of inflammation in both hypertension and atherosclerosis and recent insights about anti-inflammatory and Treg-promoting effects of SCFAs, we hypothesized that the SCFA propionate protects from AngII-induced cardiac and vascular damage. To test our hypothesis, we treated AngII-infused wild-type NMRI (WT) and AngII-infused apolipoprotein E knockout ($ApoE^{-/-}$) mice with C3 and analyzed inflammatory response, cardiac remodeling, and atherosclerotic lesion burden. Our data underscore the importance of propionate for cardiovascular health.

METHODS

The authors declare that all supporting data and analytical methods are available within the article and its online-only Data Supplement. The data, analytical methods, and study

materials that support the findings of this study are available from the corresponding author on reasonable request.

Animal Ethics

All experiments were in accordance with the German/European law for animal protection and were approved by the local ethic committees (G0280/13, G250/12, and G301/18). Mice were maintained on a 12:12 hour day:night cycle with constant access to food and water.

AngII-Induced Hypertension in WT Mice

Twelve-week-old male NMRI mice (purchased from Janvier Labs, outbred strain, not genetically altered, referred to as wild-type [WT] in the article), received AngII infusion (1.44 mg·kg^{-1}·d^{-1}, Calbiochem) for 14 days via subcutaneous osmotic minipumps (Alzet). Implantation was performed under isoflurane anesthesia. Mice were fed a purified diet low in fiber (Ssniff, S0087-E050). To study the effects of propionate, mice received sodium propionate (200 mmol/L, Sigma-Aldrich) or sodium chloride as control (200 mmol/L, Sigma-Aldrich) in the drinking water ad libitum. On day 13, echocardiography was performed under isoflurane anesthesia. After 14 days of AngII infusion, the mice were euthanized; blood and organs were collected for further analysis. In a subset of mice, blood pressure was measured using an implantable subcutaneous radiotelemetry transmitter (Data Science International), implanted on day −10 before AngII infusion.

Treg depletion in WT mice was achieved by intraperitoneal injections of anti-CD25 antibody (clone PC61, kindly provided by T. Hünig, University of Würzburg, Germany; 250 µg on days −1, 2, and 5 of AngII infusion). Control mice received the IgG1 isotype (Bio X Cell). Control and Treg-depleted mice received a low-fiber diet, sodium propionate in drinking water, AngII infusion subcutaneously, and implantable radiotelemetry blood pressure transmitters.

All mice were held in 1 room of the animal facility. Animals were age-matched, stratified for their body weight, and randomly assigned to the different treatment groups (n=18 WT Sham, n=36 WT AngII, n=33 WT AngII+C3, n=4 WT AngII+C3+IgG, n=4 WT AngII+C3+PC61). Two mice from the WT AngII+C3 group were excluded because of suture insufficiency at the implantation site of the minipump. Mice assigned to the same treatment group were held in the same cage. Cages were inhabited by 2 to 3 mice. All researchers were blinded during the experiment and analysis. Measured values were excluded if a technical failure of the analysis occurred or by statistical testing described below. Animal numbers for the WT experiment were a priori calculated with G*power software (Heinrich-Heine-Universität Düsseldorf) and an estimated effect size from the literature. For Treg depletion experiments, sample sizes were calculated using G*power and the estimated effect size from the WT experiments. Exact numbers are shown in the respective figures.

AngII-Induced Atherosclerosis in ApoE$^{-/-}$ Mice

To verify the effects of propionate in another AngII-dependent cardiovascular mouse model, we used ApoE$^{-/-}$ mice. In line with the NC3Rs recommendation, we reduced sample sizes by working without a sham group. ApoE$^{-/-}$mice (Taconic) were backcrossed on a C57BL/6 background at least 10 times. Eight-week-old mice received sodium propionate (200 mmol/L, Sigma-Aldrich) or sodium chloride as control (200 mmol/L, VWR) in the drinking water ad libitum during the whole experimental period, starting 5 days before the implantation of the osmotic minipumps. AngII osmotic minipumps (0.72 mg·kg^{-1}·d^{-1}, Sigma-Aldrich) were implanted subcutaneously as described previously.[29] In the fourth week of AngII infusion, systolic blood pressure was measured in conscious mice by tail-cuff plethysmography (BP-98A; Softron). During week 4, 10 measurements per mouse were recorded daily. For habituation during week 3 of AngII minipump implantation, mice were trained daily for 5 consecutive days as follows. Mice were set daily for at least 15 minutes in the mice restrainer; each day at least 20 blood pressure measurements were performed. Systolic blood pressure mean was calculated from all measured days per mouse. After 4 weeks of AngII infusion, mice were euthanized, and blood and organs were collected and used for further analyses.

For ApoE$^{-/-}$ experiments, housing, randomization, blinding, and exclusion were performed as described for the WT experiments. Thirty mice were randomly assigned per group. None of the mice were excluded during the experiment. Sample sizes were calculated using G*power and the estimated effect size from the WT experiments. Exact numbers are shown in the respective figures.

Statistical Analysis

Outliers identified by Grubbs test were excluded, and normality was assessed by Kolmogorov-Smirnov test. In groups with $n < 5$, normality could not be assessed and nonparametric distribution was assumed. To compare 2 groups, a 1-tailed unpaired *t* test or 1-tailed Mann-Whitney test was used, as appropriate. To compare >2 groups, a 1-way ANOVA followed by post hoc Tukey test or a Kruskal-Wallis test with post hoc Dunn test was used, as appropriate. Survival of the mice was visualized by Kaplan-Meier curves and statistically compared by using a 1-tailed log-rank test. Statistical analyses were performed using GraphPad Prism 6. Blood pressure time courses measured by telemetry were compared using linear mixed model calculations in R (Version 3.1.1, R Foundation). We calculated a model for each time point by including all time points before. Thereby, we received a specific time point for each longitudinal analysis where the *P* value fell short of 0.05. To compare the blood pressure area under the curve per week of AngII infusion, we used a 2-way repeated-measures ANOVA followed by a post hoc Sidak test (GraphPad Prism 6). A *P* value <0.05 was considered statistically significant.

RESULTS

Propionate Prevents AngII-Induced Systemic Inflammatory Response

To investigate the effect of propionate (C3) on immune homeostasis in an established model for hypertensive cardiac damage, WT mice were infused with AngII (1.44 mg·kg^{-1}·d^{-1}) for 2 weeks and concomitantly

ORIGINAL RESEARCH ARTICLE

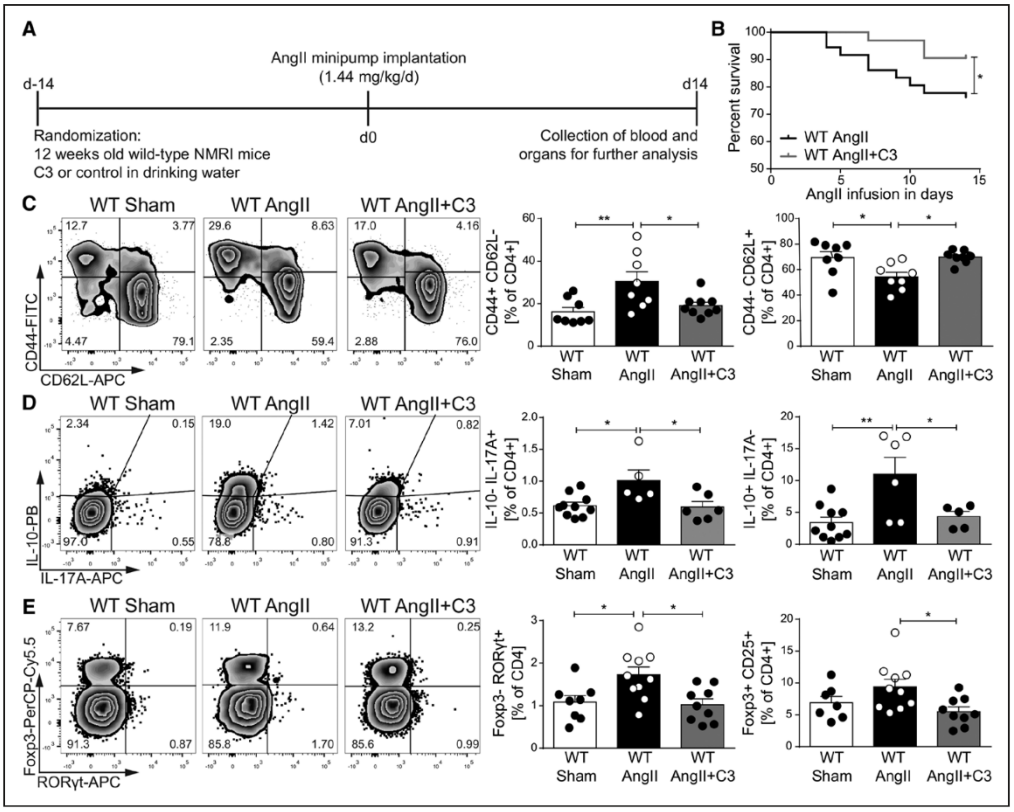

Figure 1. Propionate provides beneficial modulation of effector T cells in AngII-infused wild-type NMRI (WT) mice.
A, AngII-infused WT mice were treated with sodium propionate (C3) or sodium chloride as a control, starting 2 weeks before AngII infusion. Saline-infused mice served as nonhypertensive control group (sham). **B**, Survival curves of AngII-infused WT mice treated with C3 or control. WT AngII n=36, WT AngII+C3 n=31, **P*<0.05 by log-rank test. **C**, After 14 days of AngII, splenocytes were analyzed for CD4⁺ effector memory (CD44⁺CD62L⁻) and naive (CD44⁻ CD62L⁺) subsets. **Left**, Representative flow cytometry plots. **Right**, Quantification in percentage of CD4⁺ cells. WT Sham n=8, WT AngII n=8, WT AngII+C3 n=9. **D**, Restimulated splenocytes were analyzed for IL-10 and IL-17A by flow cytometry. **Left**, Representative flow cytometry plots. **Right**, Quantification in percentage of CD4⁺. WT Sham n=10, WT AngII n=5 to 6, WT AngII+C3 n=5 to 6. **E**, Quantification of FoxP3⁺CD25⁺ and RORγt⁺ in CD4⁺ splenocytes. **Left**, Representative flow cytometry plots. **Right**, Quantification in percentage of CD4⁺. WT Sham n=7 to 8, WT AngII n=10, WT AngII+C3 n=9. **P*<0.05, ***P*<0.01, 1-way ANOVA and Tukey post hoc for **C** through **E**. AngII indicates angiotensin II; APC, Allophycocyanin; FITC, fluorescein isothiocyanate; IL, interleukin; PB, Pacific Blue; and PerCP-Cy5.5, Peridinin-chlorophyll protein cyanine 5.5.

treated with C3 (sodium propionate, 200 mmol/L) or control (sodium chloride, 200 mmol/L) in the drinking water (Figure 1A). Saline-infused WT controls served as nonhypertensive shams. To specifically investigate the effect of exogenous C3, mice were fed a fiber-depleted purified diet to reduce intestinal SCFA production. C3 administration significantly increased C3 serum levels in AngII-infused WT mice as measured by gas chromatography–mass spectrometry (Figure IA in the online-only Data Supplement). C3 was well tolerated, as indicated by similar body weights in mice treated with C3 or control (Figure IB in the online-only Data Supplement). C3 significantly improved the survival in comparison with control-treated AngII-infused WT mice (Figure 1B). To investigate the role of C3 on systemic inflammation, spleens were harvested after 14 days and analyzed by flow cytometry. In comparison with sham-treated mice, AngII increased splenic CD4⁺ T_{EM} (CD44⁺CD62L⁻) and conversely decreased CD4⁺ naive T cells (T_N; CD44⁻ CD62L⁺), indicating a significant inflammatory response. The increase in T_{EM} and the decrease in T_N were prevented by C3 treatment (Figure 1C). CD4⁺ central memory T cells (C44⁺CD62L⁺) remained unaffected (Figure IC in the online-only Data Supplement). Further analysis of splenic Th17 cells revealed an increase in CD4⁺IL-17A⁺IL-10⁻ and CD4⁺RORγt⁺Foxp3⁻ frequencies after AngII infusion, which was normalized by C3 treatment (Figure 1D and 1E). Splenic Th1 frequencies, as measured by CD4⁺Tbet⁺ (Figure ID in the online-only Data Supplement) and CD4⁺interferon-γ⁺ cells (Figure

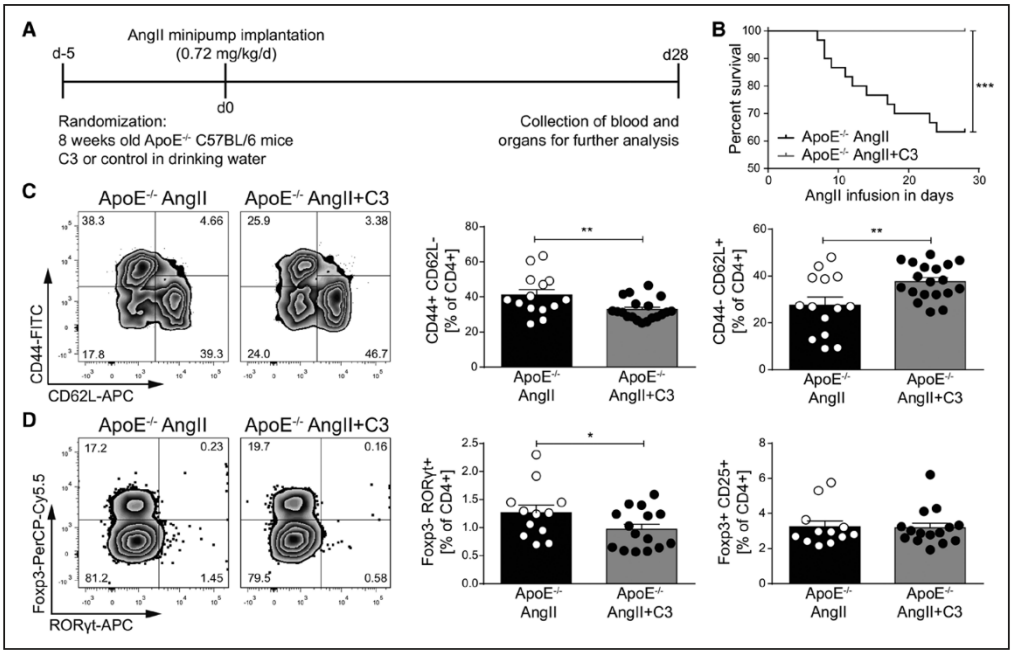

Figure 2. Propionate provides beneficial modulation of effector T cells in AngII-infused ApoE$^{-/-}$ mice.
A, AngII-infused ApoE$^{-/-}$ mice were treated with C3 or sodium chloride, starting 5 days before minipump implantation. **B**, Survival curves of AngII-infused ApoE$^{-/-}$ mice treated with C3 or control. n=30 per group, ***P<0.001 by log-rank test. **C**, After 28 days of AngII infusion, splenocytes were analyzed for CD4$^+$ effector memory (CD44$^+$CD62L$^-$) and naive (CD44$^-$CD62L$^+$) subsets. **Left**, Representative flow cytometry plots. **Right**, Quantification in percentage of CD4$^+$. ApoE$^{-/-}$ AngII n=15, ApoE$^{-/-}$ AngII+C3 n=19. **D**, Quantification of FoxP3$^+$CD25$^+$ and RORγt$^+$ in CD4$^+$ splenocytes. **Left**, Representative flow cytometry plots. **Right**, Quantification in percentage of CD4$^+$. ApoE$^{-/-}$ AngII n=12, ApoE$^{-/-}$ AngII+C3 n=15. *P<0.05, **P<0.01, by 1-tailed t test. AngII indicates angiotensin II; APC, Allophycocyanin; ApoE$^{-/-}$, apolipoprotein E knockout–deficient; C3, propionate; FITC, fluorescein isothiocyanate; and PerCP-Cy5.5, Peridinin-chlorophyll protein cyanine 5.5.

IE in the online-only Data Supplement), were not affected. It is interesting to note that Treg frequencies (CD4$^+$CD25$^+$Foxp3$^+$ and CD4$^+$IL-10$^+$IL-17A$^-$) increased after AngII, signaling a compensatory Treg response to the hypertensive stimulus, which was not observed on C3 treatment (Figure 1C and 1D).

We next tested whether C3 also affects immune homeostasis in hypertensive mice prone to develop atherosclerosis. Therefore, we infused atherosclerosis-prone ApoE$^{-/-}$ mice fed a normal chow with AngII (0.72 mg·kg^{-1}·d^{-1}) for 4 weeks and administered C3 or control (200 mmol/L) via the drinking water (Figure 2A). Similar to WT mice, C3 had no nutritive effect (Figure IF in the online-only Data Supplement). C3 treatment protected AngII-infused ApoE$^{-/-}$ mice from aortic rupture and thereby reduced mortality during the 4 weeks of AngII infusion (Figure 2B). In congruence with our findings in hypertensive mice without atherosclerosis, C3 reduced splenic T_{EM} and increased splenic T_N populations in AngII-infused ApoE$^{-/-}$ (Figure 2C), whereas splenic central memory T cells were not significantly regulated (Figure IG in the online-only Data Supplement). In addition, C3 treatment significantly reduced CD4$^+$Foxp3$^-$RORγt$^+$ Th17 cells, whereas CD4$^+$CD25$^+$FoxP3$^+$ Treg were not affected (Figure 2D). Concordant with WT, no significant regulation of Th1 cells was observed (Figure IH in the online-only Data Supplement). Our data suggest that C3 treatment ameliorates systemic inflammation in hypertensive mice with and without atherosclerosis.

Propionate Attenuates Vascular Inflammation and Atherosclerosis

Inflammation of the vascular wall is a hallmark of atherosclerosis and is amplified in the presence of elevated AngII levels.[9] To investigate if C3 modulates the atherosclerotic inflammatory response, we analyzed aortic immune cells from AngII-infused ApoE$^{-/-}$ by flow cytometry. Aortic CD4$^+$, CD8$^+$ T cell, and F4/80$^+$ macrophage numbers were reduced after C3 treatment (Figure 3A, Figure IIA in the online-only Data Supplement). Similar to splenic immune cells, the frequencies of aortic CD4$^+$ T_{EM} decreased and CD4$^+$ T_N increased after C3 treatment, whereas CD4$^+$ central memory T cells remained unaltered (Figure 3B, Figure IIB and IIC in the online-only Data Supplement).

ORIGINAL RESEARCH ARTICLE

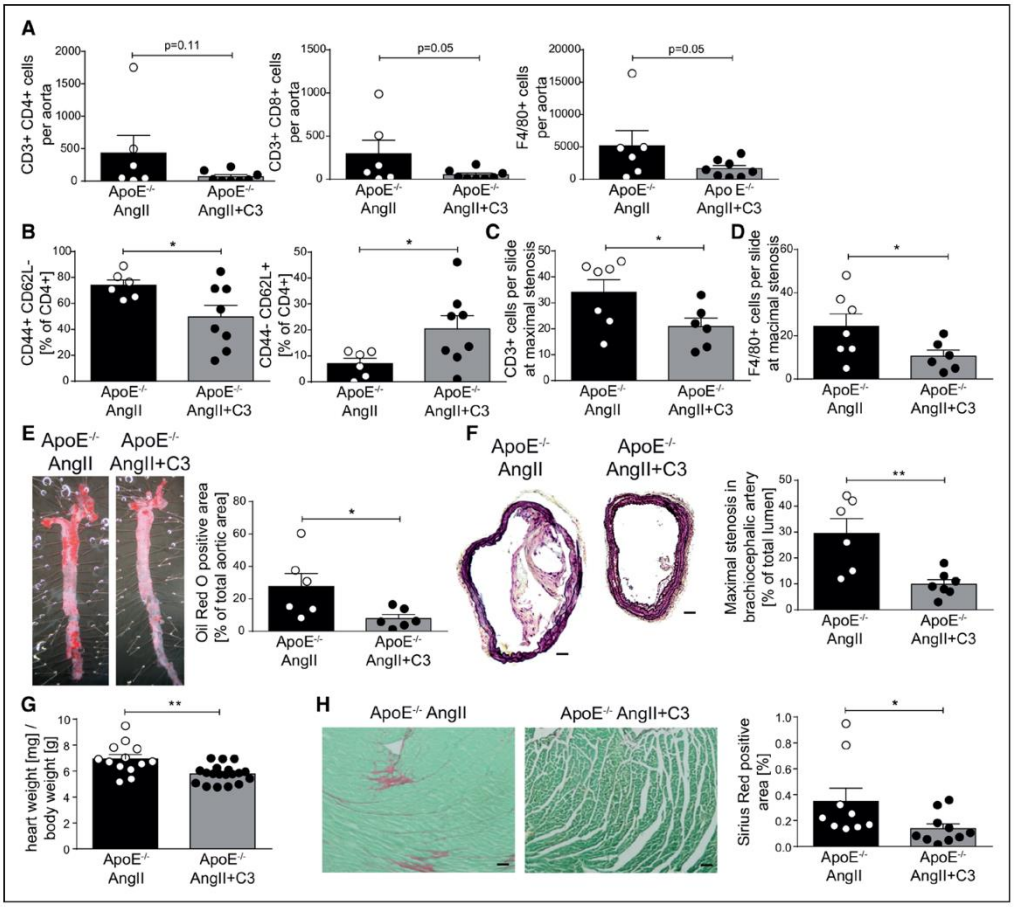

Figure 3. Propionate reduces aortic inflammation and atherosclerotic lesion burden in AngII-infused ApoE$^{-/-}$.
A, Single-cell suspensions from whole aortas of were analyzed for T helper ($CD3^+CD4^+$), cytotoxic T cells ($CD3^+CD8^+$), and macrophages ($F4/80^+$) by flow cytometry. **B**, Aortic $CD4^+$ T cells were analyzed for $CD4^+$ effector memory ($CD44^+CD62L^-$) and naive ($CD44^-CD62L^+$) subsets by flow cytometry. **C** and **D**, Quantification of CD3 and F4/80 positive cells in sections of the brachiocephalic artery, respectively. **E**, En face Oil Red O staining of whole aortas for the quantification of atherosclerotic lesion burden. **Left,** Representative aortas. **Right,** Quantification. **F**, The degree of stenosis in the brachiocephalic artery was determined in Movat-stained cross-sections. **Left**, Representative sections (scale bar=100 μm). **Right**, Quantification. **A** through **F**, ApoE$^{-/-}$ AngII n=6, ApoE$^{-/-}$ AngII+C3 n=8. **G**, Cardiac hypertrophy index (heart weight [mg]/body weight [g]) of AngII-infused ApoE$^{-/-}$ mice treated with C3 or control, ApoE$^{-/-}$ AngII n=16, ApoE$^{-/-}$ AngII+C3 n=21. **H**, Left ventricular cardiac fibrosis as analyzed by Sirius red staining. **Left**, Representative photomicrographs (scale bar=100 μm). **Right**, Quantification. ApoE$^{-/-}$ AngII n=9, ApoE$^{-/-}$ AngII+C3 n=10. *P<0.05, **P<0.01 by 1-tailed t test or Mann-Whitney test. AngII indicates angiotensin II; ApoE$^{-/-}$, apolipoprotein E knockout–deficient; and C3, propionate.

Further verification by immunohistochemical staining was obtained in atherosclerotic plaques of the brachiocephalic artery. Fewer $CD3^+$ T cells and $F4/80^+$ macrophages were detected in brachiocephalic artery sections from C3-treated AngII-infused ApoE$^{-/-}$ mice (Figure 3C and 3D). To determine whether these potentially beneficial effects would translate into a reduction in atherosclerotic lesion burden, we performed en face Oil Red O staining of whole aortas. Aortic atherosclerotic lesion burden was significantly reduced in C3-treated mice (Figure 3E). Likewise, considerably less stenosis of the brachiocephalic artery was detected in C3-treated mice (Figure 3F). Because AngII infusion may induce cardiac remodeling in addition to atherosclerosis, we measured heart weight and analyzed cardiac fibrosis in AngII-infused ApoE$^{-/-}$ by Sirius red staining. Hypertrophy index and interstitial fibrosis were significantly attenuated in C3-treated AngII-infused ApoE$^{-/-}$ (Figure 3G through 3H). C3 did not affect serum levels of total cholesterol, triglycerides, high-density lipoprotein, or low-density lipoprotein cholesterol (Table I in the online-only Data

Supplement). Taken together, C3 treatment reduced vascular inflammation, atherosclerotic lesion burden, and cardiac remodeling in AngII-infused ApoE$^{-/-}$independent of blood lipid levels.

Propionate Ameliorates Cardiac Immune Cell Infiltration and Remodeling

Alongside vascular injury, hypertension generates an inflammatory response in the heart, which promotes cardiac remodeling.[30] Flow cytometric analysis of heart-infiltrating lymphocytes on day 14 of AngII infusion in WT mice revealed a significant increase in the number of cardiac CD4$^+$ T cells, CD8$^+$ T cells, and F4/80$^+$ macrophages, which was significantly decreased by C3 treatment (Figure 4A through 4E). These results could be confirmed by analysis of CD4 and CD8 immunofluorescence of cardiac cryosections (Figure IIIA and IIIB in the online-only Data Supplement). We further analyzed the proportion of Th17, Treg, and Th1 subsets among infiltrating cardiac T cells. The AngII-induced increase in cardiac CD4$^+$ RORγt$^+$Foxp3$^-$ frequencies was prevented by C3 treatment, whereas the fraction of CD4$^+$FoxP3$^+$RORγt$^-$ T cells and CD4$^+$T-bet$^+$ T cells was similar between groups (Figure 4F, Figure IIIC in the online-only Data Supplement). IL-10 mRNA levels in cardiac tissue were analyzed by quantitative polymerase chain reaction. In line with IL-10 expression in CD4$^+$ splenocytes, C3 prevented the AngII-induced increase in *Il-10* expression (Figure IIID in the online-only Data Supplement).

As expected, AngII increased the cardiac hypertrophy index after 14 days of infusion, an effect that was prevented by C3 treatment (Figure 4G). We confirmed this finding using echocardiography, which revealed an increased left ventricular wall thickness after AngII infusion and a significant reduction on C3 treatment (Figure 4H). Accordingly, the AngII-induced increase in cardiac brain natriuretic peptide (*Nppb*) and β-myosin heavy chain (*Mhy7*) mRNA expression was prevented by C3 treatment as measured by quantitative polymerase chain reaction (Figure 4I and 4J). C3 treatment also prevented the AngII-induced increase in interstitial and perivascular cardiac fibrosis as measured by fibronectin and collagen I immunofluorescence, respectively (Figure 4K and 4L). Consistently, the number of cardiac fibroblasts analyzed using fibroblast-specific protein 1 immunofluorescence was similarly regulated (Figure 4M). Cardiac mRNA expression of connective tissue growth factor (*Ctgf*) and neutrophil gelatinase–associated lipocalin (*Ngal*) also confirmed the antifibrotic effect (Figure IIIE and IIIF in the online-only Data Supplement).

HDAC inhibitory properties have been attributed to SCFAs,[31] and HDAC inhibition is known to inhibit AngII-induced cardiac hypertrophy and fibrosis.[32] To address this potential mechanism of action, we cultured rat neonatal cardiomyocytes in vitro in the presence or absence of AngII and tested the effect of C3 on atrial natriuretic peptide (*Nppa*) mRNA expression as a sensitive hypertrophy marker in comparison with the known class I and II HDAC inhibitor trichostatin A. In contrast to trichostatin A, C3 did not reduce *Nppa* mRNA expression (Figure IV in the online-only Data Supplement), suggesting that the effect of C3 on AngII-induced cardiac hypertrophy is HDAC-independent.

Effect of Propionate Depends on Treg

C3 has been shown to promote Treg generation and function.[22] We hypothesized that the observed beneficial effects of C3 in AngII-infused hypertensive WT mice are Treg-dependent. To test this hypothesis, we depleted Tregs in C3-treated AngII-infused WT mice by injecting anti-CD25 antibody (intraperitoneal injections of antibody clone PC61 on days –1, 2, and 5 of AngII infusion). We assessed inflammation and cardiac fibrosis in comparison with nondepleted C3-treated AngII-infused WT mice receiving IgG control antibodies intraperitoneally; Treg depletion was well tolerated and had no effect on body weight (Figure VA in the online-only Data Supplement). On day 14 of AngII infusion, splenic Tregs were still significantly depleted in comparison with the IgG control group (Figure 5A). Treg-depleted AngII-infused WT mice treated with C3 displayed a significant increase in splenic CD4$^+$IL-17A$^+$ cell frequencies in comparison with nondepleted mice (Figure 5B), reinforced by a similar trend in splenic CD4$^+$RORγt$^+$ Foxp3$^-$ frequencies (Figure VB in the online-only Data Supplement). Splenic Th1 cells, as measured by interferon-γ and T-bet expression in CD4$^+$ cells, were not regulated (Figure VC and VD in the online-only Data Supplement). The inhibitory effect of C3 on splenic CD4$^+$ T_{EM} frequencies was abrogated in Treg-depleted mice (Figure 5C), without altering central memory T cells or T_N populations (Figure VE and VF in the online-only Data Supplement). Significantly more CD4$^+$ and CD8$^+$ lymphocytes could be detected in heart sections of Treg-depleted AngII-infused mice treated with C3 (Figure 5D and 5E). Cardiac hypertrophy measured by echocardiography and hypertrophy index was only nonsignificantly increased in Treg-depleted C3-treated AngII-infused mice in comparison with mice injected with IgG (Figure 5F, Figure VG in the online-only Data Supplement). However, hearts from Treg-depleted mice displayed a significantly increased interstitial and perivascular fibrosis, as well as increased numbers of fibroblast-specific protein 1$^+$ cells (Figure 5G through 5I). These findings suggest that Treg may partially mediate the cardioprotective effects of C3.

ORIGINAL RESEARCH ARTICLE

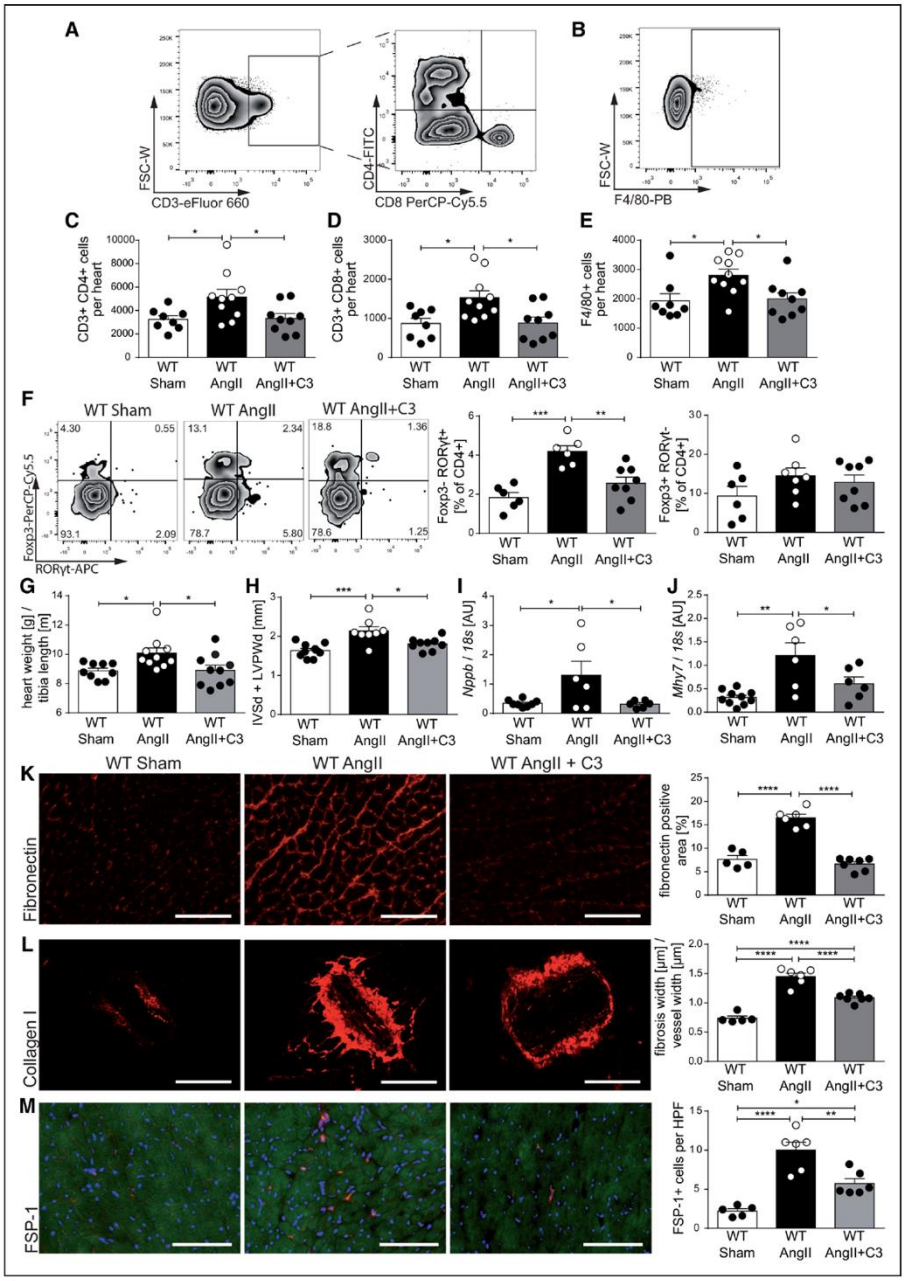

Figure 4. Propionate attenuates hypertensive cardiac damage in AngII-infused wild-type NMRI (WT) mice.
A through **E**, Single cells were isolated from hearts of sham-infused or AngII-infused WT mice treated with C3 or control and analyzed by flow cytometry for T helper cells ($CD3^+CD4^+$), cytotoxic T cells ($CD3^+CD8^+$), and macrophages ($F4/80^+$), as well. **A** and **B**, Representative ratings. **C** through **E**, The respective quantifications. WT Sham n=8, WT AngII n=10, WT AngII+C3 n=9. **F**, Analysis of $CD4^+FoxP3^+$ and $CD4^+ROR\gamma t^+$ cells in heart single-cell suspensions. **Left**, Representative flow cytometry plots. **Right**, Quantifications. WT Sham n=6, WT AngII n=6 to 7, WT AngII+C3 n=8. **G**, Cardiac hypertrophy index (heart weight [g]/tibia length [m]), (WT Sham n=9, WT AngII n=10, WT AngII+C3 n=10). **H**, Left ventricular wall thickness (sum of IVSd and LVPWd) as measured by (*Continued*)

Moderate Blood Pressure–Lowering Effect of Propionate

Recent studies have shown that C3 may directly influence vasomotor function.[26] To achieve C3-induced vasorelaxation in isolated perfused kidneys, very high, supraphysiological concentrations (3–100 mmol/L) were needed (data not shown). In addition, atomic force microscopy–based nanoindentation measurements in ApoE$^{-/-}$ mice revealed that C3 treatment softens endothelial cells in comparison with control treatment (data not shown). Next, we examined whether chronic oral C3 treatment influences blood pressure in AngII-infused WT mice and performed continuous radiotelemetric blood pressure measurements. Systolic and diastolic blood pressures in C3-treated WT mice were not affected in the initial phase, but were lowered toward the second week of AngII infusion, reaching statistical significance from day 11 and day 12 on (Figure 6A and 6C). Calculating the area under the curve for both weeks of AngII infusion separately, a significant difference in systolic and diastolic blood pressure was seen only for the second week (Figure 6B and 6D). This pattern was confirmed in the ApoE$^{-/-}$ model, because tail-cuff measurements of the systolic blood pressure were significantly lower in C3-treated mice during the last week of AngII infusion (Figure VIA in the online-only Data Supplement). In parallel with the reduced blood pressure, endothelial dysfunction in both mouse models was significantly ameliorated by C3 treatment as shown by ex vivo analysis of endothelium-dependent relaxation (Figure VIB and VIC in the online-only Data Supplement). To analyze whether C3 affects endothelial dysfunction in an immune cell–free setting, we incubated isolated mesenteric rings from untreated healthy mice with IL-17A and AngII for 24 hours in vitro (Figure VID in the online-only Data Supplement). Coincubation with C3 under cell culture conditions did not prevent endothelial dysfunction, making a direct endothelium-mediated effect of C3 less likely (Figure VID in the online-only Data Supplement).

To elucidate if the blood pressure–lowering effect of C3 is influenced directly by Treg, we measured blood pressure by radiotelemetry in C3-treated AngII-infused WT mice receiving the Treg-depleting anti-CD25 antibody or IgG control. However, systolic and diastolic blood pressures were similar in the initial and late phases of AngII infusion. (Figure VIE and VIF in the online-only Data Supplement). Therefore, the blood pressure–lowering effect of chronic C3 treatment cannot be ascribed to a single mechanism.

Propionate Reduces Susceptibility to Ventricular Arrhythmias

To further explore if the beneficial effects of C3 treatment on AngII-induced cardiac remodeling led to an improved functional outcome, we assessed the susceptibility of AngII-infused WT mice treated with C3 or control to ventricular arrhythmias by in vivo cardiac electrophysiological studies. Ventricular tachyarrhythmias are prognostically relevant in hypertensive heart disease.[33] Susceptibility to ventricular tachyarrhythmias was significantly lower in C3-treated animals (5 of 7 C3-treated mice could not be triggered at all), whereas sustained tachyarrhythmias could be triggered in 85% of control-treated mice (Figure 7A and 7B). Connexin 43, a major gap junction protein required for electric integrity, was relocated from the intercalated disk to the lateral border of the cardiomyocytes on AngII infusion as shown by immunofluorescence (Figure 7C). Consequently, the degree of connexin 43 colocalization with N-cadherin (localized at the intercalated disc) was reduced on AngII infusion in comparison with sham-infused mice and maintained by concomitant C3 treatment (Figure 7C). These data show that C3 improves cardiac electric remodeling.

DISCUSSION

Metabolites released by the gut microbiota exert an important influence on the cardiovascular health of their host. SCFAs, end products of bacterial metabolism in the intestine, which are primarily derived from dietary fibers, have been attributed health-promoting properties in several diseases, in particular because of their potent action on immune cells.[25] Epidemiological studies suggest that sufficient fiber intake may be beneficial in hypertension,[34] but we lack a comprehensive understanding of the underlying mechanisms. The current study demonstrates that the SCFA propionate prevents target organ damage in hypertensive mice with and without atherosclerosis by maintaining immune homeostasis.

Hypertension stands out among health risk factors because it promotes several cardiovascular diseases, including hypertensive heart disease and atherosclerosis. Beyond blood pressure control, the need to address the inflammatory response to hypertensive stimuli has been

Figure 4 Continued. echocardiography (WT Sham n=9, WT AngII n=8, WT AngII+C3 n=9). Cardiac *Nppb* (**I**) and *Mhy7* (**J**) expression as measured by qPCR at the end of the treatment (WT Sham n=10, WT AngII n=6, WT AngII+C3 n=6). **K** through **M**, Immunofluorescence analysis of cardiac left ventricular fibrosis using fibronectin (**K**), collagen I (**L**), and FSP-1 (**M**) antibodies (WT Sham n=5, WT AngII n=6, WT AngII+C3 n=7). **Left**, Representative photomicrographs (scale bar=100 µm). **Right**, Quantifications. **P*<0.05, ***P*<0.01, ****P*<0.001, *****P*<0.0001 by 1-way ANOVA and Tukey post hoc. AngII indicates angiotensin II; APC, Allophycocyanin; AU, arbitrary unit; C3, propionate; FITC, fluorescein isothiocyanate; FSC-W, forward scatter width; FSP-1, fibroblast-specific protein 1; HPF, high-power field; IVSd, interventricular septal thickness at diastole; LVPWd, left ventricular posterior wall end diastole; PB, Pacific Blue; PerCP-Cy5.5, Peridinin-chlorophyll protein cyanine 5.5; and qPCR, quantitative polymerase chain reaction.

ORIGINAL RESEARCH ARTICLE

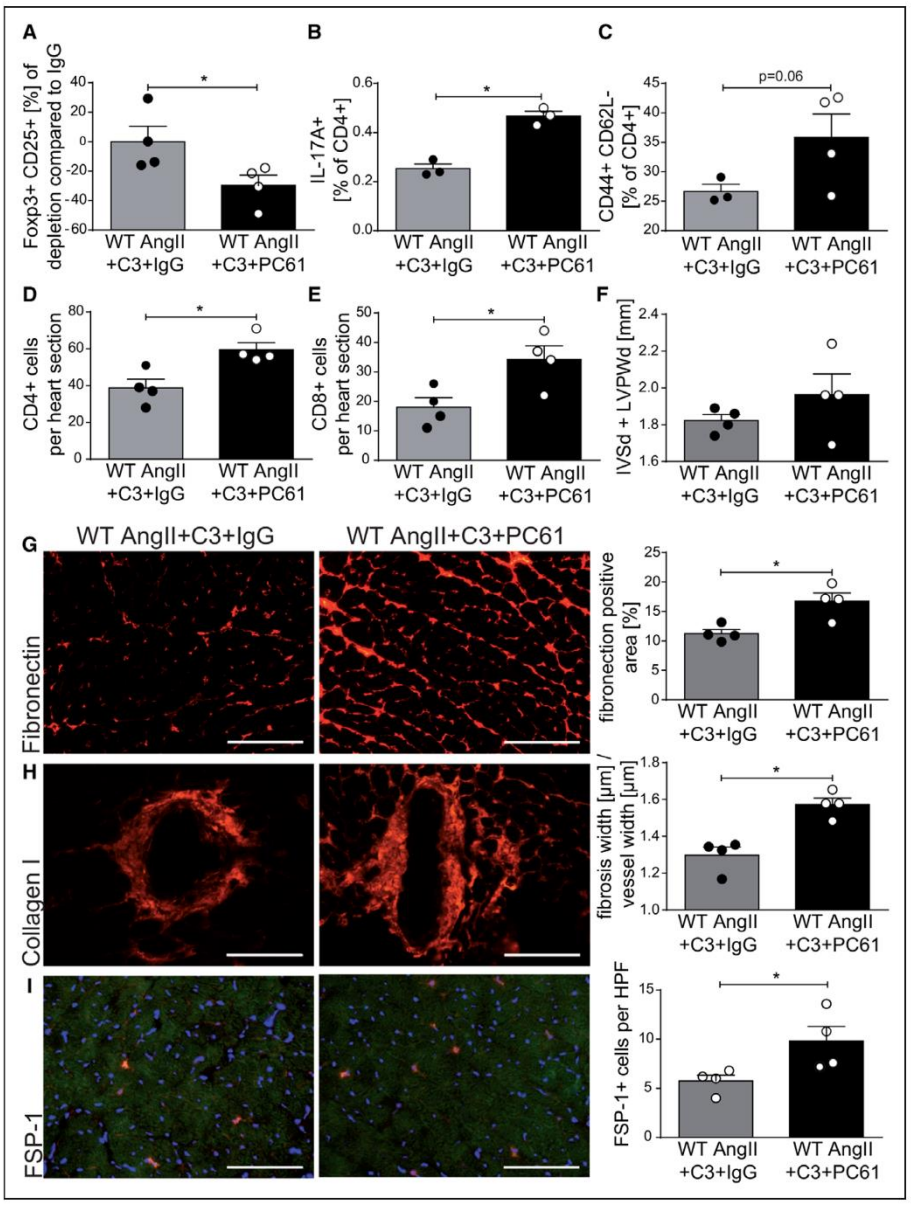

Figure 5. Depletion of regulatory T cells abrogates the effect of propionate in AngII-infused wild-type NMRI (WT) mice.
AngII-infused WT mice received propionate treatment with intraperitoneal injections of anti-CD25 (PC61) or IgG control. **A**, Relative reduction in splenic $CD4^+CD25^+Foxp3^+$ regulatory T cells at day 14 of AngII infusion in comparison with IgG control. **B**, IL-17A production in $CD4^+$ restimulated splenocytes measured by flow cytometry. **C**, Splenic effector memory T cell ($CD4^+CD44^+CD62L^-$) frequencies. **D** and **E**, Analysis of $CD4^+$ (**D**) and $CD8^+$ (**E**) lymphocytes in heart sections using immunofluorescence. **F**, Left ventricular wall thickness (sum of IVSd and LVPWd) as measured by echocardiography. **G** through **I**, Immunofluorescence analysis of left ventricular fibrosis using fibronectin (**G**), collagen I (**H**), and FSP-1 (**I**) antibodies. **Left**, Representative photomicrographs (scale bars=100 µm). **Right**, quantification. **A, D** through **I**, WT AngII+C3+IgG n=4, WT AngII+C3+PC61 n=4; **B** and **C**, WT AngII+C3+IgG n=3, WT AngII+C3+PC61 n=4, **P*<0.05 by 1-tailed Mann-Whitney test. AngII indicates angiotensin II; C3, propionate; FSP-1, fibroblast-specific protein 1; IgG, immunoglobulin G; IL, interleukin; IVSd, interventricular septal thickness at diastole; and LVPWd, left ventricular posterior wall end diastole.

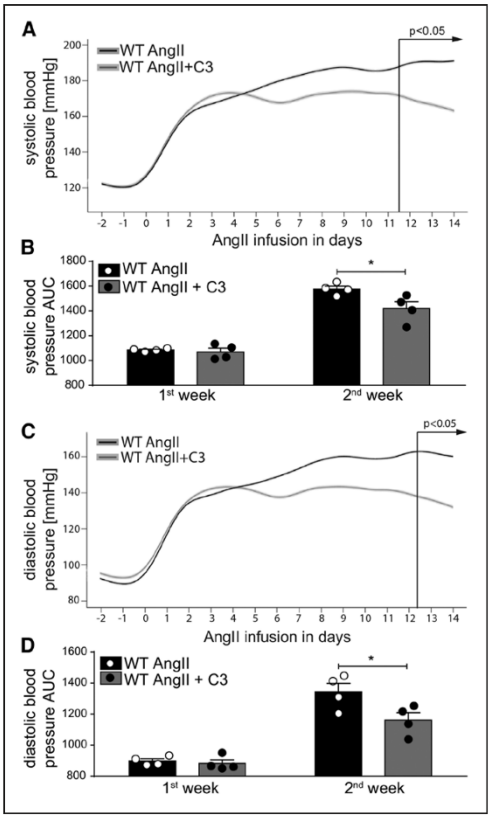

Figure 6. Propionate treatment shows a blood pressure–lowering effect confined to the second week of AngII infusion.
A through **D**, Systolic and diastolic blood pressure were measured continuously by radiotelemetry in AngII-infused WT mice treated with C3 or control. **A** and **C,** Shown are smoothened curves over time for systolic and diastolic blood pressure, respectively. *P* values by linear mixed model. **B** and **D**, Shown are systolic and diastolic pressures calculated as AUC in week 1 and week 2 of AngII infusion, respectively. n=4 per group. **P*<0.05 by 2-way repeated-measurement ANOVA and Sidak post hoc. AngII indicates angiotensin II; AUC, area under the curve; C3, propionate; and WT, wild-type NMRI.

recognized.[35] In particular, effector T cells and macrophages are activated in hypertension and mediate damage to the heart and the vasculature. Experimental evidence suggests that immunosuppression[11] or adoptive transfer of Treg[13,14] limits hypertensive target organ damage, although potential side effects prevent further translation of these interventions.

Propionate improved the survival in both WT and ApoE$^{-/-}$ mice and attenuated the systemic T cell response to AngII as indicated by reduced splenic T_{EM} frequencies together with less proinflammatory Th17 cells. It is more important that this anti-inflammatory effect was also detectable in the respective target organs, because fewer T cells and macrophages infiltrated the heart and the aorta, respectively. AngII-induced cardiac hypertrophy and fibrosis were attenuated by propionate in both mouse models. In ApoE$^{-/-}$ mice, propionate treatment led to a reduced atherosclerotic lesion burden despite unaltered blood lipid levels.

Our data expand on recent observations demonstrating the cardioprotective and renoprotective effects of a high-fiber diet in uninephrectomized deoxycorticosterone acetate–treated hypertensive mice.[28] The authors ascribe the observed cardiorenal protection to acetate, another SCFA, and demonstrate a beneficial gene regulation in hearts and kidneys from uninephrectomized deoxycorticosterone acetate mice fed a high-fiber diet or supplemented with acetate. The authors also describe decreased blood pressures at the end of the treatment.[28] Our current study expands on the cardiovascular protective effects of SCFAs, pointing to an important contribution of immune homeostasis in the SCFA-mediated effect.

Activation of T cells can be observed in response to hypertensive stimuli, indicated by increased T_{EM}.[36] The balance of Treg and effector T cells is critically important in hypertension and hypertensive end-organ damage. Tregs are known to limit target organ damage in hypertension, because adoptive transfer of Treg has been shown to dampen AngII-induced cardiac[13] and vascular[14] damage. Moreover, depletion of Treg accelerates atherosclerosis in hypercholesterolemic mice.[15] Increased proportions of T_{EM} are associated with the development of atherosclerosis in humans and mice.[37,38] In addition to the significant effect on T_{EM}, our data suggest that the propionate effect is also Treg-dependent, because Treg depletion abrogated the propionate effect on systemic and cardiac inflammation, and on cardiac fibrosis, as well. It is interesting to note that we observed an increase in splenic Treg frequencies in response to AngII along with an increase in Th17 cells, suggesting that Tregs counterbalance the AngII-elicited effector Th17 response. This observation is supported by a study showing increased plasma levels of the anti-inflammatory cytokine IL-10 in AngII-infused mice.[14] Likewise, serum IL-10 is increased in hypercholesterolemic mice,[39] and human atherosclerotic lesions show substantial IL-10 expression.[40] Enrichment of Treg in nonlymphoid tissues in response to inflammatory stimuli or injury can be observed in various contexts,[41] likely as a compensatory response. It is most important that propionate treatment in our study preserved the balance of Th17 and Treg in AngII-infused mice. Furthermore, Treg depletion abrogated the anti-inflammatory effect of propionate, indicated by increased Th17 and T_{EM} frequencies.

The current picture of SCFA signaling to host cells is complex, because both the interaction with Gpr and olfactory receptor 78,[26] and HDAC inhibitory properties, as well, have been described. Propionate is known

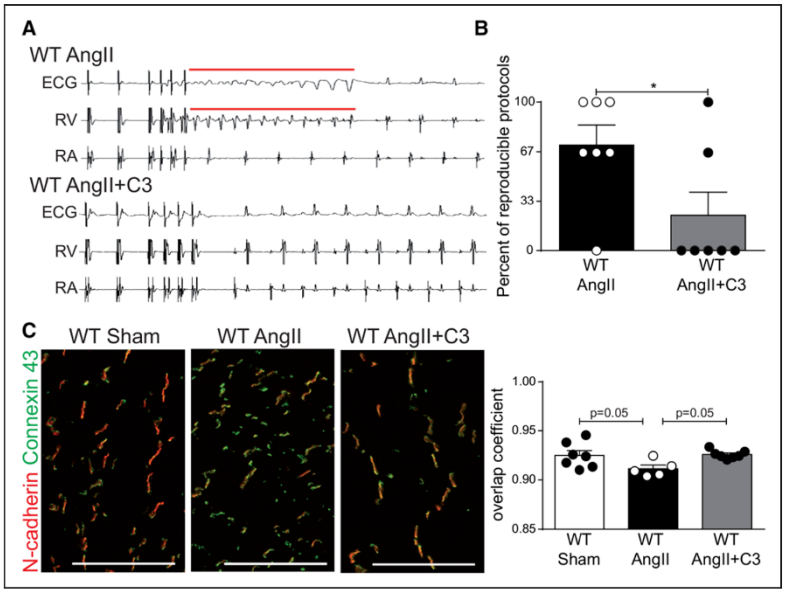

Figure 7. Propionate reduces susceptibility to ventricular arrhythmias in AngII-infused wild-type NMRI (WT) mice.
In vivo programmed electric ventricular stimulations were performed in AngII-infused WT mice treated with C3 or control. **A**, Representative original tracings showing the induction of ventricular tachyarrhythmia. Surface ECG, right ventricular (RV), and right atrial (RA) recordings are shown. **B**, Quantification of ventricular arrhythmias susceptibility. n=7 per group, **P*<0.05 by Mann-Whitney test. **C**, Immunofluorescent costaining of connexin 43 (green) and N-cadherin (red) in cardiac cryosections from sham-infused or AngII-infused WT mice treated with C3 or control. WT Sham n=7, WT AngII n=5, WT AngII+C3 n=7. Representative photomicrographs (scale bar=100 µm) and quantification of colocalization. *P* values by 1-way ANOVA and Tukey post hoc. AngII indicates angiotensin II; and C3, propionate.

to bind to Gpr41 and Gpr43, and independent studies have shown that either Gpr41[42] or Gpr43,[21] but also HDAC inhibition,[22] may account for the propionate effect on immune cells. Direct propionate signaling to nonimmune cells such as cardiomyocytes may also play a role, because the inhibition of HDAC activity is known to inhibit cardiomyocyte hypertrophy.[32] To distinguish effects mediated by immune cells from direct effects on cardiomyocytes, we tested the ability of propionate to inhibit AngII-induced hypertrophy of rat primary neonatal cardiomyocytes in comparison with the established HDAC inhibitor trichostatin A. However, propionate failed to inhibit cardiomyocyte hypertrophy. These data, together with the abrogation of the propionate effects by Treg depletion, suggest that T cells substantially contribute to the protective effect of propionate. Further studies are warranted to dissect other potentially protective pleiotropic effects of propionate.

Our data demonstrate that, in addition to beneficial immunomodulatory effects, propionate moderately reduced blood pressure in both models. Endothelial dysfunction is associated with the development of essential hypertension.[43] In isolated mesenteric arteries of AngII-infused WT mice and in isolated perfused kidneys of AngII-infused ApoE$^{-/-}$ mice, we could show that chronic C3 treatment improved endothelium-dependent vasodilation. Earlier reports described acute vasodilation in response to propionate and other SCFAs.[26] Similarly, we observed a C3-induced vasodilation in isolated perfused kidneys, albeit only at supraphysiological concentrations. Propionate was previously shown to activate Gpr41 located in the vascular endothelium, mediating the vasodilating effect of propionate, although the downstream signaling cascades are less clear.[27] In isolated mesenteric rings, C3 failed to improve endothelial function in a short-term experiment. Nevertheless, we cannot exclude that chronic Gpr41-mediated antihypertensive effects of propionate on the endothelium may have contributed to target organ protection. However, blood pressure reduction was observed only toward the late phase of AngII infusion, suggesting rather a chronic effect of propionate on hypertension, thereby arguing against a direct endothelium-dependent effect.

It is important to note that an increased occurrence of ventricular tachycardia can be observed in hypertensive patients with left ventricular hypertrophy, which is prognostically relevant.[33] Spatial redistribution of gap junction proteins is characteristic of pathological electric remodeling and has been described in the human hypertrophic myocardium.[44] We show that propionate improves electric remodeling with a reduced suscep-

tibility to programmed ventricular tachycardia in vivo. Our observation is confirmed by attenuated cardiac gap junction remodeling in propionate-treated mice, as indicated by a reduced lateralization of connexin 43 in cardiomyocytes. Similarly, beneficial effects were observed earlier in AngII-infused mice after adoptive Treg transfer.[13]

In conclusion, propionate treatment protects from cardiac damage and reduces atherosclerosis in experimental hypertension. Target organ protection by propionate is at least partially dependent on Treg, although other pleiotropic effects likely contribute to this result. Our data provide further experimental evidence for the importance of microbiota-derived SCFAs in promoting host cardiovascular health. Hypertension and atherosclerosis account for a substantial proportion of worldwide cardiovascular morbidity and mortality. Propionate could be important in improving cardiovascular health, because both atherosclerosis and hypertensive cardiac remodeling were significantly reduced on propionate treatment in our study. It is interesting to note that several subsets of gut bacteria are capable of producing propionate,[45] some of which were shown to be less abundant in experimental hypertension[46] and hypertensive patients.[17] Consequently, oral supplementation with propionate or its precursors may be beneficial in hypertensive individuals to prevent damage to target organs. Current hypertension guidelines recommend lifestyle modifications before the initiation of any pharmacological antihypertensive treatment.[47] Dietary augmentation of propionate is an affordable intervention, and our observations suggest that this could be a novel approach to prevent hypertensive damage to target organs.

ARTICLE INFORMATION

Received June 27, 2018; accepted October 18, 2018.

The online-only Data Supplement is available with this article at https://www.ahajournals.org/doi/suppl/10.1161/CIRCULATIONAHA.118.036652.

Authors

Hendrik Bartolomaeus; András Balogh, MD, PhD; Mina Yakoub, MSc; Susanne Homann, PhD; Lajos Markó, MD, PhD; Sascha Höges; Dmitry Tsvetkov, MD; Alexander Krannich, PhD; Sebastian Wundersitz; Ellen G. Avery, MSc; Nadine Haase, PhD; Kristin Kräker, MSc; Lydia Hering, PhD; Martina Maase, PhD; Kristina Kusche-Vihrog, PhD; Maria Grandoch, MD; Jens Fielitz, MD; Stefan Kempa, PhD; Maik Gollasch, MD, PhD; Zhaxybay Zhumadilov, MD, PhD; Samat Kozhakhmetov, PhD; Almagul Kushugulova, MD, PhD; Kai-Uwe Eckardt, MD; Ralf Dechend, MD; Lars Christian Rump, MD; Sofia K. Forslund, PhD; Dominik N. Müller, PhD*; Johannes Stegbauer, MD*; Nicola Wilck, MD*

Correspondence

Dominik N. Müller, PhD, Experimental and Clinical Research Center & Max Delbruck Center for Molecular Medicine in the Helmholtz Association, Lindenberger Weg 80, 13125 Berlin, Germany. Email dominik.mueller@mdc-berlin.de

Affiliations

Experimental and Clinical Research Center, a Cooperation of Charité-Universitätsmedizin Berlin and Max Delbruck Center for Molecular Medicine, Germany (H.B., A.B., L.M., D.T., S.W., E.G.A., N.H., K.K., J.F., M.G., R.D., S.K.F., D.N.M., N.W.). Charité-Universitätsmedizin Berlin, Corporate Member of Freie Universität Berlin, Humboldt-Universität zu Berlin, and Berlin Institute of Health, Germany (H.B., A.B., L.M., D.T., S.W., E.G.A., J.B., R.D., S.K.F., D.N.M., N.W.). Max Delbruck Center for Molecular Medicine in the Helmholtz Association, Berlin, Germany (H.B., A.B., L.M., A. Krannich, E.G.A., N.H., K.K., S. Kempa, R.D., S.K.F., D.N.M., N.W.). DZHK (German Centre for Cardiovascular Research), partner site Berlin (H.B., A.B., L.M., S.W., E.G.A., N.H., K.K., J.F., R.D., D.N.M., N.W.). Berlin Institute of Health, Germany (H.B., A.B., L.M., E.G.A., N.H., K.K., R.D., S.K.F., D.N.M., N.W.). Department of Nephrology, Medical Faculty, University Hospital Düsseldorf, Heinrich-Heine-University, Germany (M.Y., S. Höges, L.H., L.C.R., J.S.). Institute of Pharmacology and Clinical Pharmacology, University Hospital, Universitätsrat, Düsseldorf, Germany (S. Homann, M.G.). Department of Pharmacology and Experimental Therapy, Institute of Experimental and Clinical Pharmacology and Toxicology, Eberhard Karls University Hospitals and Clinics and Interfaculty Center of Pharmacogenomics and Drug Research, Tübingen, Germany (D.T.). Institute of Physiology II, University of Münster, Germany (M.M., K.K.-V.). DZHK (German Centre for Cardiovascular Research), partner site Greifswald (J.F.). Integrative Proteomics and Metabolomics Platform, Berlin Institute for Medical Systems Biology, Germany (S. Kempa). Medizinische Klinik mit Schwerpunkt Nephrologie und Internistische Intensivmedizin Charité – Universitätsmedizin Berlin, Germany (M.G., K.-U.E., N.W.). National Laboratory Astana Nazarbayev University, Kazakhstan (Z.Z., S. Kozhakhmetov, A. Kushugalova). Department of Cardiology and Nephrology, HELIOS-Klinikum, Berlin, Germany (R.D.). European Molecular Biology Laboratory, Structural and Computational Biology Unit, Heidelberg, Germany (S.K.F.).

Acknowledgments

We thank Gabriele N'diaye, Ilona Kramer, May-Britt Köhler, Jana Czychi, Martin Taube, Dr Sabine Bartel, and Christina Schwandt for technical assistance, and Thomas Hünig for the provision of the PC61 antibody. Drs Wilck, Müller, and Stegbauer and H. Bartolomaeus designed the study. H. Bartolomaeus and Drs Wilck, Balogh, Markó, Avery, Haase, and Kräker performed experiments in wild-type NMRI mice, and analyzed and interpreted the data. Drs Yakoub, Homann, Höges, Hering, Maase, Kusche-Vihrog, Grandoch, and Stegbauer performed experiments in ApoE$^{-/-}$ mice, and analyzed and interpreted the data. Drs A. Kushugulova, S. Kozhakhmetov, Zhumadilov, Dechend, Eckardt, Rump, and Forslund helped with data analysis and interpretation. Drs Wundersitz and Fielitz performed and analyzed neonatal cardiomyocyte experiments. S. Kempa performed and analyzed gas chromatography–mass spectrometry measurements. Dr Krannich performed statistical analyses. Dr Wilck, H. Bartolomaeus, and Drs Stegbauer and Müller wrote the manuscript with input from all authors.

Sources of Funding

Dr Wilck is participant in the Clinician Scientist Program funded by the Berlin Institute of Health. Drs Yakoub, Grandoch, Rump, S. Homann, and Stegbauer were supported by the DFG (German Research Foundation) (IRTG 1902). Dr Fielitz received funding from the DZHK (German Center for Cardiovascular Research) (81Z5400153) and the DFG (German Research Foundation) (FI 965/5-2).

Disclosures

None.

REFERENCES

1. Wenzel U, Turner JE, Krebs C, Kurts C, Harrison DG, Ehmke H. Immune mechanisms in arterial hypertension. *J Am Soc Nephrol*. 2016;27:677–686. doi: 10.1681/ASN.2015050562
2. Rudemiller NP, Crowley SD. Interactions between the immune and the renin-angiotensin systems in hypertension. *Hypertension*. 2016;68:289–296. doi: 10.1161/HYPERTENSIONAHA.116.06591
3. Itani HA, Harrison DG. Memories that last in hypertension. *Am J Physiol Renal Physiol*. 2015;308:F1197–F1199. doi: 10.1152/ajprenal.00633.2014
4. Markó L, Kvakan H, Park JK, Qadri F, Spallek B, Binger KJ, Bowman EP, Kleinewietfeld M, Fokuhl V, Dechend R, Müller DN. Interferon-γ signaling inhibition ameliorates angiotensin II-induced cardiac damage. *Hypertension*. 2012;60:1430–1436. doi: 10.1161/HYPERTENSIONAHA.112.199265
5. Madhur MS, Lob HE, McCann LA, Iwakura Y, Blinder Y, Guzik TJ, Harrison DG. Interleukin 17 promotes angiotensin II-induced hypertension and vascular dysfunction. *Hypertension*. 2010;55:500–507. doi: 10.1161/HYPERTENSIONAHA.109.145094

6. Didion SP, Kinzenbaw DA, Schrader LI, Chu Y, Faraci FM. Endogenous interleukin-10 inhibits angiotensin II-induced vascular dysfunction. *Hypertension*. 2009;54:619–624. doi: 10.1161/HYPERTENSIONAHA.109.137158
7. Rosendorff C, Lackland DT, Allison M, Aronow WS, Black HR, Blumenthal RS, Cannon CP, de Lemos JA, Elliott WJ, Findeiss L, Gersh BJ, Gore JM, Levy D, Long JB, O'Connor CM, O'Gara PT, Ogedegbe O, Oparil S, White WB; American Heart Association; American College of Cardiology; American Society of Hypertension. Treatment of hypertension in patients with coronary artery disease: a scientific statement from the American Heart Association, American College of Cardiology, and American Society of Hypertension. *J Am Coll Cardiol*. 2015;65:1998–2038. doi: 10.1016/j.jacc.2015.02.038
8. Hansson GK, Hermansson A. The immune system in atherosclerosis. *Nat Immunol*. 2011;12:204–212. doi: 10.1038/ni.2001
9. Mazzolai L, Duchosal MA, Korber M, Bouzourene K, Aubert JF, Hao H, Vallet V, Brunner HR, Nussberger J, Gabbiani G, Hayoz D. Endogenous angiotensin II induces atherosclerotic plaque vulnerability and elicits a Th1 response in ApoE-/- mice. *Hypertension*. 2004;44:277–282. doi: 10.1161/01.HYP.0000140269.55873.7b
10. Ridker PM, Everett BM, Thuren T, MacFadyen JG, Chang WH, Ballantyne C, Fonseca F, Nicolau J, Koenig W, Anker SD, Kastelein JJP, Cornel JH, Pais P, Pella D, Genest J, Cifkova R, Lorenzatti A, Forster T, Kobalava Z, Vida-Simiti L, Flather M, Shimokawa H, Ogawa H, Dellborg M, Rossi PRF, Troquay RPT, Libby P, Glynn RJ; CANTOS Trial Group. Antiinflammatory therapy with canakinumab for atherosclerotic disease. *N Engl J Med*. 2017;377:1119–1131. doi: 10.1056/NEJMoa1707914
11. Muller DN, Shagdarsuren E, Park JK, Dechend R, Mervaala E, Hampich F, Fiebeler A, Ju X, Finckenberg P, Theuer J, Viedt C, Kreuzer J, Heidecke H, Haller H, Zenke M, Luft FC. Immunosuppressive treatment protects against angiotensin II-induced renal damage. *Am J Pathol*. 2002;161:1679–1693. doi: 10.1016/S0002-9440(10)64445-8
12. Bäck M, Hansson GK. Anti-inflammatory therapies for atherosclerosis. *Nat Rev Cardiol*. 2015;12:199–211. doi: 10.1038/nrcardio.2015.5
13. Kvakan H, Kleinewietfeld M, Qadri F, Park JK, Fischer R, Schwarz I, Rahn HP, Plehm R, Wellner M, Elitok S, Gratze P, Dechend R, Luft FC, Muller DN. Regulatory T cells ameliorate angiotensin II-induced cardiac damage. *Circulation*. 2009;119:2904–2912. doi: 10.1161/CIRCULATIONAHA.108.832782
14. Barhoumi T, Kasal DA, Li MW, Shbat L, Laurant P, Neves MF, Paradis P, Schiffrin EL. T regulatory lymphocytes prevent angiotensin II-induced hypertension and vascular injury. *Hypertension*. 2011;57:469–476. doi: 10.1161/HYPERTENSIONAHA.110.162941
15. Ait-Oufella H, Salomon BL, Potteaux S, Robertson AK, Gourdy P, Zoll J, Merval R, Esposito B, Cohen JL, Fisson S, Flavell RA, Hansson GK, Klatzmann D, Tedgui A, Mallat Z. Natural regulatory T cells control the development of atherosclerosis in mice. *Nat Med*. 2006;12:178–180. doi: 10.1038/nm1343
16. Tang WH, Hazen SL. The contributory role of gut microbiota in cardiovascular disease. *J Clin Invest*. 2014;124:4204–4211. doi: 10.1172/JCI72331
17. Li J, Zhao F, Wang Y, Chen J, Tao J, Tian G, Wu S, Liu W, Cui Q, Geng B, Zhang W, Weldon R, Auguste K, Yang L, Liu X, Chen L, Yang X, Zhu B, Cai J. Gut microbiota dysbiosis contributes to the development of hypertension. *Microbiome*. 2017;5:14. doi: 10.1186/s40168-016-0222-x
18. Wilck N, Matus MG, Kearney SM, Olesen SW, Forslund K, Bartolomaeus H, Haase S, Mähler A, Balogh A, Markó L, Vvedenskaya O, Kleiner FH, Tsvetkov D, Klug L, Costea PI, Sunagawa S, Maier L, Rakova N, Schatz V, Neubert P, Frätzer C, Krannich A, Gollasch M, Grohme DA, Côrte-Real BF, Gerlach RG, Basic M, Typas A, Wu C, Titze JM, Jantsch J, Boschmann M, Dechend R, Kleinewietfeld M, Kempa S, Bork P, Linker RA, Alm EJ, Müller DN. Salt-responsive gut commensal modulates TH17 axis and disease. *Nature*. 2017;551:585–589. doi: 10.1038/nature24628
19. Karlsson FH, Fåk F, Nookaew I, Tremaroli V, Fagerberg B, Petranovic D, Bäckhed F, Nielsen J. Symptomatic atherosclerosis is associated with an altered gut metagenome. *Nat Commun*. 2012;3:1245. doi: 10.1038/ncomms2266
20. Cummings JH, Pomare EW, Branch WJ, Naylor CP, Macfarlane GT. Short chain fatty acids in human large intestine, portal, hepatic and venous blood. *Gut*. 1987;28:1221–1227.
21. Smith PM, Howitt MR, Panikov N, Michaud M, Gallini CA, Bohlooly-Y M, Glickman JN, Garrett WS. The microbial metabolites, short-chain fatty acids, regulate colonic Treg cell homeostasis. *Science*. 2013;341:569–573. doi: 10.1126/science.1241165
22. Arpaia N, Campbell C, Fan X, Dikiy S, van der Veeken J, deRoos P, Liu H, Cross JR, Pfeffer K, Coffer PJ, Rudensky AY. Metabolites produced by commensal bacteria promote peripheral regulatory T-cell generation. *Nature*. 2013;504:451–455. doi: 10.1038/nature12726
23. Haghikia A, Jörg S, Duscha A, Berg J, Manzel A, Waschbisch A, Hammer A, Lee DH, May C, Wilck N, Balogh A, Ostermann AI, Schebb NH, Akkad DA, Grohme DA, Kleinewietfeld M, Kempa S, Thöne J, Demir S, Müller DN, Gold R, Linker RA. Dietary fatty acids directly impact central nervous system autoimmunity via the small intestine. *Immunity*. 2015;43:817–829. doi: 10.1016/j.immuni.2015.09.007
24. Park J, Kim M, Kang SG, Jannasch AH, Cooper B, Patterson J, Kim CH. Short-chain fatty acids induce both effector and regulatory T cells by suppression of histone deacetylases and regulation of the mTOR-S6K pathway. *Mucosal Immunol*. 2015;8:80–93. doi: 10.1038/mi.2014.44
25. Koh A, De Vadder F, Kovatcheva-Datchary P, Bäckhed F. From dietary fiber to host physiology: short-chain fatty acids as key bacterial metabolites. *Cell*. 2016;165:1332–1345. doi: 10.1016/j.cell.2016.05.041
26. Pluznick JL, Protzko RJ, Gevorgyan H, Peterlin Z, Sipos A, Han J, Brunet I, Wan LX, Rey F, Wang T, Firestein SJ, Yanagisawa M, Gordon JI, Eichmann A, Peti-Peterdi J, Caplan MJ. Olfactory receptor responding to gut microbiota-derived signals plays a role in renin secretion and blood pressure regulation. *Proc Natl Acad Sci U S A*. 2013;110:4410–4415. doi: 10.1073/pnas.1215927110
27. Natarajan N, Hori D, Flavahan S, Steppan J, Flavahan NA, Berkowitz DE, Pluznick JL. Microbial short chain fatty acid metabolites lower blood pressure via endothelial G protein-coupled receptor 41. *Physiol Genomics*. 2016;48:826–834. doi: 10.1152/physiolgenomics.00089.2016
28. Marques FZ, Nelson E, Chu PY, Horlock D, Fiedler A, Ziemann M, Tan JK, Kuruppu S, Rajapakse NW, El-Osta A, Mackay CR, Kaye DM. High-fiber diet and acetate supplementation change the gut microbiota and prevent the development of hypertension and heart failure in hypertensive mice. *Circulation*. 2017;135:964–977. doi: 10.1161/CIRCULATIONAHA.116.024545
29. Stegbauer J, Chen D, Herrera M, Sparks MA, Yang T, Königshausen E, Gurley SB, Coffman TM. Resistance to hypertension mediated by intercalated cells of the collecting duct. *JCI Insight*. 2017;2:e92720. doi: 10.1172/jci.insight.92720
30. Nicoletti A, Heudes D, Mandet C, Hinglais N, Bariety J, Michel JB. Inflammatory cells and myocardial fibrosis: spatial and temporal distribution in renovascular hypertensive rats. *Cardiovasc Res*. 1996;32:1096–1107.
31. Waldecker M, Kautenburger T, Daumann H, Busch C, Schrenk D. Inhibition of histone-deacetylase activity by short-chain fatty acids and some polyphenol metabolites formed in the colon. *J Nutr Biochem*. 2008;19:587–593. doi: 10.1016/j.jnutbio.2007.08.002
32. Kee HJ, Sohn IS, Nam KI, Park JE, Qian YR, Yin Z, Ahn Y, Jeong MH, Bang YJ, Kim N, Kim JK, Kim KK, Epstein JA, Kook H. Inhibition of histone deacetylation blocks cardiac hypertrophy induced by angiotensin II infusion and aortic banding. *Circulation*. 2006;113:51–59. doi: 10.1161/CIRCULATIONAHA.105.559724
33. McLenachan JM, Henderson E, Morris KI, Dargie HJ. Ventricular arrhythmias in patients with hypertensive left ventricular hypertrophy. *N Engl J Med*. 1987;317:787–792. doi: 10.1056/NEJM198709243171302
34. Streppel MT, Arends LR, van't Veer P, Grobbee DE, Geleijnse JM. Dietary fiber and blood pressure: a meta-analysis of randomized placebo-controlled trials. *Arch Intern Med*. 2005;165:150–156. doi: 10.1001/archinte.165.2.150
35. Caillon A, Schiffrin EL. Role of inflammation and immunity in hypertension: recent epidemiological, laboratory, and clinical evidence. *Curr Hypertens Rep*. 2016;18:21. doi: 10.1007/s11906-016-0628-7
36. Itani HA, Xiao L, Saleh MA, Wu J, Pilkinton MA, Dale BL, Barbaro NR, Foss JD, Kirabo A, Montaniel KR, Norlander AE, Chen W, Sato R, Navar LG, Mallal SA, Madhur MS, Bernstein KE, Harrison DG. CD70 exacerbates blood pressure elevation and renal damage in response to repeated hypertensive stimuli. *Circ Res*. 2016;118:1233–1243. doi: 10.1161/CIRCRESAHA.115.308111
37. Ammirati E, Cianflone D, Vecchio V, Banfi M, Vermi AC, De Metrio M, Grigore L, Pellegatta F, Pirillo A, Garlaschelli K, Manfredi AA, Catapano AL, Maseri A, Palini AG, Norata GD. Effector memory T cells are associated with atherosclerosis in humans and animal models. *J Am Heart Assoc*. 2012;1:27–41. doi: 10.1161/JAHA.111.000125
38. Klingenberg R, Gerdes N, Badeau RM, Gisterå A, Strodthoff D, Ketelhuth DF, Lundberg AM, Rudling M, Nilsson SK, Olivecrona G, Zoller S, Lohmann C, Lüscher TF, Jauhiainen M, Sparwasser T, Hansson GK. Depletion of FOXP3+ regulatory T cells promotes hypercholesterolemia and atherosclerosis. *J Clin Invest*. 2013;123:1323–1334. doi: 10.1172/JCI63891
39. Xie JJ, Wang J, Tang TT, Chen J, Gao XL, Yuan J, Zhou ZH, Liao MY, Yao R, Yu X, Wang D, Cheng Y, Liao YH, Cheng X. The Th17/Treg functional im-

balance during atherogenesis in ApoE(-/-) mice. *Cytokine*. 2010;49:185–193. doi: 10.1016/j.cyto.2009.09.007
40. Mallat Z, Heymes C, Ohan J, Faggin E, Lesèche G, Tedgui A. Expression of interleukin-10 in advanced human atherosclerotic plaques: relation to inducible nitric oxide synthase expression and cell death. *Arterioscler Thromb Vasc Biol*. 1999;19:611–616.
41. Burzyn D, Benoist C, Mathis D. Regulatory T cells in nonlymphoid tissues. *Nat Immunol*. 2013;14:1007–1013. doi: 10.1038/ni.2683
42. Trompette A, Gollwitzer ES, Yadava K, Sichelstiel AK, Sprenger N, Ngom-Bru C, Blanchard C, Junt T, Nicod LP, Harris NL, Marsland BJ. Gut microbiota metabolism of dietary fiber influences allergic airway disease and hematopoiesis. *Nat Med*. 2014;20:159–166. doi: 10.1038/nm.3444
43. Yang G, Istas G, Höges S, Yakoub M, Hendgen-Cotta U, Rassaf T, Rodriguez-Mateos A, Hering L, Grandoch M, Mergia E, Rump LC, Stegbauer J. Angiotensin-(1-7)-induced Mas receptor activation attenuates atherosclerosis through a nitric oxide-dependent mechanism in apolipoproteinE-KO mice. *Pflugers Arch*. 2018;470:661–667. doi: 10.1007/s00424-018-2108-1
44. Kostin S, Dammer S, Hein S, Klovekorn WP, Bauer EP, Schaper J. Connexin 43 expression and distribution in compensated and decompensated cardiac hypertrophy in patients with aortic stenosis. *Cardiovasc Res*. 2004;62:426–436. doi: 10.1016/j.cardiores.2003.12.010
45. Louis P, Flint HJ. Formation of propionate and butyrate by the human colonic microbiota. *Environ Microbiol*. 2017;19:29–41. doi: 10.1111/1462-2920.13589
46. Yang T, Santisteban MM, Rodriguez V, Li E, Ahmari N, Carvajal JM, Zadeh M, Gong M, Qi Y, Zubcevic J, Sahay B, Pepine CJ, Raizada MK, Mohamadzadeh M. Gut dysbiosis is linked to hypertension. *Hypertension*. 2015;65:1331–1340. doi: 10.1161/HYPERTENSIONAHA.115.05315
47. Whelton PK, Carey RM, Aronow WS, Casey DE Jr, Collins KJ, Dennison Himmelfarb C, DePalma SM, Gidding S, Jamerson KA, Jones DW, MacLaughlin EJ, Muntner P, Ovbiagele B, Smith SC Jr, Spencer CC, Stafford RS, Taler SJ, Thomas RJ, Williams KA Sr, Williamson JD, Wright JT Jr. 2017 ACC/AHA/AAPA/ABC/ACPM/AGS/APhA/ASH/ASPC/NMA/PCNA Guideline for the Prevention, Detection, Evaluation, and Management of High Blood Pressure in Adults: A Report of the American College of Cardiology/American Heart Association Task Force on Clinical Practice Guidelines. *Circulation*. 2018;138:e484–e594. doi: 10.1161/CIR.0000000000000596

3 DISKUSSION

3.1 Das UPS in der Atherosklerose – ein therapeutisches Angriffsziel?

Für die Hypothese, nach der das Ubiquitin-Proteasom-System (UPS) ein Angriffsziel für neuartige Therapiestrategien in der Atherosklerose sein könnte, sprechen verschiedene Beobachtungen. Zunächst die Feststellung, dass verschiedene für die Pathophysiologie der Atherosklerose wichtige Prozesse wie die Inflammation, die Proliferation vaskulärer glatter Muskelzellen, der oxidative Stress und die gestörte Proteinhomöostase durch das Ubiquitin-Proteasom-System (UPS) beeinflusst oder gar entscheidend reguliert werden[113]. So ist das UPS essentiell für die Aktivierung des pro-inflammatorischen Transkriptionsfaktors NF-κB, insbesondere durch die proteasomale Degradation des inhibitorischen Proteins IκBα, welches die nukleäre Translokation von NF-κB und damit NF-κB-abhängige pro-inflammatorische Genexpression verhindert. Studien, welche Anzeichen für eine erhöhte proteasomale Aktivität, mehr NF-κB und weniger IκBα in atherosklerotischen Plaques der *Arteria carotis* nachweisen konnten, sprechen für einen relevanten Zusammenhang von NF-κB und UPS in der Atherosklerose[52, 114-117]. Allerdings ist die Frage, ob das UPS in der Atherosklerose überaktiv oder aber insuffizient ist, durchaus umstritten[54, 113, 118, 119], da andere Autoren in histologischen Analysen vermehrt Ubiquitin als Anzeichen für ein möglicherweise überlastetes UPS darstellen konnten[120]. Die in diesem Zusammenhang relevante Aktivierung der *unfolded protein response* als Zeichen der gestörten Proteinhomöostase wurde bereits in Tiermodellen der Atherosklerose beschrieben[121]. Letztendlich ist es durchaus denkbar, dass das UPS in der Atherosklerose phasenspezifisch reguliert ist: In frühen Phasen könnte ein aktivierter Zustand des UPS eine vermehrte NF-κB-Aktivierung und Inflammationsförderung bewirken, während ein möglicherweise insuffizient agierendes UPS in späten Phasen durch vermehrt anfallende oxidativ geschädigte Proteine apparent wird, was wiederum zur Bildung von Protein-Aggregaten, Zelltod und Plaque-Instabilisierung führen könnte[118]. Beide Szenarien – Überaktivität in frühen und Insuffizienz in späten Stadien – könnten unterschiedliche (phasenspezifische) Konsequenzen für den Effekt niedrigdosierter Proteasominhibition auf die Atherosklerose haben[53, 122]. Unabhängig davon beweisen die anti-proliferativen Effekte höherdosierter Proteasominhibition auf die Intimaproliferation (relevant im Kontext der lokalen Behandlung der Neointima-Bildung nach Stentimplantation), dass das UPS auch für weitere klinische Indikationen im Rahmen der Atherosklerose ein relevantes Angriffsziel sein kann[123].

In der Zusammenschau ist das UPS als zentrales proteolytisches System in vielerlei Hinsicht ein potentiell vielversprechendes Angriffsziel für neuartige therapeutische Strategien zur Progressionshemmung der Atherosklerose. Gleichzeitig sind die zentrale Bedeutung des UPS für die zelluläre Homöostase, konzentrationsabhängige Effekte von Proteasominhibitoren als auch die möglicherweise

phasenspezifische Regulation des UPS in der Atherosklerose enorme Herausforderungen für die gezielte Modulation relevanter pathophysiologischer Prozesse der Atherosklerose.

In der vorliegenden Arbeit wurden zwei unterschiedliche Strategien der Beeinflussung des UPS im atherosklerotischen Mausmodell verfolgt, um Erkenntnisse zur Rolle der UPS in der Atherosklerose zu gewinnen: (I) Die systemische Behandlung mittels niedrigdosierter Proteasominhibition und (II) der genetische Knockout immunoproteasomealer Untereinheiten.

3.1.1 Niedrigdosierte Proteasominhibition

Originalpublikation 1 der vorliegenden Arbeit zeigt, dass eine niedrigdosierte Proteasominhibition mit dem Proteasominhibitor Bortezomib die frühe Atherosklerose (6 Wochen Western Diät und begleitende Bortezomib-Behandlung) im LDLR-/- Mausmodell inhibiert[122]. Als für die Hemmung dieser frühen Atherosklerose verantwortliche Mechanismen konnten anti-inflammatorische und anti-oxidative Effekte identifiziert werden. Da u.a. mit dem endothelialen Adhäsionsmolekül VCAM-1, dem Zytokin IL-6 und dem Chemokin MCP-1 mehrere NF-κB-Zielgene durch Bortezomib-Behandlung reduziert wurden, könnten diese Befunde die Hypothese, dass in frühen Atherosklerose-Stadien die Krankheitsprogression durch eine vermehrte UPS-abhängige NF-κB-Aktivierung und -Genexpression getrieben ist, bestätigen. Durch den Einsatz niedriger Bortezomib-Konzentrationen wurden keine toxischen Nebenwirkungen festgestellt. Interessanterweise konnten wir in einer nachfolgenden Studie im selben Mausmodell zeigen, dass dieselbe Bortezomib-Dosis und Therapiedauer in einem späteren Atherosklerose-Stadium, d.h. bei einer vorbestehenden, fortgeschrittenen Atherosklerose (24 Wochen Western Diät, davon in den letzten 6 Wochen Bortezomib-Behandlung), keine Progressionshemmung bewirkte zugunsten ungünstiger, Plaque-destabilisierender Effekte[124]. Diese beiden Studien im LDLR-/- Mausmodell demonstrieren Stadien-abhängige Effekte niedrigdosierter Proteasominhibition und unterstützen damit indirekt die Vermutung, dass das UPS in der Atherosklerose phasenspezifisch reguliert sein könnte. Im Gegensatz dazu zeigten van Herck et al. in einem anderen Mausmodell der Atherosklerose, in dem Plaques im ApoE-Knockout Mausmodell durch Verengung der Arteria carotis induziert werden, dass eine 4-wöchige Bortezomib-Behandlung zwar nicht die Größe früher oder fortgeschrittenerer Plaques beeinflusst, wohl aber die Zusammensetzung fortgeschrittenerer Plaques durch Förderung von Plaqueinstabilität[125]. Allerdings wurden hier deutlich höhere Bortezomib-Konzentrationen verwendet[125]. Herrmann et al. wiederum zeigten in mit einer Hochcholesterol-Diät gefütterten Schweinen, dass eine 12-wöchige Proteasominhibition mit dem Inhibitor MLN-273 einen fördernden Einfluss auf die Atherosklerose hat[53]. Dagegen hat die Proteasominhibition mit dem Inhibitor MG132 im Kaninchenmodell der Urämie-induzierten Atherosklerose vorteilhafte Effekte[126].

Zusammenfassend lässt sich festhalten, dass die Vergleichbarkeit der ausschließlich experimentellen Studien zum Effekt von Proteasominhibitoren auf die Atherosklerose eingeschränkt ist. Unterschiedliche Tiermodelle, Atherosklerose-Stadien, unterschiedliche Proteasominhibitoren und insbesondere unterschiedliche Konzentrationen und Behandlungsdauern erschweren die Vergleichbarkeit. In Ermangelung eines klaren Bildes verbietet sich somit derzeit die Translation in klinische Studien. Ein klinisches Szenario, in dem eine derart prävalente chronische Erkrankung wie die Atherosklerose mit langfristiger und potentiell toxischer Proteasominhibition behandelt wird, ist derzeit nicht vorstellbar. Kardiovaskuläre Ereignisse im Rahmen der Therapie des Multiplen Myeloms (MM) durch hochdosierte Proteasominhibition mit Bortezomib oder Carfilzomib verdeutlichen das Potential für Nebenwirkungen im kardiovaskulären System[127, 128]. Dabei stehen vor allem kardiotoxische Effekte im Vordergrund. Auch wenn die der vorliegenden Arbeit zugrundeliegenden experimentellen Studien deutlich geringere Proteasominhibitor-Dosierungen als für die MM-Therapie verwendet haben, sind spezifischere Ansätze zur Beeinflussung des UPS notwendig, um die Atherosklerose effizient und nebenwirkungsarm zu beeinflussen. Möglicherweise versprechen Inhibitoren des Immunoproteasoms oder die Beeinflussung von E3-Ligasen des UPS eine spezifischere Ansteuerung von Atherosklerose-relevanten Prozessen ohne Nebenwirkungen unspezifischer Proteasominhibition.

3.1.2 Das Immunoproteasom

Der Hypothese von Originalpublikation 2 liegen Vorarbeiten zur Rolle der immunoproteasomalen Untereinheit β5i/LMP7 bei der Bewältigung von Zytokin-induziertem oxidativem Stress zugrunde. Währen Seifert et al.[92] die effiziente β5i/LMP7-abhängige Degradation geschädigter Proteine zeigten, konnte dies von Nathan et al.[91] nicht bestätigt werden. In beiden Publikationen wurde als *in vivo* Modell der Inflammation die experimentelle Autoimmunenzephalitis (EAE) verwendet[91, 92]. Da die Atherosklerose sowohl durch vaskulär-systemische Inflammation und erhöhte Zytokin-Expression gekennzeichnet ist, als auch durch oxidativen Stress, untersucht Originalpublikation 2 für die genetische β5i/LMP7 Defizienz in LDLR-/- Mäusen, ob frühe und fortgeschrittene Atherosklerose-Stadien beeinflusst werden. Im Ergebnis konnte festgestellt werden, dass im Vergleich zu β5i/LMP7-exprimierenden LDLR-/- Mäusen β5i/LMP7-defiziente LDLR-/- Mäuse eine vergleichbare Atherosklerose sowohl in frühen als auch fortgeschrittenen Stadien aufwiesen. Es konnten weder vermehrte Ubiquitin-Akkumulationen in Plaques β5i/LMP7-defizienter Mäuse detektiert werden, noch signifikante Unterschiede in der Plaque-Größe oder Ausdehnung des nekrotischen Kerns. Damit widerspricht Originalpublikation 2 im Kontext der Atherosklerose der Hypothese, dass β5i/LMP7-haltige Proteasomen im Vergleich zu Standardproteasomen eine höhere Kapazität für den Abbau polyubiquitinierter Proteine haben. Damit trägt Originalpublikation 2 zur Debatte über die Bedeutung der immunoproteasomalen Untereinheit β5i/LMP7 für den Zytokin-induzierten oxidativen Stress bei, wenngleich die gewonnen Ergebnisse in

einem Atherosklerose-Modell erhoben wurden und nicht auf andere Erkrankungen und Modelle generalisierbar sind. Darüber hinaus bestätigt die Studie, dass eine β5i/LMP7-Defizienz zur Bildung von Proteasom-Subtypen führt, wobei β5i/LMP7 durch seine entsprechende Standard-Untereinheit β5 ersetzt werden kann. Unterschiedliche Proteasom-Subtypen sind in verschiedenen Spezies und Organen untersucht worden und deren proteolytische Aktivität verglichen worden, wobei unterschiedliche Charakteristika demonstriert wurden[129-131]. Originalpublikation 2 konnte jedoch keine Unterschiede in der proteolytischen Aktivität feststellen, gemessen in Lysaten von Makrophagen. Zudem konnten keine Unterschiede in der Akkumulation polyubiquitinierter Proteine in Makrophagen nach oxidativem Stress nachgewiesen werden, im Einklang mit den Beobachtungen von Nathan et al[91]. Zusammenfassend demonstriert die Arbeit die erstaunliche Plastizität des Proteasoms mit unterschiedlichen Proteasom-Subtypen und konnte keine Aggravation der Atherosklerose bei β5i/LMP7-Defizienz nachweisen. Sie schließt jedoch nicht aus, dass immunoproteasomale Untereinheiten von therapeutischem Nutzen in der Atherosklerose sein könnten, da selektive Inhibitoren des Immunoproteasoms (ONX-0914: Inhibition von β5i/LMP7 und β1i/LMP2; KZR-329: selektive Inhibition von β5i/LMP7; KZR-504: selektive Inhibition von β1i/LMP2[132]) erhältlich sind. In klassischen Mausmodellen der Atherosklerose sind diese selektiven Inhibitoren jedoch derzeit nicht untersucht. Interessanterweise verhindert die Ko-Inhibition von β5i/LMP7 und β1i/LMP2 im Mausmodell eine Transplantat-Arteriosklerose von aortalen Allografts[133]. Es ist möglich, dass die unter 3.1.1 bereits diskutierten stadien- und konzentrationsabhängigen Effekte von älteren Proteasominhibitoren auch bei neueren, selektiveren Inhibitoren des Immunoproteasoms zu berücksichtigen sind.

3.2 Das Mikrobiom, Inflammation und Endorganschaden in der Hypertonie

Die Aktivierung unterschiedlichster Immunzellen kennzeichnet die arterielle Hypertonie. Aktivierte Immunzellen (z.B. T-Zellen) können in Zielorgane wie Herz und Niere einwandern, wo u.a. die Freisetzung pro-inflammatorischer Zytokine zum hypertensiven Endorganschaden beiträgt. Die Modulation dieser pro-inflammatorischen Antwort wird als ein vielversprechendes therapeutisches Ziel erachtet, jedoch durch heutige medikamentöse Therapiestandards nicht zufriedenstellend erreicht. Ein tieferes Verständnis für endogene Modulatoren der Inflammation in der arteriellen Hypertonie ist nötig, um neuartige therapeutische Ansätze zu entwickeln. Das intestinale Mikrobiom, d.h. die Gesamtheit der im Darm vorhandenen Bakterien sowie deren Gene, ist ein auf Umwelteinflüsse höchst responsives Ökosystem mit profundem Einfluss auf das Immunsystem. Umweltfaktoren wie die Ernährung (z.B. Salz, Fasern) können Veränderungen der Zusammensetzung sowie der Funktion des Mikrobioms verursachen und somit inflammatorische Prozesse vorteilhaft oder aber zum Nachteil des Wirts beeinflussen. Essentiell in diesem Zusammenhang ist die Tatsache, dass Bakterien aus Nahrungsbestandteilen Metabolite generieren, die vom Wirt resorbiert werden und die Differenzierung und Funktion von Immunzellen beeinflussen können. Auf diese Weise können intestinale Bakterien auch darmferne Organe beeinflussen, wodurch sich unterschiedliche Kommunikationsachsen identifizieren lassen (z.B. Darm-Niere, Darm-Herz). Ein genaueres Verständnis der Wechselwirkung von Ernährung und Mikrobiom, Metaboliten mikrobieller Herkunft und Immunsystem sowie der Auswirkungen auf die Hypertonie könnte zukünftig eine gezielte, personalisierte Beeinflussung des Mikrobioms zur Organprotektion in der Hypertonie ermöglichen.

Die in diese Habilitationsschrift zum Thema Mikrobiom eingehenden Publikationen (Originalarbeiten 3-5) haben zum Ziel, den Einfluss des Mikrobioms und seiner Einflussfaktoren auf die Inflammation bei Bluthochdruck näher zu charakterisieren. Zum einen wurden relevante Umweltfaktoren (z. B. die salzreiche Ernährung (Originalpublikation 4), Ballaststoffgehalt der Nahrung (Originalpublikation 5)) in Bezug auf Zusammensetzung und Funktion des Mikrobioms näher charakterisiert und die Auswirkung auf die inflammatorische Antwort untersucht. Zum anderen wurde durch den Vergleich des Endorganschadens von keimfreien (Engl. *germ-free*) und kolonisierten hypertensiven Mäusen untersucht, welchen grundlegenden Einfluss die Anwesenheit von Darmbakterien hat (Originalpublikation 3). Letztere Publikation demonstriert, dass der hypertensive renale und kardiale Endorganschaden in Abwesenheit intestinaler Mikrobiota aggraviert ist, wobei die Nieren im Vergleich zum Herz eine ausgeprägtere Inflammation sowie deutlichere Organschäden aufwiesen. Die Ursache für den aggravierten Organschaden keimfreier hypertensiver Mäuse ist möglicherweise in der Abwesenheit kurzkettiger Fettsäuren (SCFA) zu sehen, deren protektive Wirkung bei Bluthochdruck u.a. aus Originalpublikation 4 und Publikationen weiterer Autoren[66] bekannt ist.

Originalpublikation 4 zeigt im Tierexperiment und an gesunden Probanden, dass die salzreiche Ernährung die Zusammensetzung und Funktion des Mikrobioms verändert. Besonders empfindlich reagierten intestinale *Lactobacillus*-Spezies, welche unter einer Hochsalzdiät vermindert nachweisbar waren. Die salzinduzierte Reduktion intestinaler *Lactobacilli* wurde von vermehrt vorkommenden, pro-inflammatorischen T-Helfer-17-Zellen (T_H17) und höheren Blutdruckwerten begleitet. Eine probiotische Behandlung mit *Lactobacillus murinus* im Tiermodell konnte sowohl den Salz-induzierten Anstieg der T_H17-Zellen als auch den Anstieg des Blutdrucks vermindern. Als in diesem Zusammenhang potentiell wichtige Mediatoren zwischen Darmmikrobiom und Immunsystem des Wirts konnten Tryptophan-Metabolite bakterieller Herkunft identifiziert werden, sogenannte Indole, welche nach bakterieller Bildung im Darm vom Wirt resorbiert werden. Die im Tiermodell beobachtete Depletion von *Lactobacillus*, der Anstieg des Blutdrucks und pro-inflammatorischer T_H17-Zellen konnte in einem Pilotversuch an gesunden männlichen Probanden bestätigt werden. Diese Ergebnisse skizzieren einen neuartigen Mechanismus, der zur Entstehung von Bluthochdruck beitragen könnte: Eine salzreiche Ernährung beeinflusst über Veränderungen im mikrobiellen Ökosystem des Darms das Immunsystem in einer Art und Weise, die Bluthochdruck und Endorganschaden fördert. Die Beeinflussung des Mikrobioms, zum Beispiel durch eine gezielte probiotische Behandlung, könnte zur einer vorteilhaften Immunmodulation und zum Schutz vor Bluthochdruck und Endorganschaden führen. Um diese Hypothese zu überprüfen, müssen randomisierte klinische Studien durchgeführt werden.

Zusätzlich zur Untersuchung Salz-induzierter, Mikrobiom-vermittelter Mechanismen untersucht Originalpublikation 5 die Wirkung kurzkettiger Fettsäuren (Engl. *short-chain fatty acids*, SCFA) auf den hypertensiven Endorganschaden. SCFA sind wichtige Vertreter immunmodulatorisch wirksamer Metabolite und entstehen vor allem aus unverdaubaren, langkettigen Kohlenhydraten der Nahrung durch die Stoffwechselaktivität bestimmter Bakterien. Erste Untersuchungen im Mausmodell der Multiplen Sklerose belegten die protektive Wirkung kurzkettiger Fettsäuren bakterieller Herkunft (z.B. Propionat) über die Förderung der Funktion von regulatorischen T-Zellen (T_{REG})[134]. Für hypertensive Mausmodelle konnten wir zeigen, dass die Behandlung mit Propionat vor Angiotensin II (AngII)-induzierten kardialen und vaskulären Endorganschäden schützt. Propionat führte neben einer verzögert eintretenden, moderaten Blutdrucksenkung zu einer signifikant abgeschwächten inflammatorischen T-Zell-Antwort auf AngII, die sowohl in der Milz als auch im Herz nachweisbar war. Das kardiale Remodeling als auch die Suszeptibilität für kardiale ventrikuläre Arrhythmien war durch Propionat deutlich vermindert. Wir konnten zeigen, dass ein Großteil der organoprotektiven Wirkung von Propionat durch T_{REG} vermittelt wird, da die experimentelle Depletion von T_{REG} die Protektion verminderte.

3.3 Ernährung, Mikrobiom, Immunsystem – eine Achse mit verschiedenen Angriffspunkten für die Behandlung kardiovaskulärer Erkrankungen

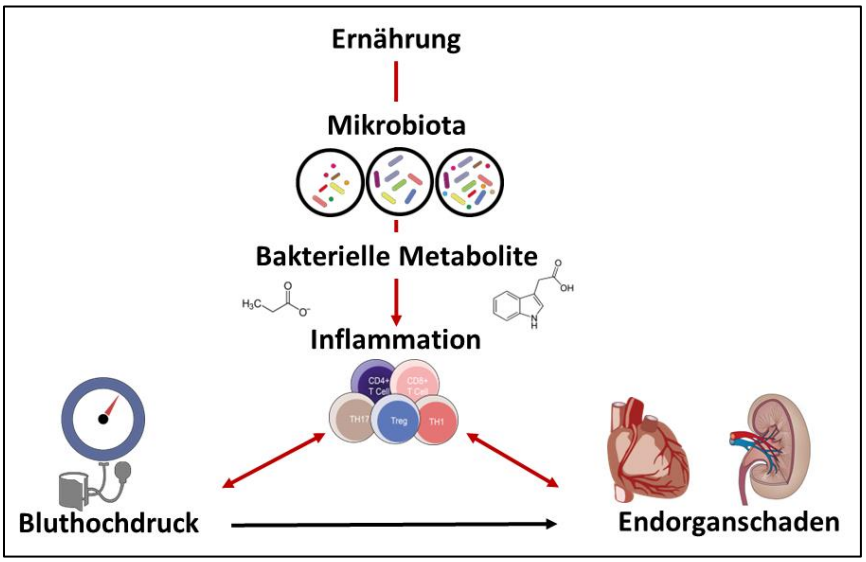

Abbildung 1: Schematische Darstellung der Modulation des hypertensiven Endorganschadens durch die Mikrobiom-Immun-Achse. Dabei können bakterielle Metabolite (SCFA, Indole) mit immunmodulatorischer Aktivität vom Wirt aufgenommen werden und so die Inflammation und das Ausmaß des hypertensiven Endorganschadens beeinflussen. Die Ernährung kann gezielt genutzt werden, um diese Achse zu nutzen, um Organprotektion bei Bluthochdruck zu erreichen. Abbildung durch den Autor erstellt.

Die hier zum Thema Mikrobiom einfließenden Publikationen weisen somit auf eine wichtige Rolle des intestinalen Mikrobiom und insbesondere mikrobieller Metabolite bei der Immunmodulation im Rahmen des Bluthochdrucks hin. Die Beeinflussung des Mikrobioms, zum Beispiel durch gezielte probiotische Behandlungen oder personalisierte diätetische Interventionen, könnte zu einer vorteilhaften Beeinflussung mikrobieller Immunmodulation über Metabolite und zum Schutz vor Bluthochdruck und Endorganschaden führen. Weitere experimentelle sowie klinische Studien sind notwendig, um dieses Potenzial näher zu charakterisieren. Mein zukünftiges Arbeitsprogramm hat zum Ziel, die Mikrobiom-Wirt-Kommunikation in der Pathogenese der Hypertonie durch Integration multimodaler Omics-Technologien im Tiermodell und im Menschen weiter zu charakterisieren. Dabei soll insbesondere auch die Bedeutung einer eingeschränkten Nierenfunktion auf diese Interaktion untersucht werden. Da zahlreiche bakterielle Metabolite renal eliminiert werden ist, liegt darin ein Ansatzpunkt, um die bei Nierenerkrankungen verstärkt auftretenden kardiovaskulären Komplikationen zu erklären und zu behandeln.

4 ZUSAMMENFASSUNG

Kardiovaskuläre Erkrankungen wie die Atherosklerose und der Bluthochdruck sind durch einen anhaltenden inflammatorischen Zustand charakterisiert, dessen Ausprägung sowohl durch intrinsisch-zelluläre Prozesse als auch extrinsisch-mikrobielle Faktoren beeinflusst werden kann.

Das Proteasom als das zentrale Proteinabbausystem diente in der vorliegenden Arbeit als zelluläre Zielstruktur, dessen Funktion im Kontext der Atherosklerose durch Anwendung eines Proteasominhibitors beeinflusst wurde. Der zentralen Rolle des Proteasoms Rechnung tragend und um toxische Effekte zu vermeiden, wurden niedrige Konzentrationen des Proteasominhibitors Bortezomib eingesetzt, um eine experimentelle Atherosklerose in LDLR -/- Mäusen zu beeinflussen. Dabei könnte ein frühes Atherosklerose-Stadium durch niedrigdosierte Proteasominhibition günstig beeinflusst werden. Mechanistisch konnten anti-oxidative und anti-inflammatorische Effekte niedrigdosierter Proteasominhibition identifiziert werden. Darüber hinaus wurde der Einfluss einer genetischen Defizienz der immunoproteasomalen Untereinheit β5i/LMP7 in LDLR -/- Mäusen untersucht, was jedoch weder die frühe noch die späte Atherosklerose im Mausmodell beeinflusste. Aus diesen Studien lässt schließen, dass das Proteasom zwar ein potentielles Ziel für zukünftige Therapien sein könnte, es jedoch einer spezifischeren Ansteuerung von Komponenten des Ubiquitin-Proteasom-Systems bedarf, um der Inflammation gezielter und nebenwirkungsarm zu begegnen.

Kardiovaskuläre Erkrankungen hängen in besonderem Maß von Umweltfaktoren, wie zum Beispiel der Ernährung, ab. Die intestinale Mikrobiota reagiert sensibel auf Umwelt und Ernährung und interagiert mit dem Immunsystem. Für viele Erkrankungen ist bereits eine Beeinflussung durch das Mikrobiom gezeigt. Die hier vorgelegten Arbeiten untersuchen die Rolle des Mikrobioms bei Bluthochdruck. Dabei konnte gezeigt werden, dass der hypertensive renale und kardiale Schaden in Abwesenheit eines Mikrobioms bei keimfreien Mäusen aggraviert ist, was auf die Abwesenheit protektiver bakterieller Metabolite hinweisen könnte. Zusätzlich wurde der Einfluss einer Hochsalzdiät auf das Mikrobiom untersucht und Lactobacillus als ein Salz-sensitives intestinales Bakterium identifiziert, welches durch Produktion eines Metaboliten die T_H17-abhängige Inflammation und den Blutdruck reguliert. Schließlich wurde in einer weiteren Arbeit die kurzkettige Fettsäure Propionat als ein protektiver bakterieller Metabolit identifiziert, welcher vor hypertensiven kardialen Schäden über zum Teil T_{REG}-abhängige Mechanismen schützt. Zusammengefasst beleuchten diese Studien das Mikrobiom als ein vielversprechendes Angriffsziel für organoprotektive Therapien bei Bluthochdruck.

5 LITERATURANGABEN

1. Diseases GBD ,Injuries C. Global burden of 369 diseases and injuries in 204 countries and territories, 1990-2019: a systematic analysis for the Global Burden of Disease Study 2019. *Lancet*. 2020;396:1204-1222 DOI: 10.1016/S0140-6736(20)30925-9.

2. Yusuf S, Joseph P, Rangarajan S, Islam S, Mente A, Hystad P, Brauer M, Kutty VR, Gupta R, Wielgosz A, et al. Modifiable risk factors, cardiovascular disease, and mortality in 155 722 individuals from 21 high-income, middle-income, and low-income countries (PURE): a prospective cohort study. *Lancet*. 2020;395:795-808 DOI: 10.1016/S0140-6736(19)32008-2.

3. Libby P, Buring JE, Badimon L, Hansson GK, Deanfield J, Bittencourt MS, Tokgozoglu L ,Lewis EF. Atherosclerosis. *Nat Rev Dis Primers*. 2019;5:56 DOI: 10.1038/s41572-019-0106-z.

4. Mielke N, Huscher D, Douros A, Ebert N, Gaedeke J, van der Giet M, Kuhlmann MK, Martus P ,Schaeffner E. Self-reported medication in community-dwelling older adults in Germany: results from the Berlin Initiative Study. *BMC Geriatr*. 2020;20:22 DOI: 10.1186/s12877-020-1430-6.

5. Knopf H ,Grams D. [Medication use of adults in Germany: results of the German Health Interview and Examination Survey for Adults (DEGS1)]. *Bundesgesundheitsblatt Gesundheitsforschung Gesundheitsschutz*. 2013;56:868-77 DOI: 10.1007/s00103-013-1667-8.

6. Hansson GK. Inflammation, atherosclerosis, and coronary artery disease. *The New England journal of medicine*. 2005;352:1685-95 DOI: 10.1056/NEJMra043430.

7. Ross R. Atherosclerosis--an inflammatory disease. *The New England journal of medicine*. 1999;340:115-26 DOI: 10.1056/NEJM199901143400207.

8. Norlander AE, Madhur MS ,Harrison DG. The immunology of hypertension. *The Journal of experimental medicine*. 2018;215:21-33 DOI: 10.1084/jem.20171773.

9. Lakoski SG, Cushman M, Palmas W, Blumenthal R, D'Agostino RB, Jr. ,Herrington DM. The relationship between blood pressure and C-reactive protein in the Multi-Ethnic Study of Atherosclerosis (MESA). *Journal of the American College of Cardiology*. 2005;46:1869-74 DOI: 10.1016/j.jacc.2005.07.050.

10. Dalekos GN, Elisaf M, Bairaktari E, Tsolas O ,Siamopoulos KC. Increased serum levels of interleukin-1beta in the systemic circulation of patients with essential hypertension: additional risk factor for atherogenesis in hypertensive patients? *The Journal of laboratory and clinical medicine*. 1997;129:300-8 DOI: 10.1016/s0022-2143(97)90178-5.

11. Emerging Risk Factors C, Kaptoge S, Di Angelantonio E, Lowe G, Pepys MB, Thompson SG, Collins R ,Danesh J. C-reactive protein concentration and risk of coronary heart disease, stroke, and mortality: an individual participant meta-analysis. *Lancet*. 2010;375:132-40 DOI: 10.1016/S0140-6736(09)61717-7.

12. Ridker PM, Glynn RJ ,Hennekens CH. C-reactive protein adds to the predictive value of total and HDL cholesterol in determining risk of first myocardial infarction. *Circulation*. 1998;97:2007-11 DOI: 10.1161/01.cir.97.20.2007.

13. Galea J, Armstrong J, Gadsdon P, Holden H, Francis SE ,Holt CM. Interleukin-1 beta in coronary arteries of patients with ischemic heart disease. *Arteriosclerosis, thrombosis, and vascular biology*. 1996;16:1000-6 DOI: 10.1161/01.atv.16.8.1000.

14. Ridker PM, Everett BM, Thuren T, MacFadyen JG, Chang WH, Ballantyne C, Fonseca F, Nicolau J, Koenig W, Anker SD, et al. Antiinflammatory Therapy with Canakinumab for Atherosclerotic Disease. *The New England journal of medicine*. 2017;377:1119-1131 DOI: 10.1056/NEJMoa1707914.

15. Levy D, Ehret GB, Rice K, Verwoert GC, Launer LJ, Dehghan A, Glazer NL, Morrison AC, Johnson AD, Aspelund T, et al. Genome-wide association study of blood pressure and hypertension. *Nature genetics*. 2009;41:677-87 DOI: 10.1038/ng.384.

16. Evangelou E, Warren HR, Mosen-Ansorena D, Mifsud B, Pazoki R, Gao H, Ntritsos G, Dimou N, Cabrera CP, Karaman I, et al. Genetic analysis of over 1 million people identifies 535 new loci associated with blood pressure traits. *Nature genetics*. 2018;50:1412-1425 DOI: 10.1038/s41588-018-0205-x.

17. Samani NJ, Erdmann J, Hall AS, Hengstenberg C, Mangino M, Mayer B, Dixon RJ, Meitinger T, Braund P, Wichmann HE, et al. Genomewide association analysis of coronary artery disease. *The New England journal of medicine*. 2007;357:443-53 DOI: 10.1056/NEJMoa072366.

18. Munoz M, Pong-Wong R, Canela-Xandri O, Rawlik K, Haley CS ,Tenesa A. Evaluating the contribution of genetics and familial shared environment to common disease using the UK Biobank. *Nature genetics*. 2016;48:980-3 DOI: 10.1038/ng.3618.

19. Khera AV, Emdin CA, Drake I, Natarajan P, Bick AG, Cook NR, Chasman DI, Baber U, Mehran R, Rader DJ, et al. Genetic Risk, Adherence to a Healthy Lifestyle, and Coronary Disease. *The New England journal of medicine*. 2016;375:2349-2358 DOI: 10.1056/NEJMoa1605086.

20. Ezzati M ,Riboli E. Behavioral and dietary risk factors for noncommunicable diseases. *The New England journal of medicine*. 2013;369:954-64 DOI: 10.1056/NEJMra1203528.

21. Meier T, Grafe K, Senn F, Sur P, Stangl GI, Dawczynski C, Marz W, Kleber ME ,Lorkowski S. Cardiovascular mortality attributable to dietary risk factors in 51 countries in the WHO European Region from 1990 to 2016: a systematic analysis of the Global Burden of Disease Study. *European journal of epidemiology*. 2019;34:37-55 DOI: 10.1007/s10654-018-0473-x.

22. Statistisches Bundesamt. Deaths caused by the 10 most frequent cardiovascular diseases. 2022, https://www.destatis.de/EN/Themes/Society-Environment/Health/Causes-Death/Tables/deaths-cardiovascular-disease-total.html.

23. Roth GA, Mensah GA, Johnson CO, Addolorato G, Ammirati E, Baddour LM, Barengo NC, Beaton AZ, Benjamin EJ, Benziger CP, et al. Global Burden of Cardiovascular Diseases and Risk Factors, 1990-2019: Update From the GBD 2019 Study. *Journal of the American College of Cardiology*. 2020;76:2982-3021 DOI: 10.1016/j.jacc.2020.11.010.

24. Blais JE, Wei Y, Yap KKW, Alwafi H, Ma TT, Brauer R, Lau WCY, Man KKC, Siu CW, Tan KCB, et al. Trends in lipid-modifying agent use in 83 countries. *Atherosclerosis*. 2021;328:44-51 DOI: 10.1016/j.atherosclerosis.2021.05.016.

25. Ridker PM, Everett BM, Pradhan A, MacFadyen JG, Solomon DH, Zaharris E, Mam V, Hasan A, Rosenberg Y, Iturriaga E, et al. Low-Dose Methotrexate for the Prevention of Atherosclerotic Events. *The New England journal of medicine*. 2019;380:752-762 DOI: 10.1056/NEJMoa1809798.

26. Tardif JC, Kouz S, Waters DD, Bertrand OF, Diaz R, Maggioni AP, Pinto FJ, Ibrahim R, Gamra H, Kiwan GS, et al. Efficacy and Safety of Low-Dose Colchicine after Myocardial Infarction. *The New England journal of medicine*. 2019;381:2497-2505 DOI: 10.1056/NEJMoa1912388.

27. Coffman TM. Under pressure: the search for the essential mechanisms of hypertension. *Nature medicine*. 2011;17:1402-9 DOI: 10.1038/nm.2541.

28. Okuda T ,Grollman A. Passive transfer of autoimmune induced hypertension in the rat by lymph node cells. *Tex Rep Biol Med*. 1967;25:257-64, https://www.ncbi.nlm.nih.gov/pubmed/6040652.

29. White FN ,Grollman A. Autoimmune Factors Associated with Infarction of the Kidney. *Nephron*. 1964;1:93-102 DOI: 10.1159/000179322.

30. Muller DN, Shagdarsuren E, Park JK, Dechend R, Mervaala E, Hampich F, Fiebeler A, Ju X, Finckenberg P, Theuer J, et al. Immunosuppressive treatment protects against angiotensin II-induced renal damage. *The American journal of pathology*. 2002;161:1679-93 DOI: 10.1016/S0002-9440(10)64445-8.

31. Mattson DL, James L, Berdan EA ,Meister CJ. Immune suppression attenuates hypertension and renal disease in the Dahl salt-sensitive rat. *Hypertension*. 2006;48:149-56 DOI: 10.1161/01.HYP.0000228320.23697.29.

32. Mervaala E, Muller DN, Park JK, Dechend R, Schmidt F, Fiebeler A, Bieringer M, Breu V, Ganten D, Haller H, et al. Cyclosporin A protects against angiotensin II-induced end-organ damage in double transgenic rats harboring human renin and angiotensinogen genes. *Hypertension*. 2000;35:360-6 DOI: 10.1161/01.hyp.35.1.360.

33. Muller DN, Dechend R, Mervaala EM, Park JK, Schmidt F, Fiebeler A, Theuer J, Breu V, Ganten D, Haller H, et al. NF-kappaB inhibition ameliorates angiotensin II-induced inflammatory damage in rats. *Hypertension*. 2000;35:193-201 DOI: 10.1161/01.hyp.35.1.193.

34. Guzik TJ, Hoch NE, Brown KA, McCann LA, Rahman A, Dikalov S, Goronzy J, Weyand C ,Harrison DG. Role of the T cell in the genesis of angiotensin II induced hypertension and vascular dysfunction. *The Journal of experimental medicine*. 2007;204:2449-60 DOI: 10.1084/jem.20070657.

35. Madhur MS, Lob HE, McCann LA, Iwakura Y, Blinder Y, Guzik TJ ,Harrison DG. Interleukin 17 promotes angiotensin II-induced hypertension and vascular dysfunction. *Hypertension*. 2010;55:500-7 DOI: 10.1161/HYPERTENSIONAHA.109.145094.

36. Marko L, Kvakan H, Park JK, Qadri F, Spallek B, Binger KJ, Bowman EP, Kleinewietfeld M, Fokuhl V, Dechend R, et al. Interferon-gamma signaling inhibition ameliorates angiotensin II-induced cardiac damage. *Hypertension*. 2012;60:1430-6 DOI: 10.1161/HYPERTENSIONAHA.112.199265.

37. Kamat NV, Thabet SR, Xiao L, Saleh MA, Kirabo A, Madhur MS, Delpire E, Harrison DG ,McDonough AA. Renal transporter activation during angiotensin-II hypertension is blunted in interferon-gamma-/- and interleukin-17A-/- mice. *Hypertension*. 2015;65:569-76 DOI: 10.1161/HYPERTENSIONAHA.114.04975.

38. Norlander AE, Saleh MA, Kamat NV, Ko B, Gnecco J, Zhu L, Dale BL, Iwakura Y, Hoover RS, McDonough AA, et al. Interleukin-17A Regulates Renal Sodium Transporters and Renal Injury in Angiotensin II-Induced Hypertension. *Hypertension*. 2016;68:167-74 DOI: 10.1161/HYPERTENSIONAHA.116.07493.

39. Itani HA, Xiao L, Saleh MA, Wu J, Pilkinton MA, Dale BL, Barbaro NR, Foss JD, Kirabo A, Montaniel KR, et al. CD70 Exacerbates Blood Pressure Elevation and Renal Damage in Response to Repeated Hypertensive Stimuli. *Circulation research*. 2016;118:1233-43 DOI: 10.1161/CIRCRESAHA.115.308111.

40. Kvakan H, Kleinewietfeld M, Qadri F, Park JK, Fischer R, Schwarz I, Rahn HP, Plehm R, Wellner M, Elitok S, et al. Regulatory T cells ameliorate angiotensin II-induced cardiac damage. *Circulation*. 2009;119:2904-12 DOI: 10.1161/CIRCULATIONAHA.108.832782.

41. Barhoumi T, Kasal DA, Li MW, Shbat L, Laurant P, Neves MF, Paradis P ,Schiffrin EL. T regulatory lymphocytes prevent angiotensin II-induced hypertension and vascular injury. *Hypertension*. 2011;57:469-76 DOI: 10.1161/HYPERTENSIONAHA.110.162941.

42. Mian MO, Barhoumi T, Briet M, Paradis P ,Schiffrin EL. Deficiency of T-regulatory cells exaggerates angiotensin II-induced microvascular injury by enhancing immune responses. *Journal of hypertension*. 2016;34:97-108 DOI: 10.1097/HJH.0000000000000761.

43. Hershko A ,Ciechanover A. The ubiquitin system. *Annu Rev Biochem*. 1998;67:425-79 DOI: 10.1146/annurev.biochem.67.1.425.

44. Goldberg AL. Protein degradation and protection against misfolded or damaged proteins. *Nature*. 2003;426:895-9 DOI: 10.1038/nature02263.

45. Coux O, Tanaka K ,Goldberg AL. Structure and functions of the 20S and 26S proteasomes. *Annu Rev Biochem*. 1996;65:801-47 DOI: 10.1146/annurev.bi.65.070196.004101.

46. Kloetzel PM ,Ossendorp F. Proteasome and peptidase function in MHC-class-I-mediated antigen presentation. *Current opinion in immunology*. 2004;16:76-81 DOI: 10.1016/j.coi.2003.11.004.

47. Ding Q, Martin S, Dimayuga E, Bruce-Keller AJ ,Keller JN. LMP2 knock-out mice have reduced proteasome activities and increased levels of oxidatively damaged proteins. *Antioxidants & redox signaling*. 2006;8:130-5 DOI: 10.1089/ars.2006.8.130.

48. Kotamraju S, Matalon S, Matsunaga T, Shang T, Hickman-Davis JM ,Kalyanaraman B. Upregulation of immunoproteasomes by nitric oxide: potential antioxidative mechanism in endothelial cells. *Free radical biology & medicine*. 2006;40:1034-44 DOI: 10.1016/j.freeradbiomed.2005.10.052.

49. Callahan MK, Wohlfert EA, Menoret A ,Srivastava PK. Heat shock up-regulates lmp2 and lmp7 and enhances presentation of immunoproteasome-dependent epitopes. *Journal of immunology (Baltimore, Md : 1950)*. 2006;177:8393-9 DOI: 10.4049/jimmunol.177.12.8393.

50. Karin M ,Ben-Neriah Y. Phosphorylation meets ubiquitination: the control of NF-[kappa]B activity. *Annual review of immunology*. 2000;18:621-63 DOI: 10.1146/annurev.immunol.18.1.621.

51. Visekruna A, Joeris T, Seidel D, Kroesen A, Loddenkemper C, Zeitz M, Kaufmann SH, Schmidt-Ullrich R ,Steinhoff U. Proteasome-mediated degradation of IkappaBalpha and processing of p105 in Crohn disease and ulcerative colitis. *The Journal of clinical investigation*. 2006;116:3195-203 DOI: 10.1172/JCI28804.

52. Marfella R, Cacciapuoti F, Grassia A, Manfredi E, De Maio G, Caruso G, Pepe M, Nittolo G ,Cacciapuoti F. Role of the ubiquitin-proteasome system in carotid plaque instability in diabetic patients. *Acta cardiologica*. 2006;61:630-6 DOI: 10.2143/AC.61.6.2017962.

53. Herrmann J, Saguner AM, Versari D, Peterson TE, Chade A, Olson M, Lerman LO ,Lerman A. Chronic proteasome inhibition contributes to coronary atherosclerosis. *Circulation research*. 2007;101:865-74 DOI: 10.1161/CIRCRESAHA.107.152959.

54. Herrmann J, Lerman LO ,Lerman A. On to the road to degradation: atherosclerosis and the proteasome. *Cardiovascular research*. 2010;85:291-302 DOI: 10.1093/cvr/cvp333.

55. Unger T, Borghi C, Charchar F, Khan NA, Poulter NR, Prabhakaran D, Ramirez A, Schlaich M, Stergiou GS, Tomaszewski M, et al. 2020 International Society of Hypertension Global Hypertension Practice Guidelines. *Hypertension*. 2020;75:1334-1357 DOI: 10.1161/HYPERTENSIONAHA.120.15026.

56. Whelton PK, Carey RM, Aronow WS, Casey DE, Jr., Collins KJ, Dennison Himmelfarb C, DePalma SM, Gidding S, Jamerson KA, Jones DW, et al. 2017 ACC/AHA/AAPA/ABC/ACPM/AGS/APhA/ASH/ASPC/NMA/PCNA Guideline for the Prevention, Detection, Evaluation, and Management of High Blood Pressure in Adults: A Report of the American College of Cardiology/American Heart Association Task Force on Clinical Practice Guidelines. *Journal of the American College of Cardiology*. 2017; DOI: 10.1016/j.jacc.2017.11.006.

57. Williams B, Mancia G, Spiering W, Agabiti Rosei E, Azizi M, Burnier M, Clement DL, Coca A, de Simone G, Dominiczak A, et al. 2018 ESC/ESH Guidelines for the management of arterial hypertension. *European heart journal*. 2018;39:3021-3104 DOI: 10.1093/eurheartj/ehy339.

58. Cummings JH, Pomare EW, Branch WJ, Naylor CP ,Macfarlane GT. Short chain fatty acids in human large intestine, portal, hepatic and venous blood. *Gut*. 1987;28:1221-7 DOI: 10.1136/gut.28.10.1221.

59. Yan Q, Gu Y, Li X, Yang W, Jia L, Chen C, Han X, Huang Y, Zhao L, Li P, et al. Alterations of the Gut Microbiome in Hypertension. *Frontiers in cellular and infection microbiology*. 2017;7:381 DOI: 10.3389/fcimb.2017.00381.

60. Yang T, Santisteban MM, Rodriguez V, Li E, Ahmari N, Carvajal JM, Zadeh M, Gong M, Qi Y, Zubcevic J, et al. Gut dysbiosis is linked to hypertension. *Hypertension*. 2015;65:1331-40 DOI: 10.1161/HYPERTENSIONAHA.115.05315.

61. Husted AS, Trauelsen M, Rudenko O, Hjorth SA ,Schwartz TW. GPCR-Mediated Signaling of Metabolites. *Cell metabolism*. 2017;25:777-796 DOI: 10.1016/j.cmet.2017.03.008.

62. Brown AJ, Goldsworthy SM, Barnes AA, Eilert MM, Tcheang L, Daniels D, Muir AI, Wigglesworth MJ, Kinghorn I, Fraser NJ, et al. The Orphan G protein-coupled receptors GPR41 and GPR43 are activated by propionate and other short chain carboxylic acids. *The Journal of biological chemistry*. 2003;278:11312-9 DOI: 10.1074/jbc.M211609200.

63. Bindels LB, Dewulf EM ,Delzenne NM. GPR43/FFA2: physiopathological relevance and therapeutic prospects. *Trends Pharmacol Sci*. 2013;34:226-32 DOI: 10.1016/j.tips.2013.02.002.

64. Pluznick JL, Protzko RJ, Gevorgyan H, Peterlin Z, Sipos A, Han J, Brunet I, Wan LX, Rey F, Wang T, et al. Olfactory receptor responding to gut microbiota-derived signals plays a role in renin secretion and blood pressure regulation. *Proceedings of the National Academy of Sciences of the United States of America*. 2013;110:4410-5 DOI: 10.1073/pnas.1215927110.

65. Natarajan N, Hori D, Flavahan S, Steppan J, Flavahan NA, Berkowitz DE ,Pluznick JL. Microbial short chain fatty acid metabolites lower blood pressure via endothelial G protein-coupled receptor 41. *Physiological genomics*. 2016;48:826-834 DOI: 10.1152/physiolgenomics.00089.2016.

66. Marques FZ, Nelson E, Chu PY, Horlock D, Fiedler A, Ziemann M, Tan JK, Kuruppu S, Rajapakse NW, El-Osta A, et al. High-Fiber Diet and Acetate Supplementation Change the Gut Microbiota and Prevent the Development of Hypertension and Heart Failure in Hypertensive Mice. *Circulation*. 2017;135:964-977 DOI: 10.1161/CIRCULATIONAHA.116.024545.

67. Wang Z, Klipfell E, Bennett BJ, Koeth R, Levison BS, Dugar B, Feldstein AE, Britt EB, Fu X, Chung YM, et al. Gut flora metabolism of phosphatidylcholine promotes cardiovascular disease. *Nature*. 2011;472:57-63 DOI: 10.1038/nature09922.

68. Tang WH, Wang Z, Kennedy DJ, Wu Y, Buffa JA, Agatisa-Boyle B, Li XS, Levison BS ,Hazen SL. Gut microbiota-dependent trimethylamine N-oxide (TMAO) pathway contributes to both development of renal insufficiency and mortality risk in chronic kidney disease. *Circulation research*. 2015;116:448-55 DOI: 10.1161/CIRCRESAHA.116.305360.

69. Zelante T, Iannitti RG, Cunha C, De Luca A, Giovannini G, Pieraccini G, Zecchi R, D'Angelo C, Massi-Benedetti C, Fallarino F, et al. Tryptophan catabolites from microbiota engage aryl hydrocarbon receptor and balance mucosal reactivity via interleukin-22. *Immunity*. 2013;39:372-85 DOI: 10.1016/j.immuni.2013.08.003.

70. Nakano T, Katsuki S, Chen M, Decano JL, Halu A, Lee LH, Pestana DVS, Kum AST, Kuromoto RK, Golden WS, et al. Uremic Toxin Indoxyl Sulfate Promotes Proinflammatory Macrophage Activation Via the Interplay of OATP2B1 and Dll4-Notch Signaling. *Circulation*. 2019;139:78-96 DOI: 10.1161/CIRCULATIONAHA.118.034588.

71. Nowak WN, Deng J, Ruan XZ ,Xu Q. Reactive Oxygen Species Generation and Atherosclerosis. *Arteriosclerosis, thrombosis, and vascular biology*. 2017;37:e41-e52 DOI: 10.1161/ATVBAHA.117.309228.

72. Schleicher E ,Friess U. Oxidative stress, AGE, and atherosclerosis. *Kidney international Supplement*. 2007;72:S17-26 DOI: 10.1038/sj.ki.5002382.

73. Davignon J ,Ganz P. Role of endothelial dysfunction in atherosclerosis. *Circulation*. 2004;109:III27-32 DOI: 10.1161/01.CIR.0000131515.03336.f8.

74. Gimbrone MA, Jr. ,Garcia-Cardena G. Endothelial Cell Dysfunction and the Pathobiology of Atherosclerosis. *Circulation research*. 2016;118:620-36 DOI: 10.1161/CIRCRESAHA.115.306301.

75. Ait-Oufella H, Taleb S, Mallat Z ,Tedgui A. Recent advances on the role of cytokines in atherosclerosis. *Arteriosclerosis, thrombosis, and vascular biology*. 2011;31:969-79 DOI: 10.1161/ATVBAHA.110.207415.

76. Basatemur GL, Jorgensen HF, Clarke MCH, Bennett MR ,Mallat Z. Vascular smooth muscle cells in atherosclerosis. *Nature reviews Cardiology*. 2019;16:727-744 DOI: 10.1038/s41569-019-0227-9.

77. Bieler S, Meiners S, Stangl V, Pohl T ,Stangl K. Comprehensive proteomic and transcriptomic analysis reveals early induction of a protective anti-oxidative stress response by low-dose proteasome inhibition. *Proteomics*. 2009;9:3257-67 DOI: 10.1002/pmic.200800927.

78. Stangl V, Lorenz M, Meiners S, Ludwig A, Bartsch C, Moobed M, Vietzke A, Kinkel HT, Baumann G ,Stangl K. Long-term up-regulation of eNOS and improvement of endothelial function by inhibition of the ubiquitin-proteasome pathway. *FASEB journal : official publication of the Federation of American Societies for Experimental Biology*. 2004;18:272-9 DOI: 10.1096/fj.03-0054com.

79. Meiners S, Ludwig A, Lorenz M, Dreger H, Baumann G, Stangl V ,Stangl K. Nontoxic proteasome inhibition activates a protective antioxidant defense response in endothelial cells. *Free radical biology & medicine*. 2006;40:2232-41 DOI: 10.1016/j.freeradbiomed.2006.03.003.

80. Westphal K, Stangl V, Fahling M, Dreger H, Weller A, Baumann G, Stangl K ,Meiners S. Human-specific induction of glutathione peroxidase-3 by proteasome inhibition in cardiovascular cells. *Free radical biology & medicine*. 2009;47:1652-60 DOI: 10.1016/j.freeradbiomed.2009.09.017.

81. Lorenz M, Wilck N, Meiners S, Ludwig A, Baumann G, Stangl K ,Stangl V. Proteasome inhibition prevents experimentally-induced endothelial dysfunction. *Life sciences*. 2009;84:929-34 DOI: 10.1016/j.lfs.2009.04.016.

82. Dreger H, Westphal K, Wilck N, Baumann G, Stangl V, Stangl K ,Meiners S. Protection of vascular cells from oxidative stress by proteasome inhibition depends on Nrf2. *Cardiovascular research*. 2010;85:395-403 DOI: 10.1093/cvr/cvp279.

83. Ludwig A, Fechner M, Wilck N, Meiners S, Grimbo N, Baumann G, Stangl V ,Stangl K. Potent anti-inflammatory effects of low-dose proteasome inhibition in the vascular system. *Journal of molecular medicine (Berlin, Germany)*. 2009;87:793-802 DOI: 10.1007/s00109-009-0469-9.

84. Shang F ,Taylor A. Ubiquitin-proteasome pathway and cellular responses to oxidative stress. *Free radical biology & medicine*. 2011;51:5-16 DOI: 10.1016/j.freeradbiomed.2011.03.031.

85. Kloetzel PM. Generation of major histocompatibility complex class I antigens: functional interplay between proteasomes and TPPII. *Nature immunology*. 2004;5:661-9 DOI: 10.1038/ni1090.

86. Griffin TA, Nandi D, Cruz M, Fehling HJ, Kaer LV, Monaco JJ ,Colbert RA. Immunoproteasome assembly: cooperative incorporation of interferon gamma (IFN-gamma)-inducible subunits. *The Journal of experimental medicine*. 1998;187:97-104 DOI: 10.1084/jem.187.1.97.

87. Groettrup M, Standera S, Stohwasser R ,Kloetzel PM. The subunits MECL-1 and LMP2 are mutually required for incorporation into the 20S proteasome. *Proceedings of the National Academy of Sciences of the United States of America*. 1997;94:8970-5 DOI: 10.1073/pnas.94.17.8970.

88. Nandi D, Woodward E, Ginsburg DB ,Monaco JJ. Intermediates in the formation of mouse 20S proteasomes: implications for the assembly of precursor beta subunits. *The EMBO journal*. 1997;16:5363-75 DOI: 10.1093/emboj/16.17.5363.

89. Cascio P, Hilton C, Kisselev AF, Rock KL ,Goldberg AL. 26S proteasomes and immunoproteasomes produce mainly N-extended versions of an antigenic peptide. *The EMBO journal*. 2001;20:2357-66 DOI: 10.1093/emboj/20.10.2357.

90. Sijts AJ, Ruppert T, Rehermann B, Schmidt M, Koszinowski U ,Kloetzel PM. Efficient generation of a hepatitis B virus cytotoxic T lymphocyte epitope requires the structural features of immunoproteasomes. *The Journal of experimental medicine*. 2000;191:503-14 DOI: 10.1084/jem.191.3.503.

91. Nathan JA, Spinnenhirn V, Schmidtke G, Basler M, Groettrup M ,Goldberg AL. Immuno- and constitutive proteasomes do not differ in their abilities to degrade ubiquitinated proteins. *Cell*. 2013;152:1184-94 DOI: 10.1016/j.cell.2013.01.037.

92. Seifert U, Bialy LP, Ebstein F, Bech-Otschir D, Voigt A, Schroter F, Prozorovski T, Lange N, Steffen J, Rieger M, et al. Immunoproteasomes preserve protein homeostasis upon interferon-induced oxidative stress. *Cell*. 2010;142:613-24 DOI: 10.1016/j.cell.2010.07.036.

93. Basler M, Dajee M, Moll C, Groettrup M ,Kirk CJ. Prevention of experimental colitis by a selective inhibitor of the immunoproteasome. *Journal of immunology (Baltimore, Md : 1950)*. 2010;185:634-41 DOI: 10.4049/jimmunol.0903182.

94. Kalim KW, Basler M, Kirk CJ ,Groettrup M. Immunoproteasome subunit LMP7 deficiency and inhibition suppresses Th1 and Th17 but enhances regulatory T cell differentiation. *Journal of immunology (Baltimore, Md : 1950)*. 2012;189:4182-93 DOI: 10.4049/jimmunol.1201183.

95. Muchamuel T, Basler M, Aujay MA, Suzuki E, Kalim KW, Lauer C, Sylvain C, Ring ER, Shields J, Jiang J, et al. A selective inhibitor of the immunoproteasome subunit LMP7 blocks cytokine production and attenuates progression of experimental arthritis. *Nature medicine*. 2009;15:781-7 DOI: 10.1038/nm.1978.

96. Collaborators GBDRF. Global, regional, and national comparative risk assessment of 84 behavioural, environmental and occupational, and metabolic risks or clusters of risks, 1990-2016: a systematic analysis for the Global Burden of Disease Study 2016. *Lancet*. 2017;390:1345-1422 DOI: 10.1016/S0140-6736(17)32366-8.

97. Collaborators GBDRF. Global burden of 87 risk factors in 204 countries and territories, 1990-2019: a systematic analysis for the Global Burden of Disease Study 2019. *Lancet*. 2020;396:1223-1249 DOI: 10.1016/S0140-6736(20)30752-2.

98. Appel LJ, Moore TJ, Obarzanek E, Vollmer WM, Svetkey LP, Sacks FM, Bray GA, Vogt TM, Cutler JA, Windhauser MM, et al. A clinical trial of the effects of dietary patterns on blood pressure. DASH Collaborative Research Group. *The New England journal of medicine*. 1997;336:1117-24 DOI: 10.1056/NEJM199704173361601.

99. Lelong H, Blacher J, Baudry J, Adriouch S, Galan P, Fezeu L, Hercberg S ,Kesse-Guyot E. Individual and Combined Effects of Dietary Factors on Risk of Incident Hypertension: Prospective Analysis From the NutriNet-Sante Cohort. *Hypertension*. 2017;70:712-720 DOI: 10.1161/HYPERTENSIONAHA.117.09622.

100. Ellison DH ,Welling P. Insights into Salt Handling and Blood Pressure. *The New England journal of medicine*. 2021;385:1981-1993 DOI: 10.1056/NEJMra2030212.

101. Mente A, O'Donnell MJ, Rangarajan S, McQueen MJ, Poirier P, Wielgosz A, Morrison H, Li W, Wang X, Di C, et al. Association of urinary sodium and potassium excretion with blood pressure. *The New England journal of medicine*. 2014;371:601-11 DOI: 10.1056/NEJMoa1311989.

102. Reynolds AN, Akerman A, Kumar S, Diep Pham HT, Coffey S ,Mann J. Dietary fibre in hypertension and cardiovascular disease management: systematic review and meta-analyses. *BMC medicine*. 2022;20:139 DOI: 10.1186/s12916-022-02328-x.

103. Streppel MT, Arends LR, van 't Veer P, Grobbee DE ,Geleijnse JM. Dietary fiber and blood pressure: a meta-analysis of randomized placebo-controlled trials. *Archives of internal medicine*. 2005;165:150-6 DOI: 10.1001/archinte.165.2.150.

104. Commission E. Survey on Member States' implementation of the EU salt reduction framework. 2014:00001-00032.

105. Klenow S, Thamm M ,Mensink GBM. Sodium intake in Germany estimated from sodium excretion measured in spot urine samples. *BMC Nutrition*. 2016;2:36 DOI: 10.1186/s40795-016-0075-5.

106. Mozaffarian D, Fahimi S, Singh GM, Micha R, Khatibzadeh S, Engell RE, Lim S, Danaei G, Ezzati M, Powles J, et al. Global sodium consumption and death from cardiovascular causes. *The New England journal of medicine*. 2014;371:624-34 DOI: 10.1056/NEJMoa1304127.

107. O'Donnell M, Mente A, Rangarajan S, McQueen MJ, Wang X, Liu L, Yan H, Lee SF, Mony P, Devanath A, et al. Urinary sodium and potassium excretion, mortality, and cardiovascular events. *The New England journal of medicine*. 2014;371:612-23 DOI: 10.1056/NEJMoa1311889.

108. Farez MF, Fiol MP, Gaitan MI, Quintana FJ ,Correale J. Sodium intake is associated with increased disease activity in multiple sclerosis. *Journal of neurology, neurosurgery, and psychiatry*. 2015;86:26-31 DOI: 10.1136/jnnp-2014-307928.

109. Kleinewietfeld M, Manzel A, Titze J, Kvakan H, Yosef N, Linker RA, Muller DN ,Hafler DA. Sodium chloride drives autoimmune disease by the induction of pathogenic TH17 cells. *Nature*. 2013;496:518-22 DOI: 10.1038/nature11868.

110. Brestoff JR ,Artis D. Commensal bacteria at the interface of host metabolism and the immune system. *Nature immunology*. 2013;14:676-84 DOI: 10.1038/ni.2640.

111. Atarashi K, Tanoue T, Oshima K, Suda W, Nagano Y, Nishikawa H, Fukuda S, Saito T, Narushima S, Hase K, et al. Treg induction by a rationally selected mixture of Clostridia strains from the human microbiota. *Nature*. 2013;500:232-6 DOI: 10.1038/nature12331.

112. Furusawa Y, Obata Y, Fukuda S, Endo TA, Nakato G, Takahashi D, Nakanishi Y, Uetake C, Kato K, Kato T, et al. Commensal microbe-derived butyrate induces the differentiation of colonic regulatory T cells. *Nature*. 2013;504:446-50 DOI: 10.1038/nature12721.

113. Wilck N ,Ludwig A. Targeting the ubiquitin-proteasome system in atherosclerosis: status quo, challenges, and perspectives. *Antioxidants & redox signaling*. 2014;21:2344-63 DOI: 10.1089/ars.2013.5805.

114. Marfella R, D'Amico M, Esposito K, Baldi A, Di Filippo C, Siniscalchi M, Sasso FC, Portoghese M, Cirillo F, Cacciapuoti F, et al. The ubiquitin-proteasome system and inflammatory activity in diabetic atherosclerotic plaques: effects of rosiglitazone treatment. *Diabetes*. 2006;55:622-32 DOI: 10.2337/diabetes.55.03.06.db05-0832.

115. Marfella R, D'Amico M, Di Filippo C, Baldi A, Siniscalchi M, Sasso FC, Portoghese M, Carbonara O, Crescenzi B, Sangiuolo P, et al. Increased activity of the ubiquitin-proteasome system in patients with symptomatic carotid disease is associated with enhanced inflammation and may destabilize the atherosclerotic plaque: effects of rosiglitazone treatment. *Journal of the American College of Cardiology*. 2006;47:2444-55 DOI: 10.1016/j.jacc.2006.01.073.

116. Marfella R, Di Filippo C, Portoghese M, Ferraraccio F, Crescenzi B, Siniscalchi M, Barbieri M, Bologna C, Rizzo MR, Rossi F, et al. Proteasome activity as a target of hormone replacement therapy-dependent plaque stabilization in postmenopausal women. *Hypertension*. 2008;51:1135-41 DOI: 10.1161/HYPERTENSIONAHA.107.105239.

117. Marfella R, Di Filippo C, Laieta MT, Vestini R, Barbieri M, Sangiulo P, Crescenzi B, Ferraraccio F, Rossi F, D'Amico M, et al. Effects of ubiquitin-proteasome system deregulation on the vascular senescence and atherosclerosis process in elderly patients. *The journals of gerontology Series A, Biological sciences and medical sciences*. 2008;63:200-3 DOI: 10.1093/gerona/63.2.200.

118. Herrmann J, Soares SM, Lerman LO ,Lerman A. Potential role of the ubiquitin-proteasome system in atherosclerosis: aspects of a protein quality disease. *Journal of the American College of Cardiology*. 2008;51:2003-10 DOI: 10.1016/j.jacc.2008.02.047.

119. Ludwig A ,Meiners S. Targeting of the proteasome worsens atherosclerosis? *Circulation research*. 2008;102:e37 DOI: 10.1161/CIRCRESAHA.107.168963.

120. Herrmann J, Edwards WD, Holmes DR, Jr., Shogren KL, Lerman LO, Ciechanover A ,Lerman A. Increased ubiquitin immunoreactivity in unstable atherosclerotic plaques associated with acute coronary syndromes. *Journal of the American College of Cardiology*. 2002;40:1919-27 DOI: 10.1016/s0735-1097(02)02564-0.

121. Zhou J, Lhotak S, Hilditch BA ,Austin RC. Activation of the unfolded protein response occurs at all stages of atherosclerotic lesion development in apolipoprotein E-deficient mice. *Circulation*. 2005;111:1814-21 DOI: 10.1161/01.CIR.0000160864.31351.C1.

122. Wilck N, Fechner M, Dreger H, Hewing B, Arias A, Meiners S, Baumann G, Stangl V, Stangl K ,Ludwig A. Attenuation of early atherogenesis in low-density lipoprotein receptor-deficient mice by proteasome inhibition. *Arteriosclerosis, thrombosis, and vascular biology*. 2012;32:1418-26 DOI: 10.1161/ATVBAHA.112.249342.

123. Meiners S, Laule M, Rother W, Guenther C, Prauka I, Muschick P, Baumann G, Kloetzel PM ,Stangl K. Ubiquitin-proteasome pathway as a new target for the prevention of restenosis. *Circulation*. 2002;105:483-9 DOI: 10.1161/hc0402.102951.

124. Wilck N, Fechner M, Dan C, Stangl V, Stangl K ,Ludwig A. The Effect of Low-Dose Proteasome Inhibition on Pre-Existing Atherosclerosis in LDL Receptor-Deficient Mice. *International journal of molecular sciences*. 2017;18 DOI: 10.3390/ijms18040781.

125. Van Herck JL, De Meyer GR, Martinet W, Bult H, Vrints CJ ,Herman AG. Proteasome inhibitor bortezomib promotes a rupture-prone plaque phenotype in ApoE-deficient mice. *Basic research in cardiology*. 2010;105:39-50 DOI: 10.1007/s00395-009-0054-y.

126. Feng B, Zhang Y, Mu J, Ye Z, Zeng W, Qi W, Luo Z, Guo Y, Yang X ,Yuan F. Preventive effect of a proteasome inhibitor on the formation of accelerated atherosclerosis in rabbits with uremia. *Journal of cardiovascular pharmacology*. 2010;55:129-38 DOI: 10.1097/FJC.0b013e3181c87f8e.

127. Chen JH, Lenihan DJ, Phillips SE, Harrell SL ,Cornell RF. Cardiac events during treatment with proteasome inhibitor therapy for multiple myeloma. *Cardiooncology*. 2017;3:4 DOI: 10.1186/s40959-017-0023-9.

128. Waxman AJ, Clasen S, Hwang WT, Garfall A, Vogl DT, Carver J, O'Quinn R, Cohen AD, Stadtmauer EA, Ky B, et al. Carfilzomib-Associated Cardiovascular Adverse Events: A Systematic Review and Meta-analysis. *JAMA Oncol*. 2018;4:e174519 DOI: 10.1001/jamaoncol.2017.4519.

129. Joeris T, Schmidt N, Ermert D, Krienke P, Visekruna A, Kuckelkorn U, Kaufmann SH ,Steinhoff U. The proteasome system in infection: impact of beta5 and LMP7 on composition, maturation and quantity of active proteasome complexes. *PloS one*. 2012;7:e39827 DOI: 10.1371/journal.pone.0039827.

130. Kloss A, Meiners S, Ludwig A ,Dahlmann B. Multiple cardiac proteasome subtypes differ in their susceptibility to proteasome inhibitors. *Cardiovascular research*. 2010;85:367-75 DOI: 10.1093/cvr/cvp217.

131. Dahlmann B, Ruppert T, Kuehn L, Merforth S ,Kloetzel PM. Different proteasome subtypes in a single tissue exhibit different enzymatic properties. *Journal of molecular biology*. 2000;303:643-53 DOI: 10.1006/jmbi.2000.4185.

132. Kisselev AF. Site-Specific Proteasome Inhibitors. *Biomolecules*. 2021;12 DOI: 10.3390/biom12010054.

133. Li J, Hu S, Johnson HWB, Kirk CJ, Xian P, Song Y, Li Y, Liu N, Groettrup M ,Basler M. Co-inhibition of immunoproteasome subunits LMP2 and LMP7 enables prevention of transplant arteriosclerosis. *Cardiovascular research*. 2023;119:1030-1045 DOI: 10.1093/cvr/cvac181.

134. Haghikia A, Jorg S, Duscha A, Berg J, Manzel A, Waschbisch A, Hammer A, Lee DH, May C, Wilck N, et al. Dietary Fatty Acids Directly Impact Central Nervous System Autoimmunity via the Small Intestine. *Immunity*. 2015;43:817-29 DOI: 10.1016/j.immuni.2015.09.007.

DANKSAGUNG

Meine Forschung und damit auch diese Arbeit wären ohne die Hilfe und den Zuspruch vieler KollegInnen und Freunde nicht möglich gewesen. Dabei hatte ich die Ehre, meine Arbeiten an der Klinik für Kardiologie, Angiologie und Intensivmedizin, Campus Charité Mitte (Kardiologisches Forschungslabor, Leitung Prof. Dr Verena Stangl, Prof. Dr. Karl Stangl), dem Experimental and Clinical Research Center (ECRC) von Charité und Max-Delbrück-Centrum für Molekulare Medizin (MDC) und schließlich der Medizinischen Klinik mit Schwerpunkt Nephrologie und Internistische Intensivmedizin (unter der Leitung von Prof. Dr. Kai-Uwe Eckardt) der Charité durchführen zu können. Dafür möchte ich mich herzlich bedanken. Ich danke allen KollegInnen, die mir hin und wieder in der Klinik den Rücken freigehalten haben.

Darüber hinaus bedanke ich mich für die Aufnahme in das BIH Clinician Scientist Programm.

Es gibt einige Freunde und KollegInnen (hier verschwimmt die Grenze glücklicherweise), die mir über die Jahre Orientierung und Rat gaben. Ohne PD Dr. Antje Ludwig wäre ich möglicherweise nicht in der Forschung geblieben. Danke Antje, für viele Gespräche mit und ohne Forschungsinhalt. Ohne die Offenheit und Förderung von Prof. Dr. Dominik N. Müller hätte meine Forschung nicht die Fahrt und Kreativität aufgenommen, die sie heute so unverzichtbar für mich macht. Ich empfinde es als Privileg, jeden Tag mit interessierten, wunderbaren WissenschaftlerInnen zu arbeiten. Danke Dr. Hendrik Bartolomaeus für unermüdlichen Vorwärtsdrang und den Spaß bei unserer Arbeit.

Meine liebe Familie hat mich immer unterstützt und mich dabei eher am Schreibtisch als auf der Wiese beobachten können. Danke für Deine Unterstützung, Laura. Danke Willem, Lorenz und Miriam für Eure Geduld.

ERKLÄRUNG

§ 4 Abs. 3 (k) der HabOMed der Charité

Hiermit erkläre ich, dass

- weder früher noch gleichzeitig ein Habilitationsverfahren durchgeführt oder angemeldet wurde,

- die vorgelegte Habilitationsschrift ohne fremde Hilfe verfasst, die beschriebenen Ergebnisse selbst gewonnen sowie die verwendeten Hilfsmittel, die Zusammenarbeit mit anderen Wissenschaftlern/Wissenschaftlerinnen und mit technischen Hilfskräften sowie die verwendete Literatur vollständig in der Habilitationsschrift angegeben wurden,

- mir die geltende Habilitationsordnung bekannt ist.

Ich erkläre ferner, dass mir die Satzung der Charité – Universitätsmedizin Berlin zur Sicherung Guter Wissenschaftlicher Praxis bekannt ist und ich mich zur Einhaltung dieser Satzung verpflichte.

…… ……..

Datum Unterschrift